

ENERGY
THAT
CHANGES



PSMA-SMA SPECIAL PROJECT – PHASE II INVESTIGATION ON MAGNETIC FLUX PROPAGATION IN FERRITE CORES

Marcin Kącki, dr. Marek S. Ryłko, Edward Herbert



Project co-sponsored by
The Power Sources Manufacturers Association

e-mail: power@psma.com

<http://www.pdma.com/>

P.O. Box 418

Mendham, NJ 07945-0418



The continuous drive to high performance energy conversion based on new wide bandgap semiconductors forces an uprising new models and design rules for high performance magnetic components. The state-of-the-art magnetic modeling assumes high frequency effects in ferrites as negligible. Ferrite manufacturers provide materials parameters as permittivity and conductivity as a constant that is common for the ferrite family range. Power loss under rectangular wave excitation are investigated predominantly by universities and research centers. Limited data availability in magnetic materials datasheets narrows design procedure to available data that incur substantial errors at high switching frequencies, the overcome of the available data limitations is motivation to start a new research project. The research work is focused on the magnetic flux distribution in the magnetic core, ferrite electrical properties and power loss for various materials, core sizes and excitations. The results are intended to be a foundation for further discussion to introduce a standardized testing procedures for magnetic materials required by a detailed design.

Due to the range of the work, the project is scoped in five main packages:

1. Large core testing – flux propagation in ferrites

- a) Flux distribution in T50 ferrite ring cores
- b) Flux distribution in T152 ferrite ring cores
- c) Design cores for equivalent circuit verification

This package is focused on the fundamentals of the magnetic flux distribution in the magnetic core. The number of experiment was carried out in order to develop the non uniform flux distribution and quantify the effect.

2. Core power loss comparison

- a) Material 3C95 (various toroid sizes)
- b) Material 3E10 (various toroid sizes)
- c) Material 3F36(various toroid sizes)

This package investigates how the flux distribution impacts core power loss under sinusoidal and rectangular voltage waveform. The results are presented as a Performance Factor and Herbert's Curve.

3. Core shape effect on power loss

- a) Laminated ferrite cores (core loss and impedance comparison)
- b) Hollowed ring cores (core loss and impedance comparison)
- c) String of beads (core loss and impedance comparison)

This package investigates core shape impact on flux distribution, power loss and inductor performance. Three cores were designed and experimentally investigated for possible performance improvement.

4. Ferrites electrical properties

- a) Measurement fixture development
- b) Sample size selection for material testing
- c) Preliminary magnetic materials tests

This package is focused on a novel method to determine the electric properties of conductivity and permittivity of ferrite cores at high frequency.



5. Rectangular wave core loss tester

- a) H-Bridge development and component selection
- b) Software development for interfacing measurement setup and data acquisition
- c) Data post-processing on the example of selected core

This package is focused on the core loss tester development for rectangular wave excitation. Reliable core loss measurement based on the rectangular excitation is essential for magnetic component design process. Further, the tester is to be employed to characterize magnetic flux distribution on the core loss in relations to the applied voltage waveform.

Acknowledgements



We would like to express our deep gratitude to Professor Charles R. Sullivan, Professor John G. Hayes and Professor Gerry W. Hurley for their valuable, constructive suggestions and research supervision during the planning and developing this research work.

We would like to offer special thanks to the SMA Magnetics R&D team for their support for research.

Finally, we wish to thank Fair-Rite Products Corporation for frame core machining and precise drilling.

References



- [1] G.R. Skutt, "High-frequency dimensional effects in ferrite-core magnetic devices," PHD Virginia Polytechnic Institute, 1996.
- [2] G.R. Skutt, F.C. Lee, "Characterization of dimensional effects in ferrite-core magnetic devices," *Power Electronics Specialist Conference*, 1996.
- [3] M. Kącki, M.S. Ryłko, J.G Hayes, C.R. Sullivan, "Magnetic material selection for EMI filter," *IEEE Energy Conversion Congress and Exposition (ECCE)*, 2017.
- [4] F.G. Brockman, P.H. Dowling, W.G. Steneck, "Dimensional effects resulting from a high dielectric constant found in a ferromagnetic ferrite," *Physical Review* 77, January 1950.
- [5] F.P. Pengfei, Z. Ning, "Magnetodielectric effect of Mn-Zn ferrite at resonant frequency," *Journal of Magnetism and Magnetic Materials*, Vol. 416, 2016.
- [6] B.D Cullity, C.D. Graham, "Introduction to magnetic materials," *John Wiley and Sons*, 2009.
- [7] E.C. Snelling, *Soft ferrites: properties and applications*, Newnes-Butterworth; 1 St Edition, 1969.
- [8] T. Todorova, V. Valchev, A. Van den Bossche, "Modeling of electrical properties of Mn-Zn ferrites taking into account the frequency of the occurrence of the dimensional resonance," *Jurnal of Electrical Engineering*, July 2018.

ENERGY
THAT
CHANGES



SECTION I – FLUX PROPAGATION IN FERRITES

Marcin Kącki, dr. Marek S. Ryłko, Edward Herbert

Sponsored by

The Power Sources Manufacturers Association

e-mail: power@psma.com, <http://www.psm.com/>

P.O. Box 418, Mendham, NJ 07945-0418

Magnetic core size, magnetic field amplitude and frequency has a strong impact on the magnetic flux distribution in the core. The magnetic flux distribution is also affected by the frequency dependent dynamic effects as eddy currents and wave propagation effect. Eddy currents are characterized by the skin effect that results in a non-uniform flux distribution in the core cross-section. Wave propagation effect is characterized by material parameters dependent dimensional resonance. This section of the project presents experimental investigation of the magnetic flux distribution in selected ferrite ring cores.

Project development:

1. Flux distribution verification based on the T50 ring core - simplified method
2. Flux distribution verification based on the T152 ring core - detailed verification based on 4 shells and 49 segment core drilling scheme
3. Core samples preparation are subsequent task of this project

Content



1

Flux distribution in T50 ferrite ring core

2

Flux distribution in T152 ferrite ring core

3

Cores selection for equivalent circuit validation

4

Conclusion and future work

5

Appendices

Flux distribution in T50 ferrite ring core



The first step was to bore two vertical and one horizontal hole in two ferrite cores made of 3E10 and 3C95 material and measure the magnetic flux distribution.

The holes divide core into two sections: inner and outer. Therefore, inner to outer core segments ratio is compared. This simplified approach allows to measure magnetic flux distribution up to the certain frequency extent where the magnetic flux skin depth effect is limited to the magnet wire loop.

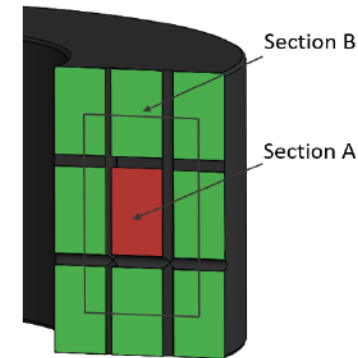
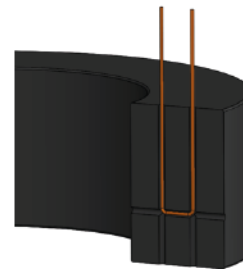
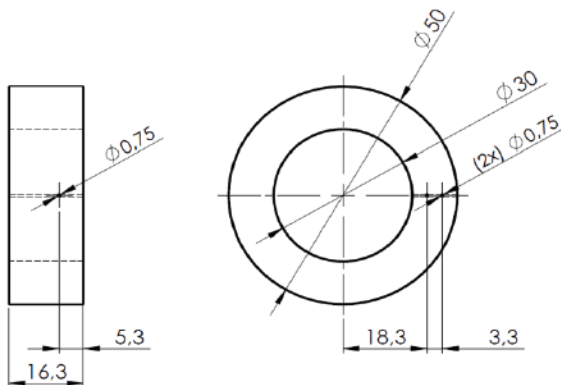
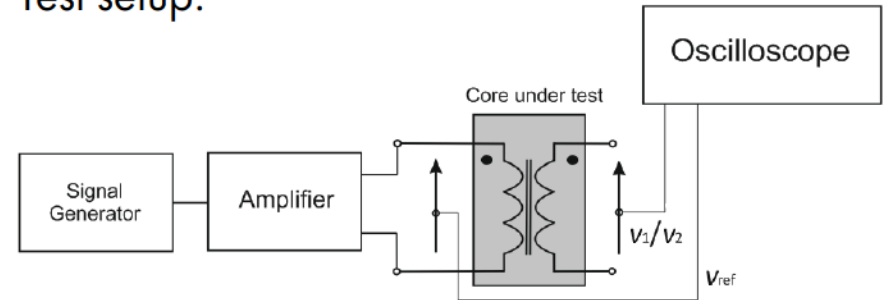
Flux distribution in T50 ferrite ring core



Three holes were bored in selected ferrite cores:

Material	3E10	3C95
Permeability	10 000	3 000
Dimensions OD x ID x H	50x30x16.5 mm	50x30x16.5 mm
Core total cross section	165 mm ²	165 mm ²
Core volume	20.7 cm ³	20.7 cm ³

Test setup:

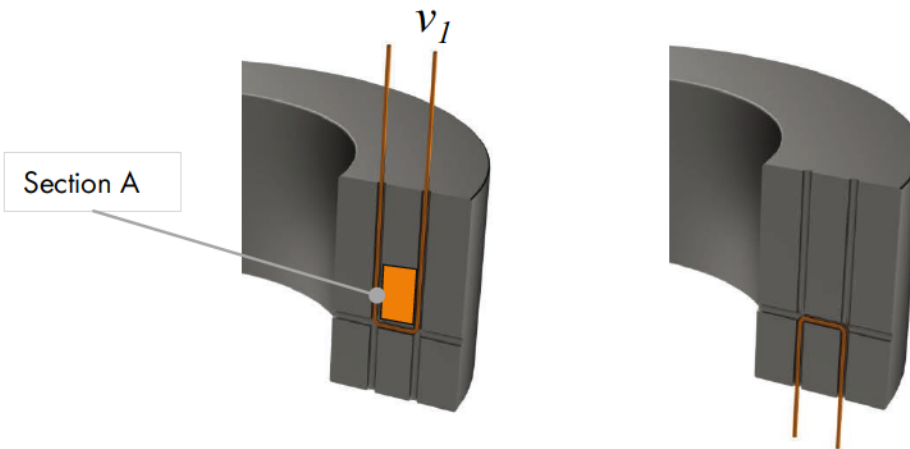
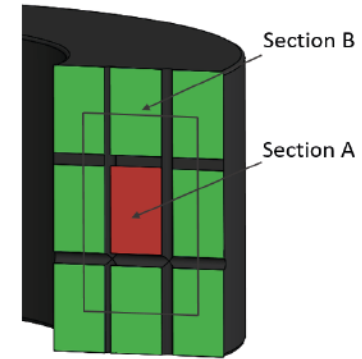


Flux distribution in T50 ferrite ring core



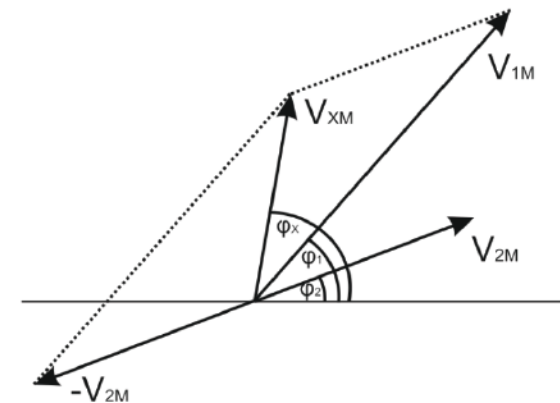
Section A voltage v_x was defined in three steps:

- V_1 measurement – section A + portion above it
- V_2 measurement
- Measured voltage subtraction: $v_x = v_1 - v_2$



$$v_1(t) = V_{1M} \sin(\omega t + \phi_1)$$

$$v_2(t) = V_{2M} \sin(\omega t + \phi_2)$$

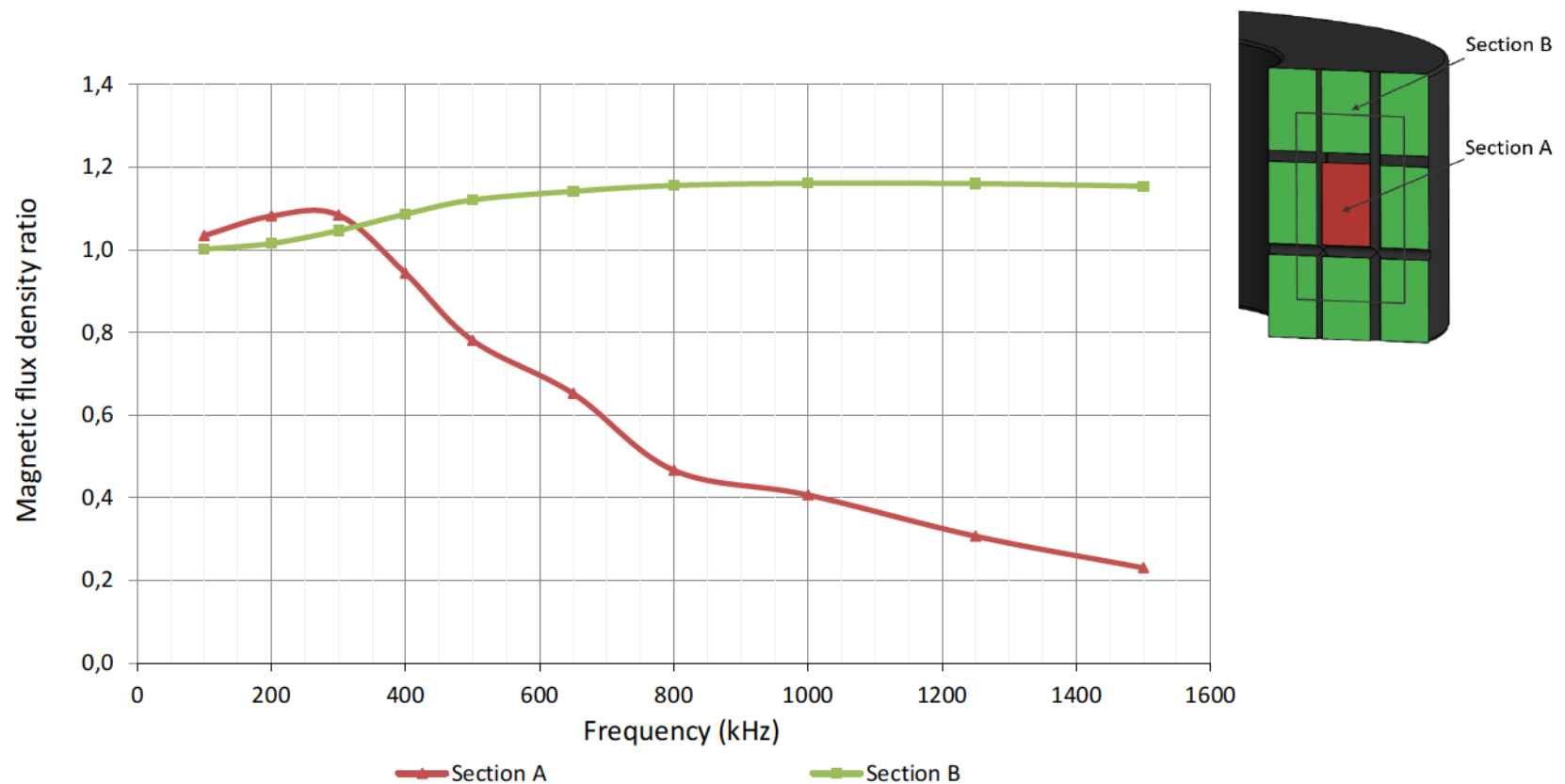


$$v_x(t) = V_{XM} \sin(\omega t + \phi_X)$$
$$v_x(t) = v_1(t) - v_2(t)$$

Flux distribution in T50 ferrite ring core



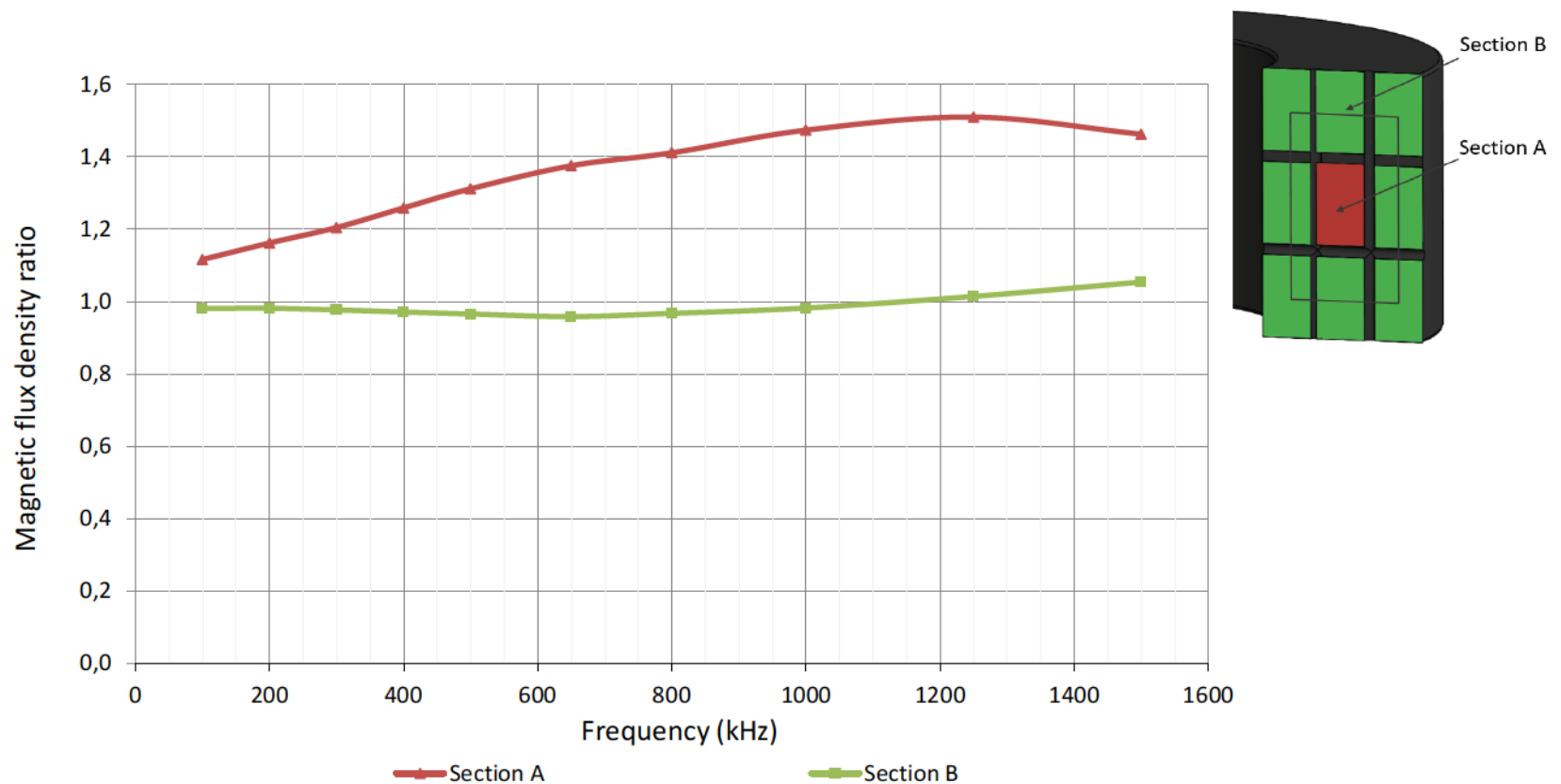
Flux distribution in the section of TX50 core made from 3E10 material:



Flux distribution in T50 ferrite ring core



Flux distribution in the section of TX50 core made from 3C95 material:



Flux distribution in T50 ferrite ring core



It is observed that magnetic flux undergoes a skin effect analogous to conductors in high permeability materials as 3E10. In extreme case, magnetic flux in the core's middle section flow in an opposite direction to the equivalent flux in the core. Lower permeability materials shows magnetic flux increase in the core's middle section caused by wave propagation effects.

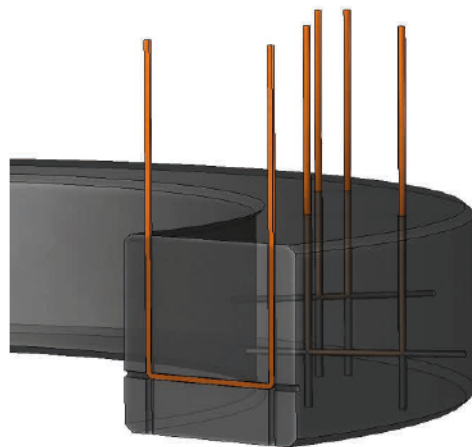
To increase measurement accuracy number of drilled holes was tripled. Flux distribution in the core was measured with higher resolution. With additional bores measured flux characteristics could be presented in four core sections instead of two. Simultaneously core size was increased from T50 to T152 that allows to develop Eddy-currents and dimensional resonance effects at lower frequency.

Flux distribution in T152 ferrite ring core

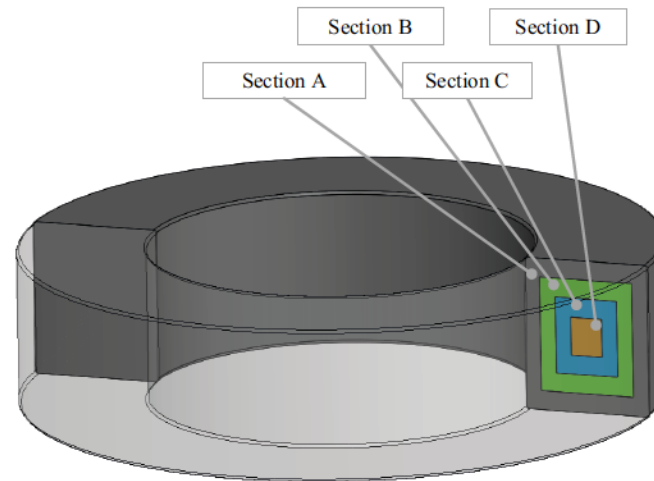
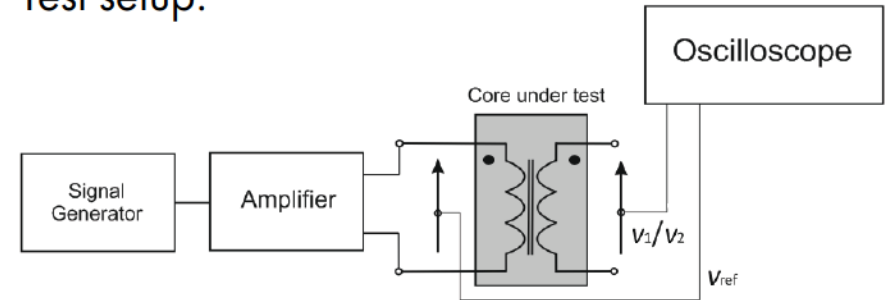


Three sets of holes were bored in selected ferrite cores:

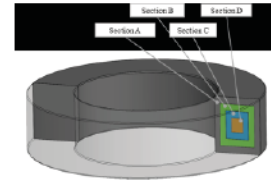
Material	3C95
Permeability	3 000
Dimensions OD x ID x H	152x104x24 mm
Core total cross section	576 mm ²
Core volume	231 cm ³



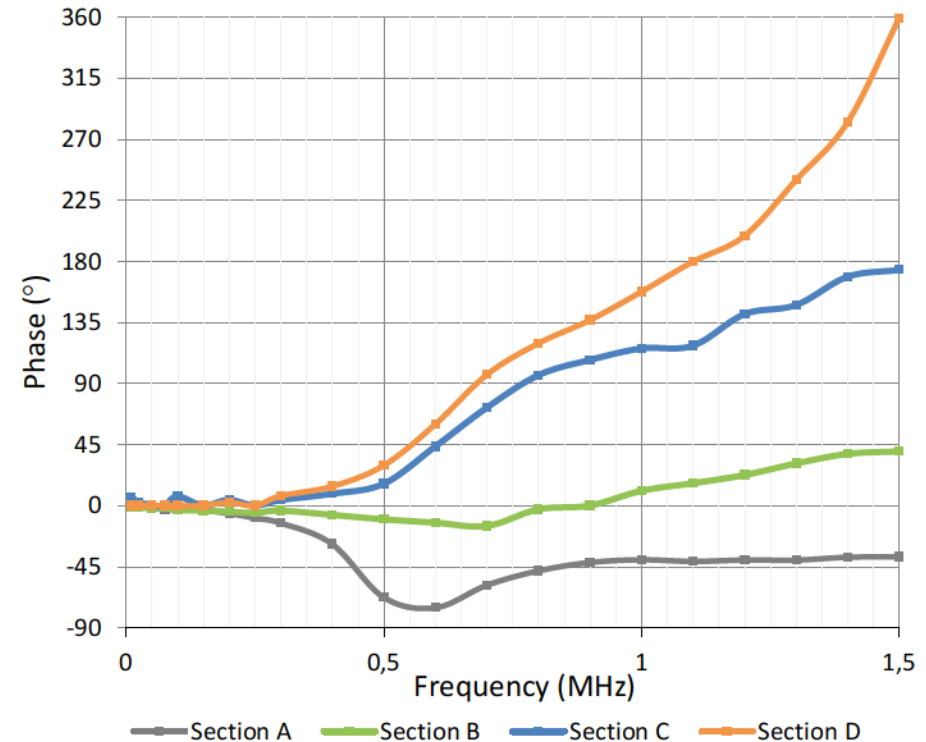
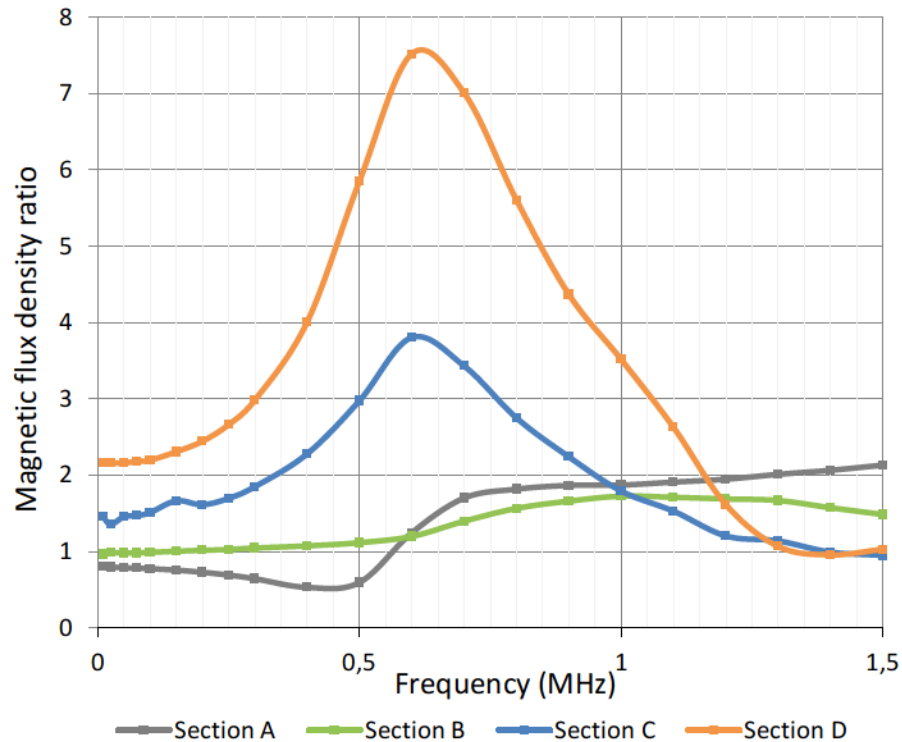
Test setup:



Flux distribution in T152 ferrite ring core



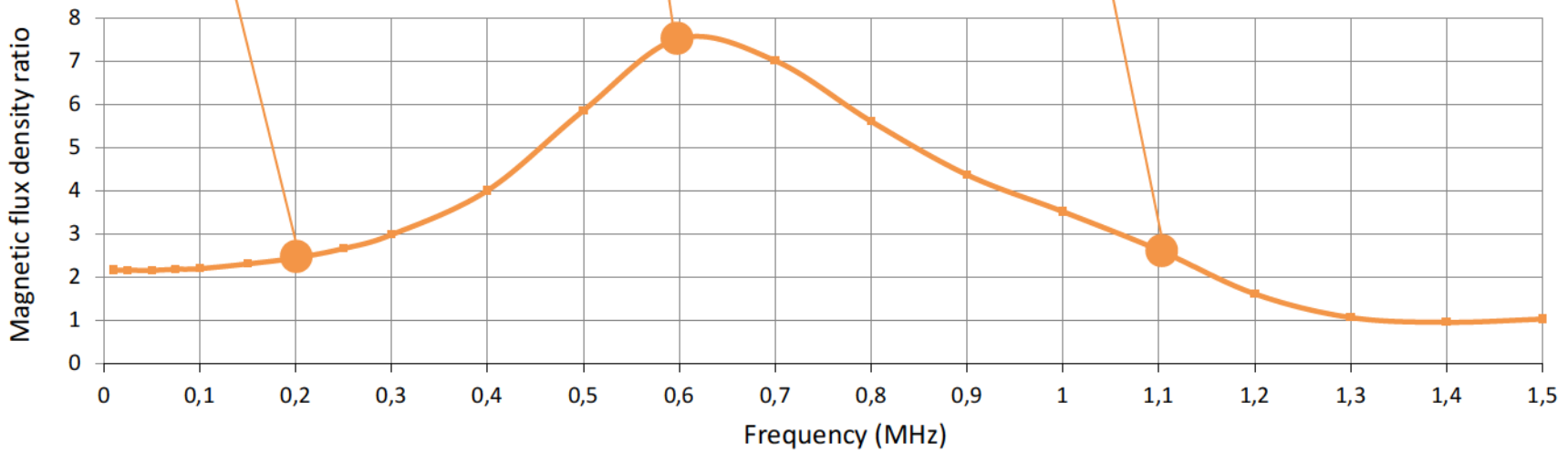
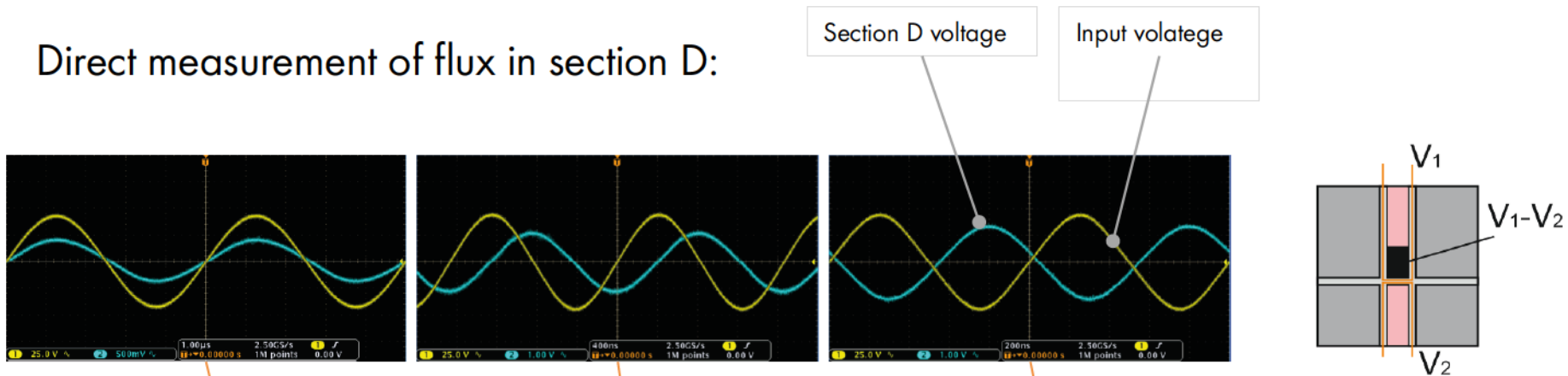
Flux distribution in the sections of TX152 core made from 3C95 material:



Flux distribution in T152 ferrite ring core



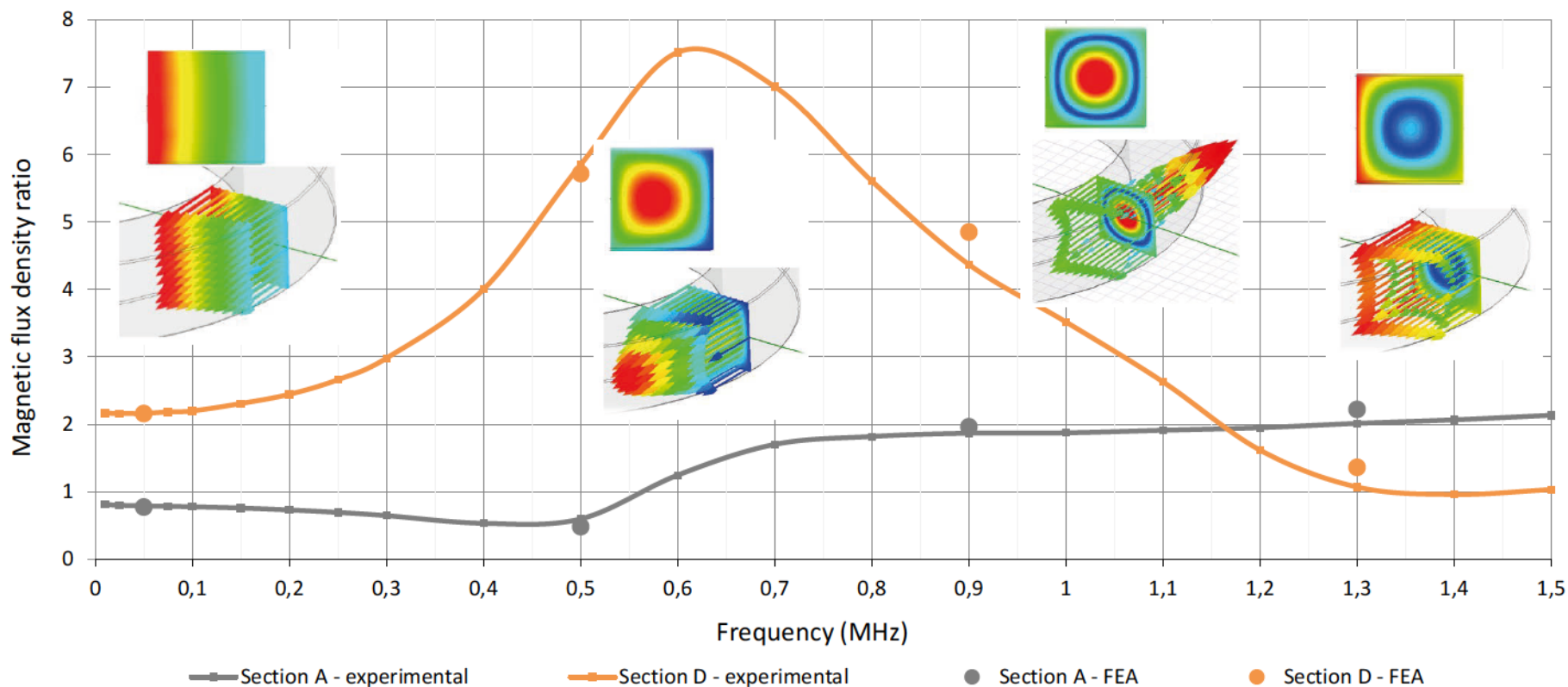
Direct measurement of flux in section D:



Flux distribution in T152 ferrite ring core



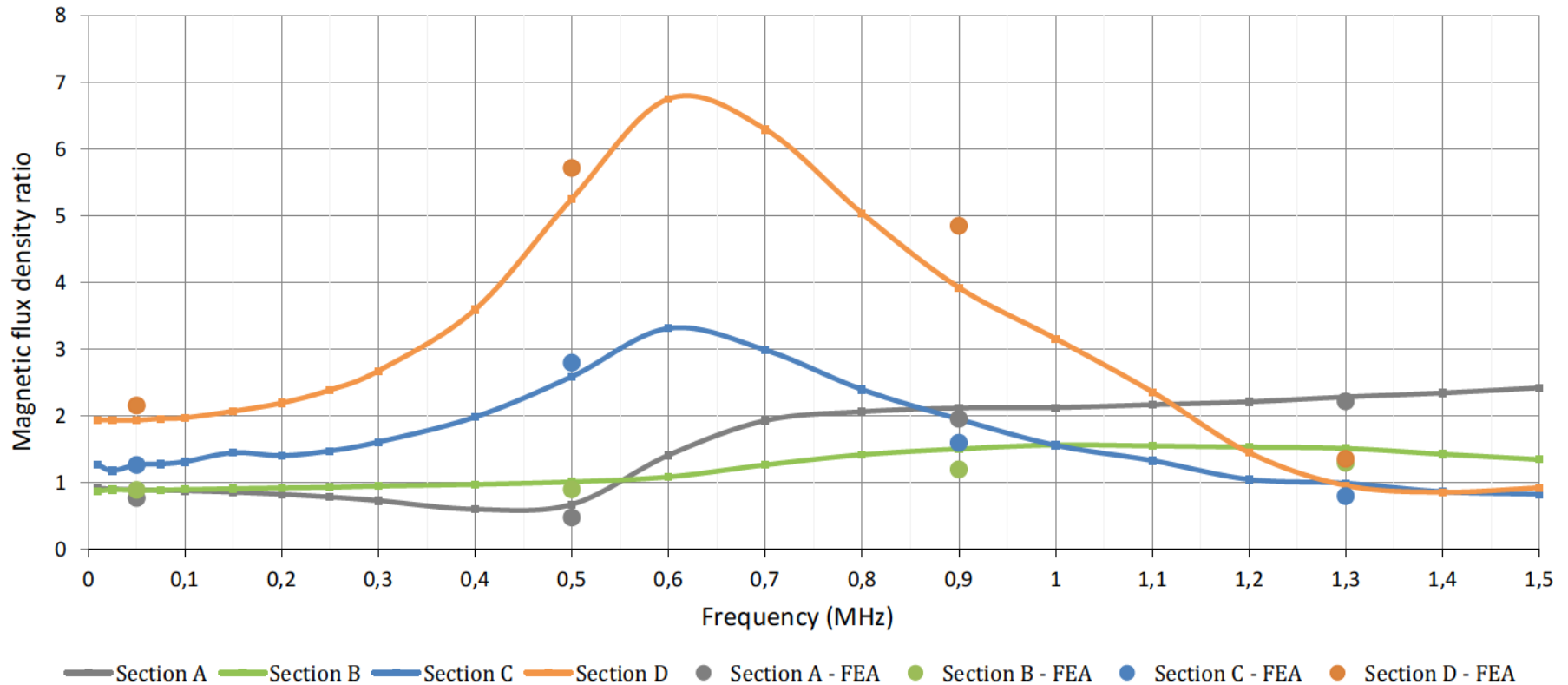
Measurement comparison with FEA



Flux distribution in T152 ferrite ring core



Measurement comparison with FEA



Measurement comparison with FEA

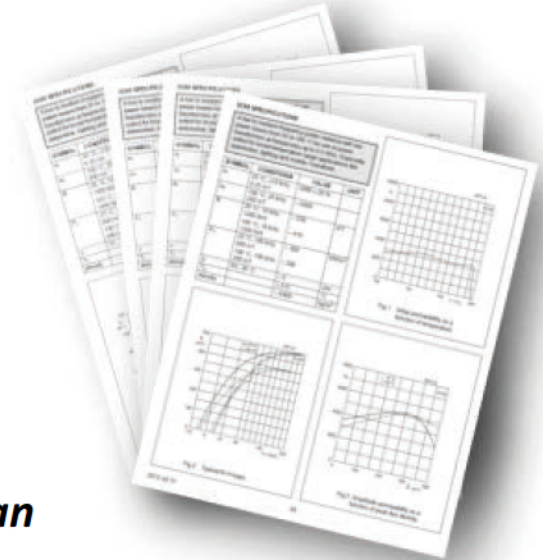


Good coherence between FEA and measurement was achieved due to accurate magnetic materials characteristic.

Magnetics materials properties required for FEA analysis:

1. Permeability frequency characteristic
2. Dielectric constant frequency characteristic
3. Conductivity frequency characteristic
4. Power loss measured at sinusoidal and square wave excitation

Calculation based on data provided by material manufacturer`s may cause significant error.



The most important is to have correct data than the most detailed equation or model.

Measurement comparison with FEA



Four simulations were performed to check the effect of core permeability, permittivity and conductivity on flux distribution:

Simulation 1 – Not corrected FEA

The first simulation shows an ideal case of a lossless core. Magnetic flux intensity is stronger at the inner radius of the core and reduces due to the effect of the reluctance path.

Simulation 2 – High permittivity

In the second simulation relative permittivity was set to 20000, large amplitude flux occurs under resonant conditions and is concentrated in the inner part of the core.

Simulation 1 – Ideal

$f = 500 \text{ kHz}$, $\mu_R = 10\,000$, $\epsilon_R = 1$, $\sigma = 0.1 \text{ S/m}$



Simulation 2 – High permittivity

$f = 500 \text{ kHz}$, $\mu_R = 10\,000$, $\epsilon_R = 20\,000$, $\sigma = 0.1 \text{ S/m}$



Measurement comparison with FEA



Simulation 3 – High conductivity

The magnetic flux density distribution is similar to current distribution in a conductor. Magnetic flux is concentrated in the outer circumference while the core center exhibits flux density weakening due to core skin effect.

Simulation 4 – All parameters

High frequency core effects are visible in FEA modeling of field distribution due to introduction of permittivity and conductivity. Only the identification of all magnetic material properties allow for a precise calculation.

Simulation 3 – High conductivity
 $f = 500 \text{ kHz}$, $\mu_R = 10\,000$, $\epsilon_R = 1$, $\sigma = 5 \text{ S/m}$



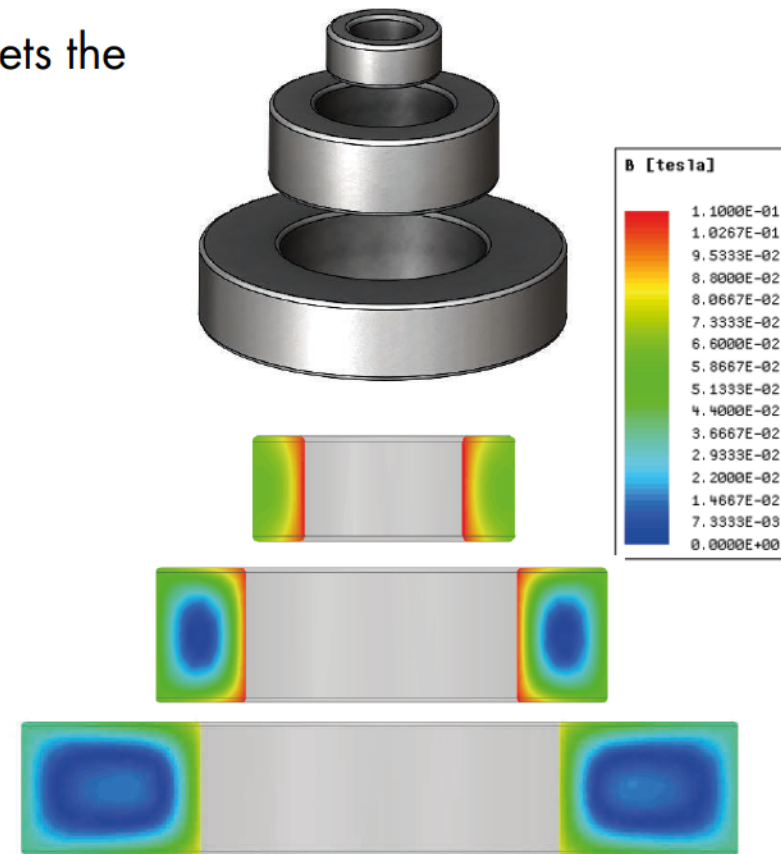
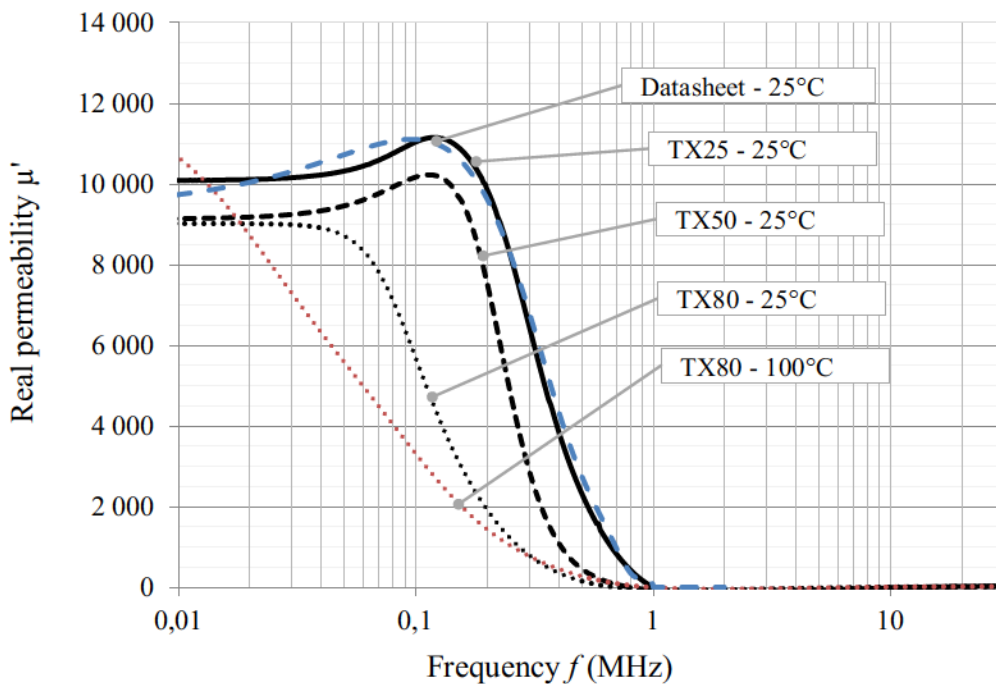
Simulation 4 – All parameters
 $f = 500 \text{ kHz}$, $\mu_R = 10\,000$, $\epsilon_R = 20\,000$, $\sigma = 5 \text{ S/m}$



Measurement comparison with FEA



FEM analysis with included magnetic material characteristics help to understand effects which sets the limit for effective core use:



$$f = 500 \text{ kHz}, \mu_R = 10\,000, \epsilon_R = 20\,000, \sigma = 5 \text{ S/m}$$

Flux distribution in T152 ferrite ring core



The flux distribution based on bored three sets of holes gives more precise data than simplified three holes model.

Results confirm that flux distribution is affected by the frequency dependent dynamic effects as eddy currents and wave propagation effect.

Shells representation give good flux distribution overview analogous to current distribution in conductors.

FEA Simulation shows good correlation with measurement up to 1.3 MHz.

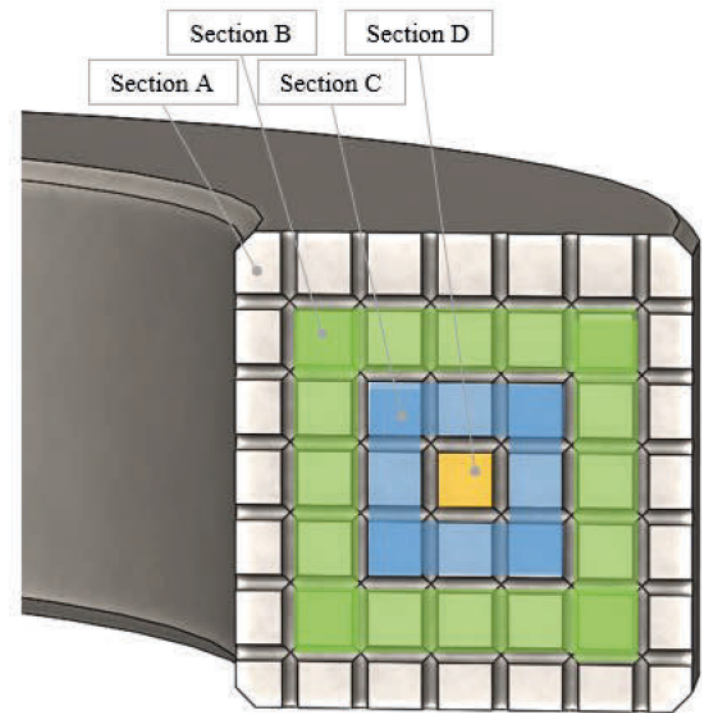
To further increase flux distribution measurement accuracy two ferrite cores T152 were drilled to obtain flux distribution in core 49 segments

Flux distribution in T152 ferrite ring core

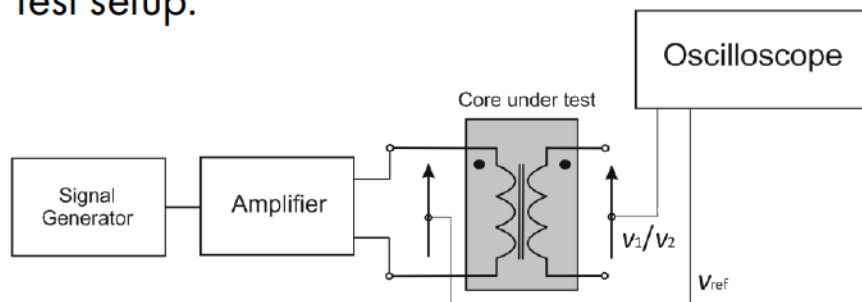


Six horizontal holes and six vertical holes equally spaced to fraction the core into 49 segments.

Material	3C95	3E10
Permeability	3 000	10 000
Dimensions OD x ID x H	152x104x24 mm	152x104x24 mm
Core total cross section	576 mm ²	576 mm ²
Core volume	231 cm ³	231 cm ³



Test setup:

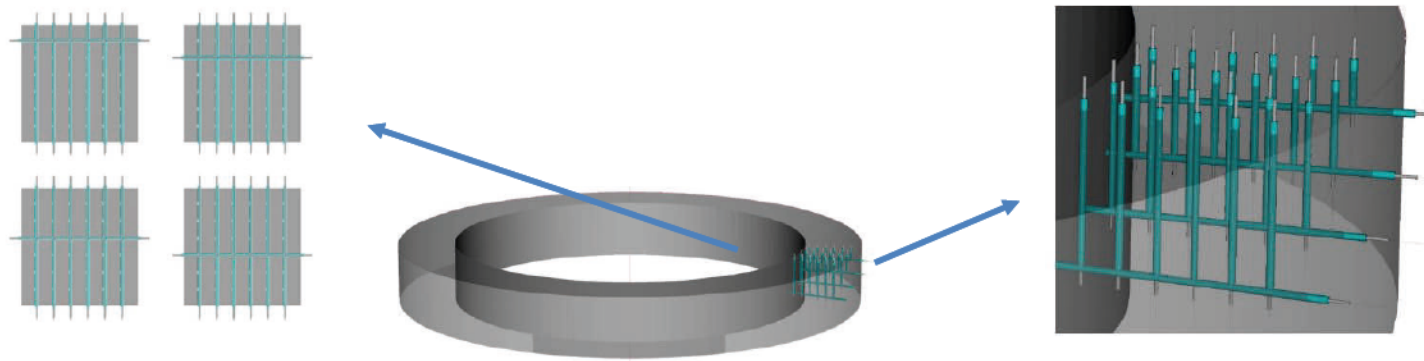


Flux distribution in T152 ferrite ring core

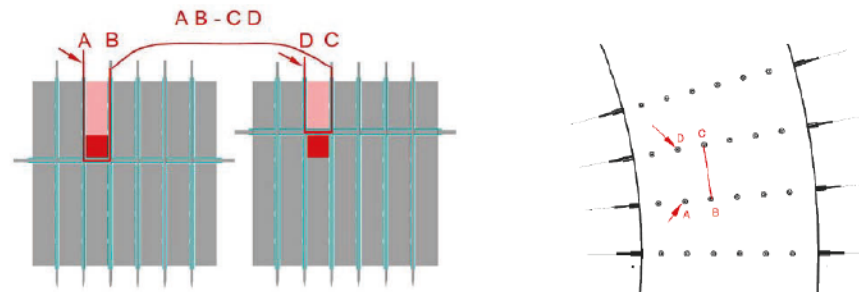


T152 core drilling scheme:

In four planes, one horizontal hole is drilled from the OD to the ID of the core.



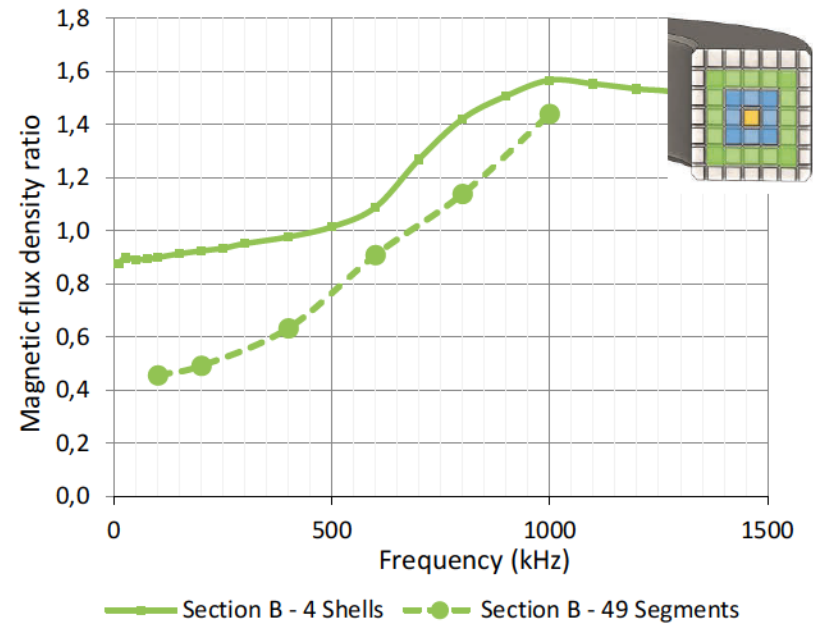
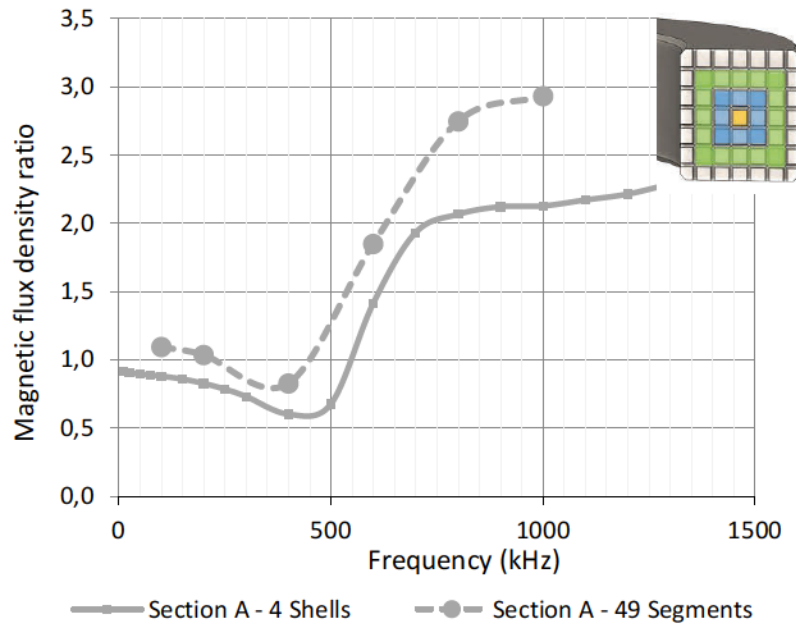
To measure the voltage on a RED segment, the presented connections were used. During the measurement pink area voltage is cancelled.



Flux distribution in T152 ferrite ring core



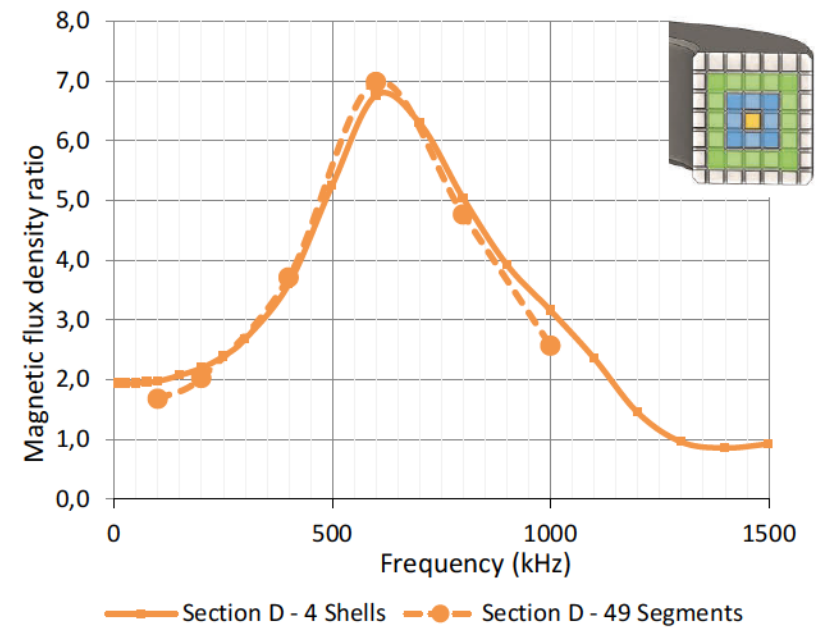
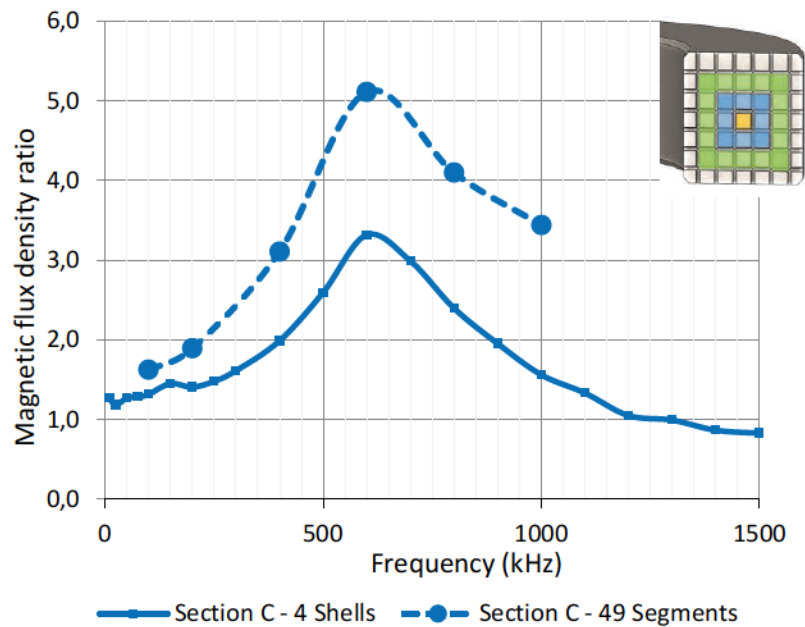
Shells and 49 segments results are contrasted for Section A and B:



Flux distribution in T152 ferrite ring core



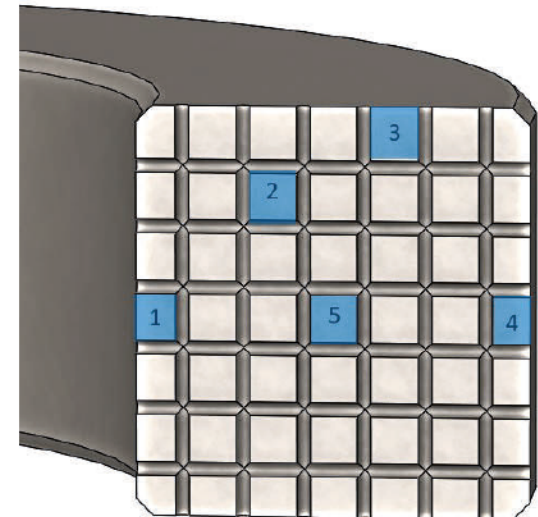
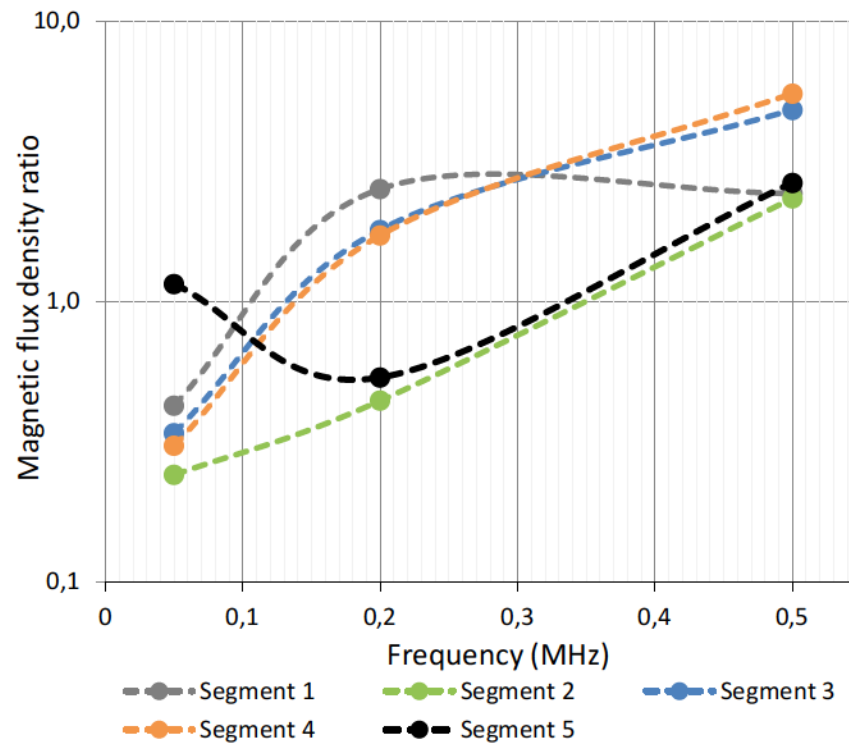
Shells and 49 segments results are contrasted for Section A and B:



Flux distribution in T152 ferrite ring core



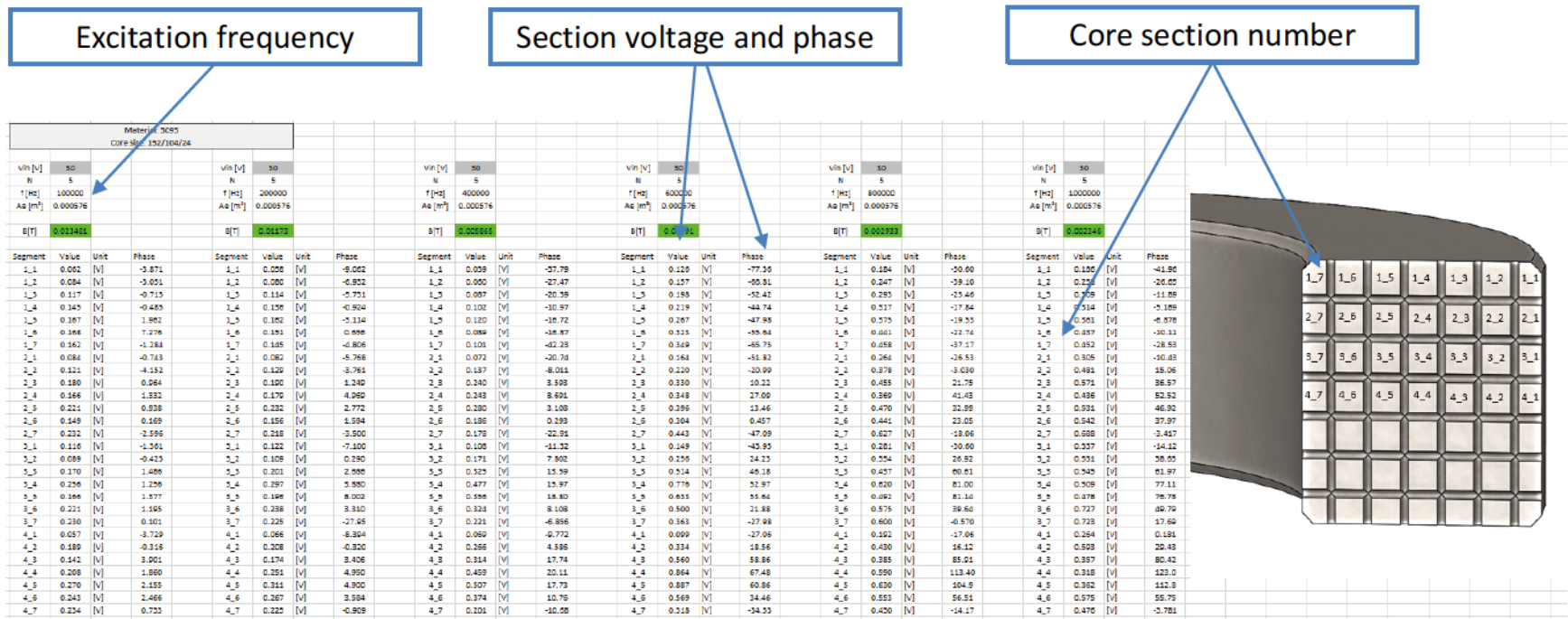
Based on the measurements any combination of the core segments could be contrasted with each other:



Flux distribution in T152 ferrite ring core



All measurement result collected in Excel files:

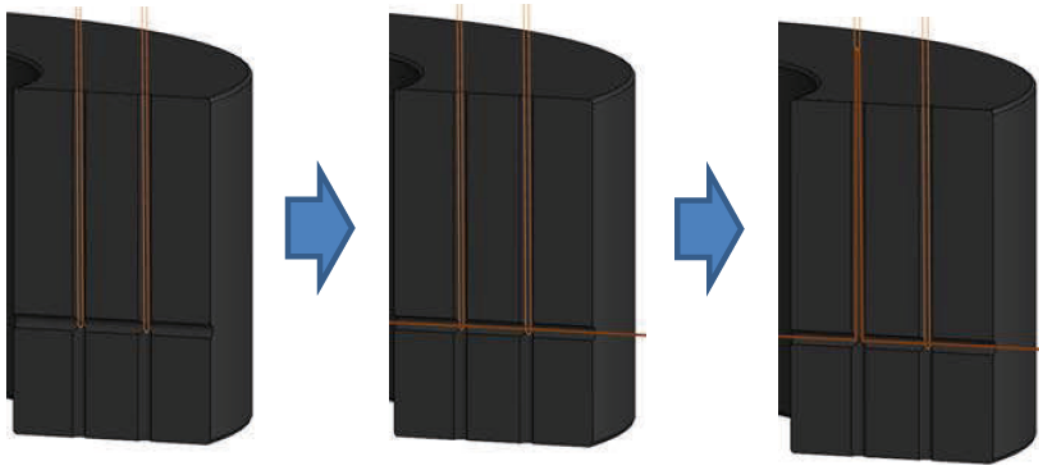


The excel file is presented in Appendix 1 - Flux propagation – 3C95

Flux distribution in T152 ferrite ring core



Sense winding placement is time consuming and challenging. Therefore, the method for permanent sense winding placement was defined. The idea is presented in pictures below:



Step 1. Insert wires (0.1mm) into each vertical hole, make small loop at the end of the inserted wire. Loops must be in line with horizontal hole.

Step 2. Insert wire into the horizontal hole. Wire diameter must be smaller than the hole radius. Thread the wire through each of the loops from first step.

Step 3. Pull wires inserted into vertical hole. Repeat for the other vertical wires

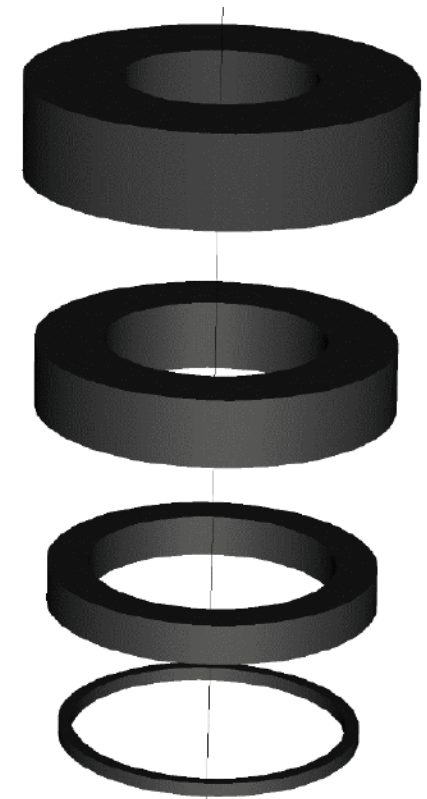


Cores equivalent circuit validation

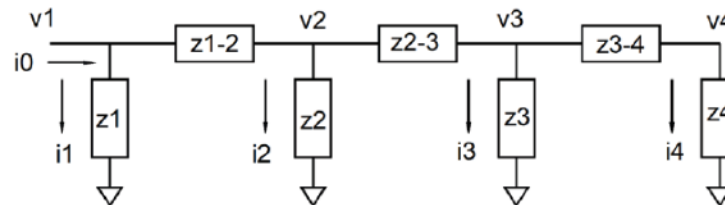
Four cores were machined for equivalent circuit validation.

Core details:

Material	3E10	3E10	3E10	3E10
Permeability	10 000	10 000	10 000	10 000
Dimensions OD x ID x H mm	80x40x20	74.3x45.7x14.3	68.6x51.4x8.6	62.9x57.1x2.9
Core total cross section	400 mm ²	204.5 mm ²	74 mm ²	8.4 mm ²
Core volume	75.3 cm ³	38.5 cm ³	13.9 cm ³	1.6 cm ³



In the next project phase core will be used to investigate core equivalent circuit:



Conclusion and future work



1. Dense mesh of holes allows to assess flux distribution in the core
2. Presented flux propagation results starting from simple three-hole model up to advanced 49 segments model confirms that magnetic flux distribution is affected by the frequency dependent dynamic effects as eddy currents and wave propagation effect
3. The three holes methods may be a subject for further discussion on the approach to standardized test for magnetic material properties

Future work

1. Flux propagation research for rectangular wave excitation

Appendices



The Appendices can be found on the PSMA website:

1. Flux propagation 4 shells - 3C95.xlsm
2. Flux propagation 49 segments - 3C95.xlsm
3. Flux propagation 49 segments - 3E10.xlsm

ENERGY
THAT
CHANGES



SECTION II – CORE POWER LOSSES COMPARISON

Marcin Kącki, dr. Marek S. Ryłko, Edward Herbert

Sponsored by

The Power Sources Manufacturers Association

e-mail: power@psma.com, <http://www.psm.com/>

P.O. Box 418, Mendham, NJ 07945-0418

This section of the project investigates how core size influence magnetic material performance. The power losses of different sized cores of the same material are measured and contrasted for sinusoidal and rectangular excitation.

Project development:

1. Core samples preparation for the tests
2. Measure power loss with sinusoidal excitation
3. Measure power loss with rectangular excitation
4. Calculate BF curve and Herbert curve

Content



1

Performance Factor curves for 3C95 material

2

Performance Factor curves for 3E10 material

3

Performance Factor curves for 3F36 material

4

Conclusion

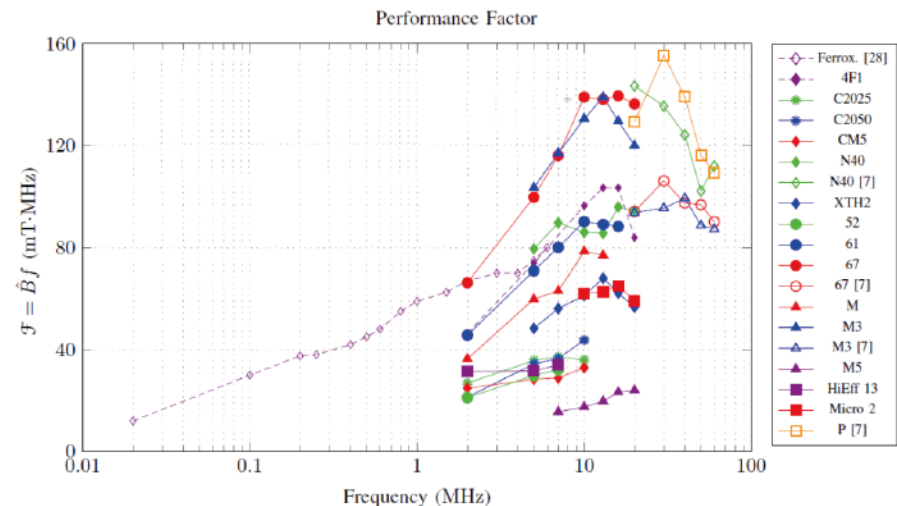
Performance factor



Performance Factor PF is commonly used comparison method. It is defined as the maximum product of peak flux density and frequency as a function of frequency at a constant power loss density. Magnetic components physical size is inversely related to PF . Performance factor is define as follows:

$$PF_{AC} = f \cdot B_{AC}$$

Market available magnetic materials performance factor comparison are limited to the small ring cores power loss measurement.



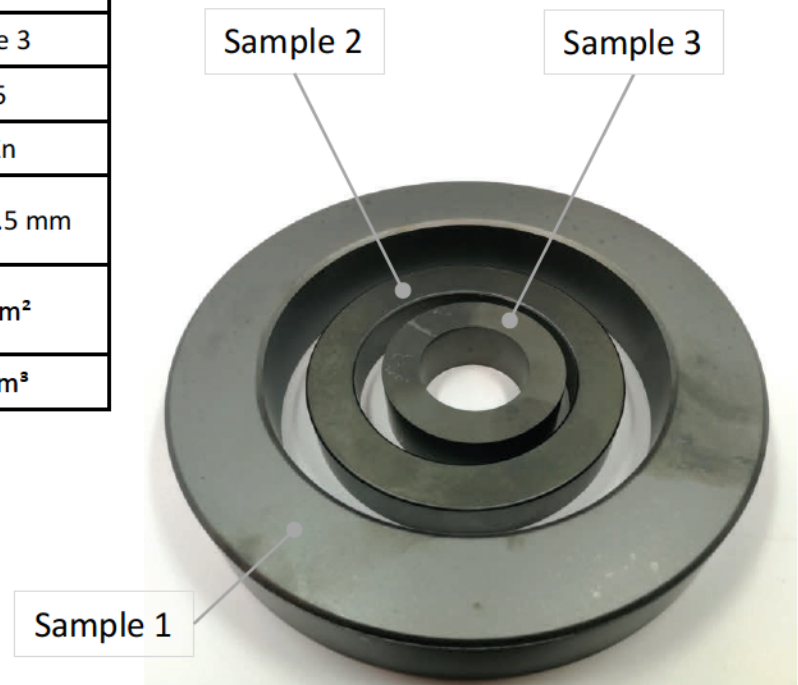
A.J. Hanson, J.A. Belk, D.J. Perreault, C.R. Sullivan, „Measurements and performance factor comparison of magnetic materials at high frequency,” *IEEE Energy Conversion Congress and Exposition (ECCE) 2015*

Performance Factor curves for 3C95



Core construction details:

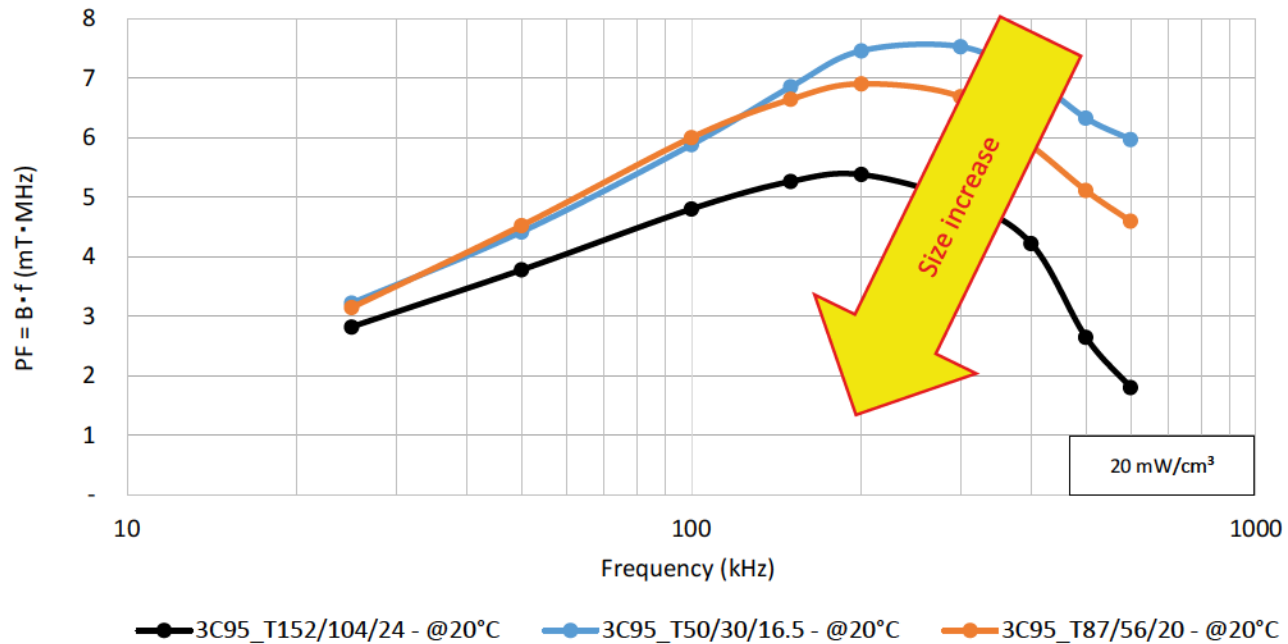
Tested samples			
	Sample 1	Sample 2	Sample 3
Material name	3C95	3C95	3C95
Material type	Mn-Zn	Mn-Zn	Mn-Zn
Dimensions OD x ID x H	152x104x24 mm	87x56x20 mm	50x30x16.5 mm
Core total cross section	571 mm ²	305 mm ²	160 mm ²
Core volume	226 cm ³	66.9 cm ³	19.3 cm ³



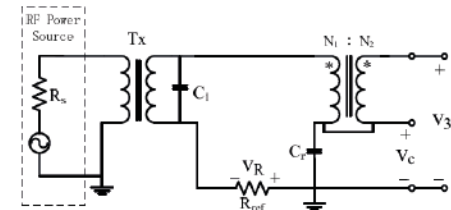
Performance Factor curves for 3C95 material



Core performance factor comparison:



Test setup:

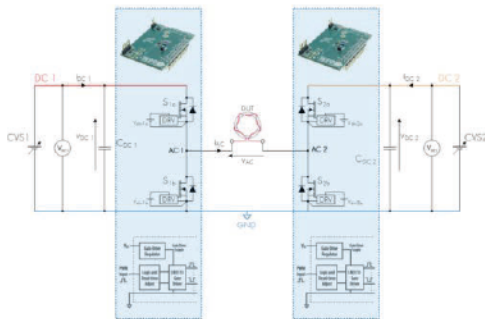


Performance Factor curves for 3C95 material

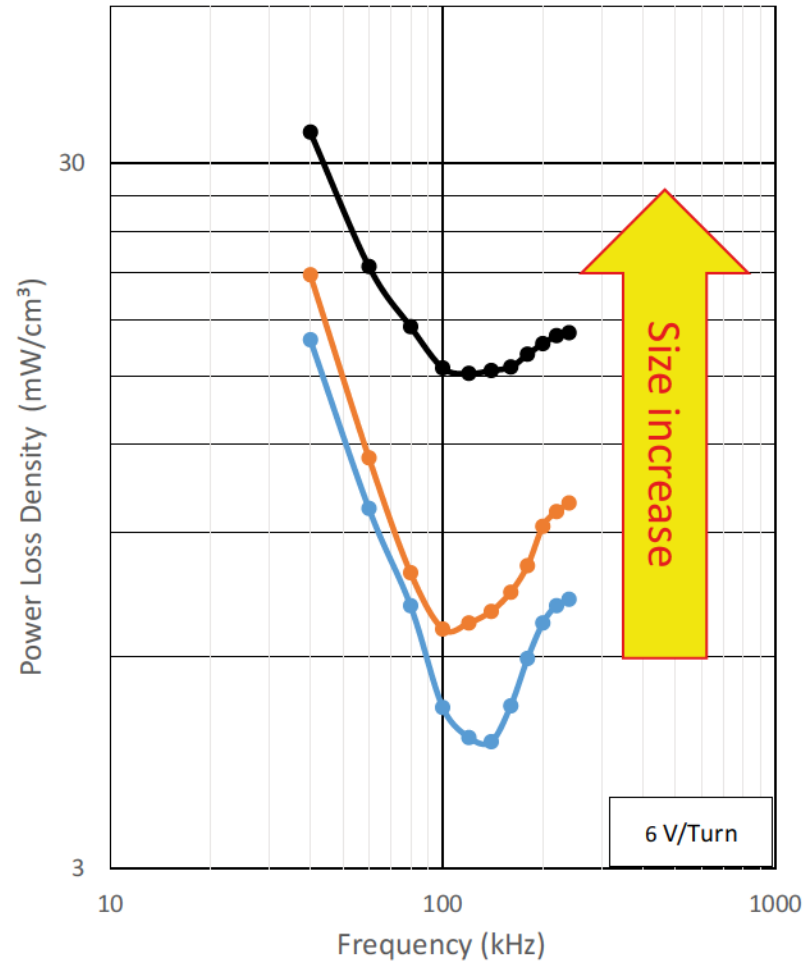


Power loss density comparison:

Test setup:



Herbert Graph



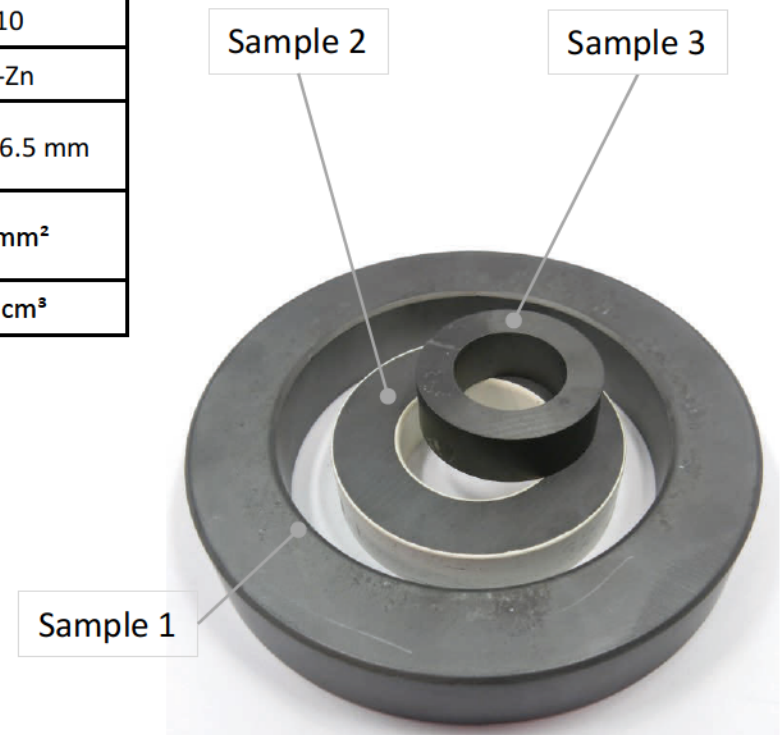
- 3C95_T152/104/24 - @20°C
- 3C95_T87/56/20 - @20°C
- 3C95_T50/30/16.5 - @20°C

Performance Factor curves for 3E10 material



Core construction details:

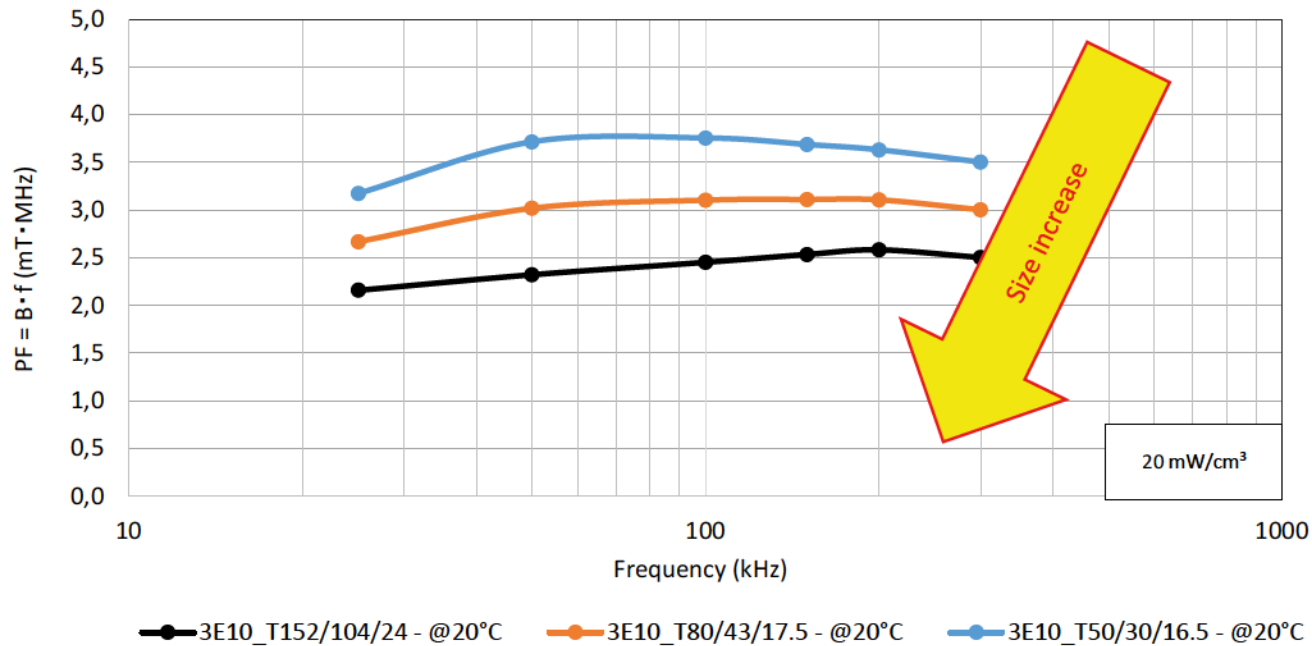
Tested samples			
	Sample 1	Sample 2	Sample 3
Material name	3E10	3E10	3E10
Material type	Mn-Zn	Mn-Zn	Mn-Zn
Dimensions OD x ID x H	152x104x24 mm	80x43x17.5 mm	50x30x16.5 mm
Core total cross section	571 mm ²	318 mm ²	160 mm ²
Core volume	226 cm ³	59.9 cm ³	19.3 cm ³



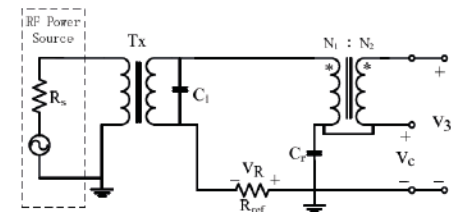
Performance Factor curves for 3E10 material



Core performance factor comparison:



Test setup:

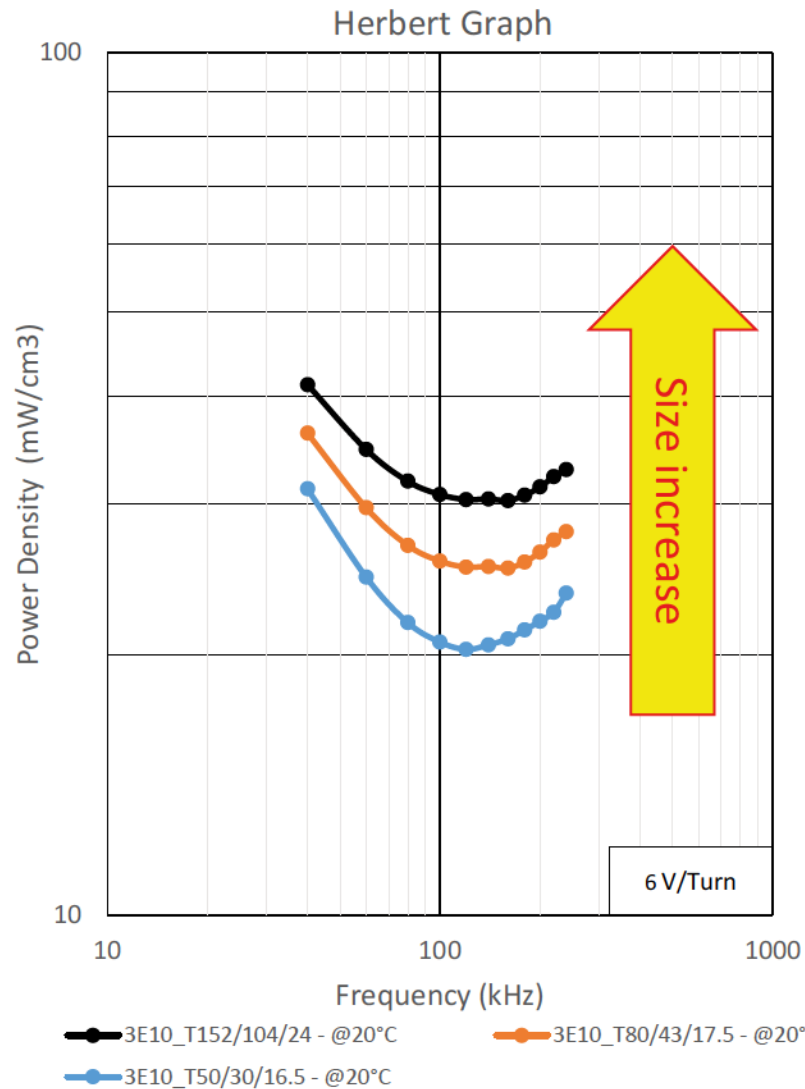
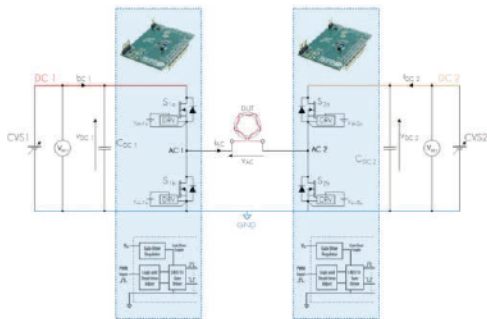


Performance Factor curves for 3E10 material



Power loss density comparison :

Test setup:

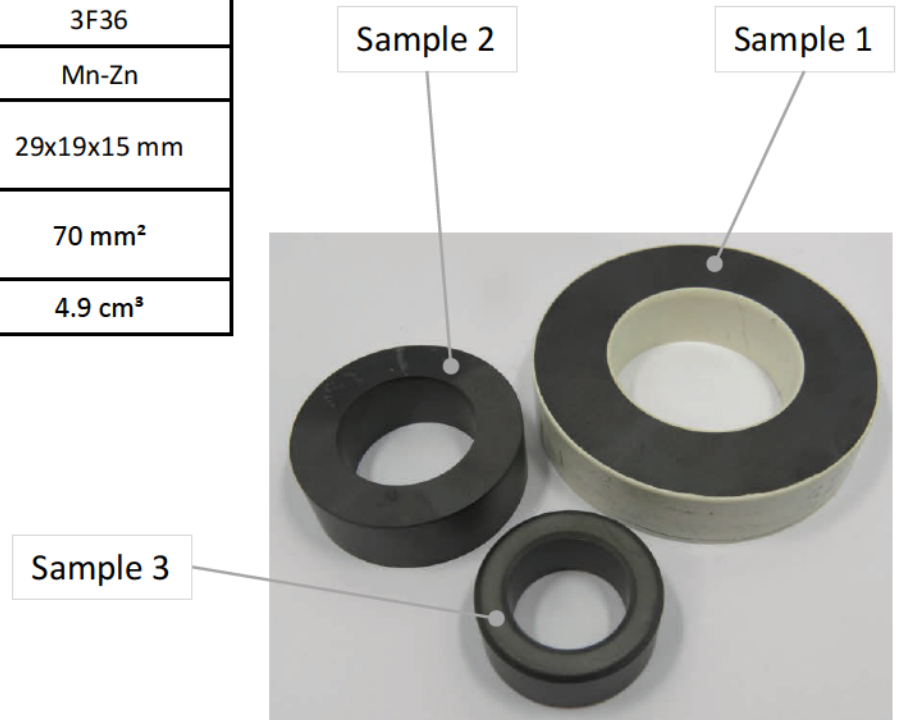


Performance Factor curves for 3F36 material



Core construction details:

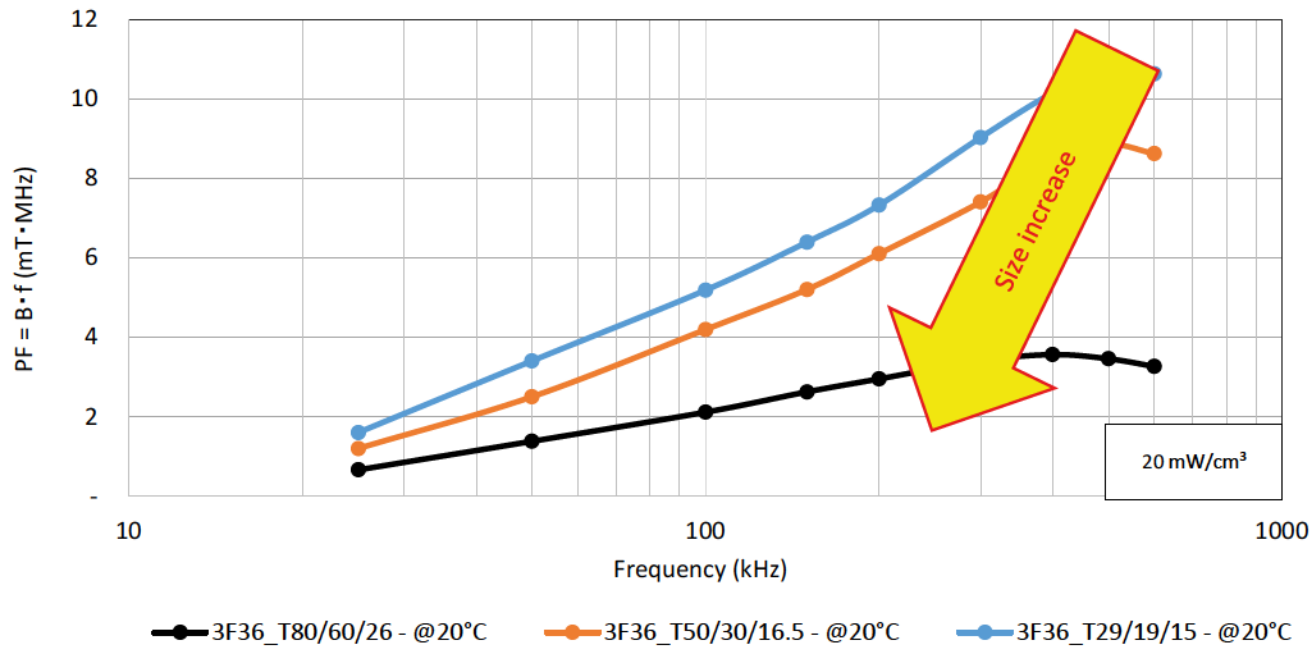
Tested samples			
	Sample 1	Sample 2	Sample 3
Material name	3F36	3F36	3F36
Material type	Mn-Zn	Mn-Zn	Mn-Zn
Dimensions OD x ID x H	80x60x26 mm	50x30x16.5 mm	29x19x15 mm
Core total cross section	255 mm ²	160 mm ²	70 mm ²
Core volume	54.8 cm ³	19.6 cm ³	4.9 cm ³



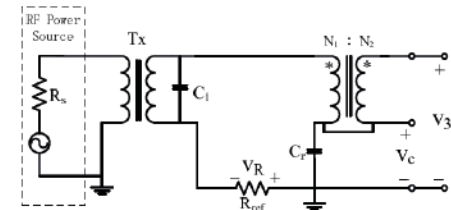
Performance Factor curves for 3F36 material



Core performance factor comparison:



Test setup:



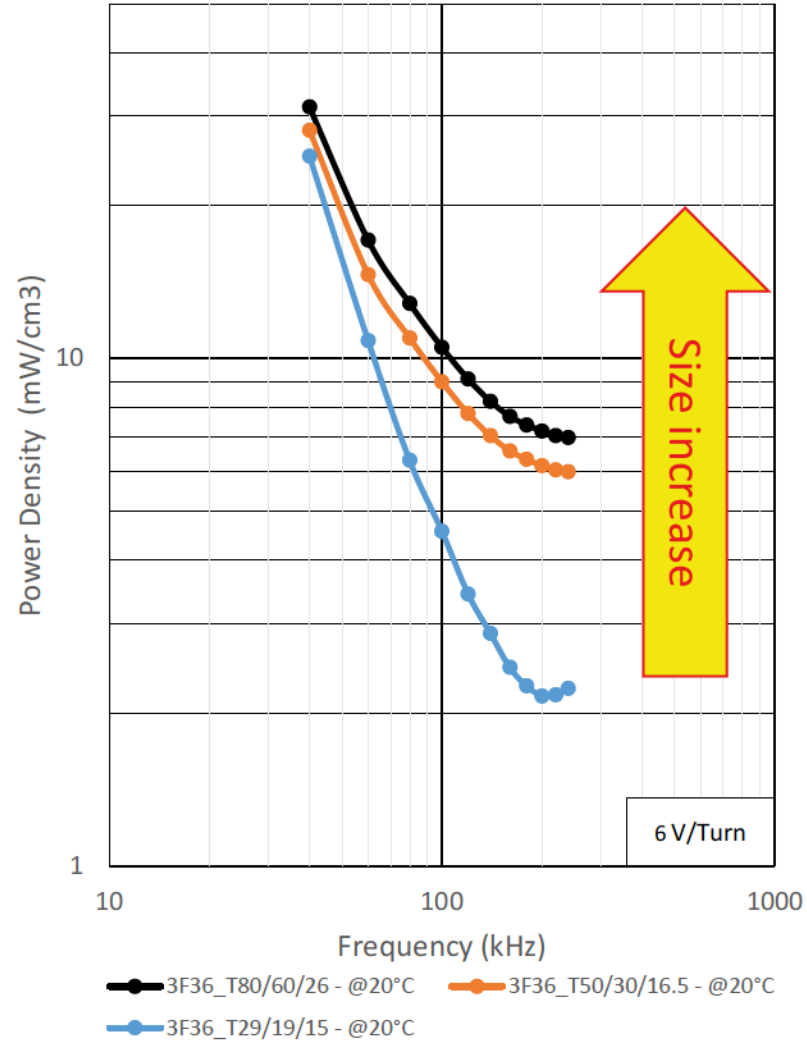
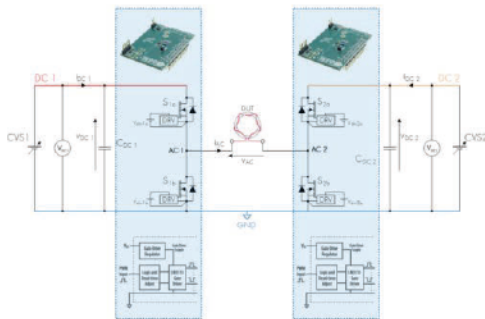
Performance Factor curves for 3F36 material



Herbert Graph

Power loss density comparison :

Test setup:



Conclusion



1. Optimum operating frequency decreases as core size increases
2. Core shape and size has significant influence on the core parameters. Core overall size optimization is as important as material selection
3. Presented core parameters analysis indicates importance of consideration of core size for application

ENERGY
THAT
CHANGES



SECTION III – CORE SHAPE EFFECT ON POWER LOSS

Marcin Kącki, dr. Marek S. Ryłko, Edward Herbert

Sponsored by

The Power Sources Manufacturers Association

e-mail: power@psma.com, <http://www.psm.com/>

P.O. Box 418, Mendham, NJ 07945-0418

Ferrite magnetic materials are subject to high frequency effects such as eddy-currents and dimensional resonance which result in non-uniform frequency-dependent magnetic flux distributions. The magnetic flux distribution is determined by the core shape; and thus, magnetic losses are core shape dependent. Therefore this section of the project investigates how core shape influence magnetic material performance

Project development:

1. Core samples preparation for the tests
2. Measure power loss with sinusoidal excitation
3. Measure power loss with rectangular excitation
4. Measure impedance characteristics

Content



1

Laminated ferrite ring cores

2

Laminated ferrite E-shape cores

3

Hollowed ferrite ring cores

4

String of beads

5

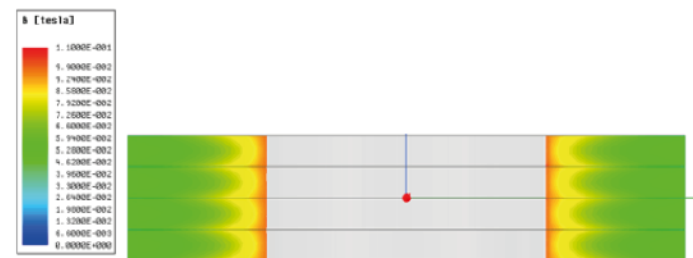
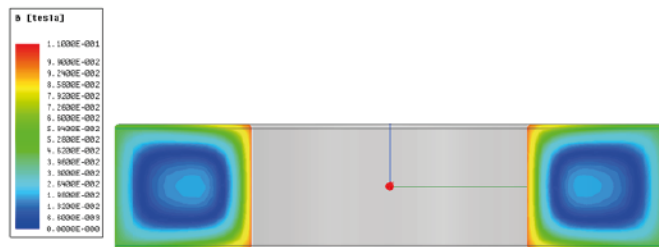
Conclusion and future work

Laminated ferrite ring core



Traditional laminated iron cores are designed and used in high power magnetics in the frequency range of 50 Hz to several kilohertz. Laminations limit the eddy current that are induced in conductive core material. Ferrite appears as a bulk highly resistive material that by intuition shall not be prone to eddy currents. However, the ferrite core high impedance is a result of the material structure that is built of small, electrically conductive, iron-oxide particles isolated by the filler. At high frequency, the ferrite core becomes dominated by capacitive effects that allows for the capacitive current to flow. The laminar structure sections the conduction path which reduce high-frequency effects.

FEA results of flux distribution in solid and laminar core at 500 kHz:



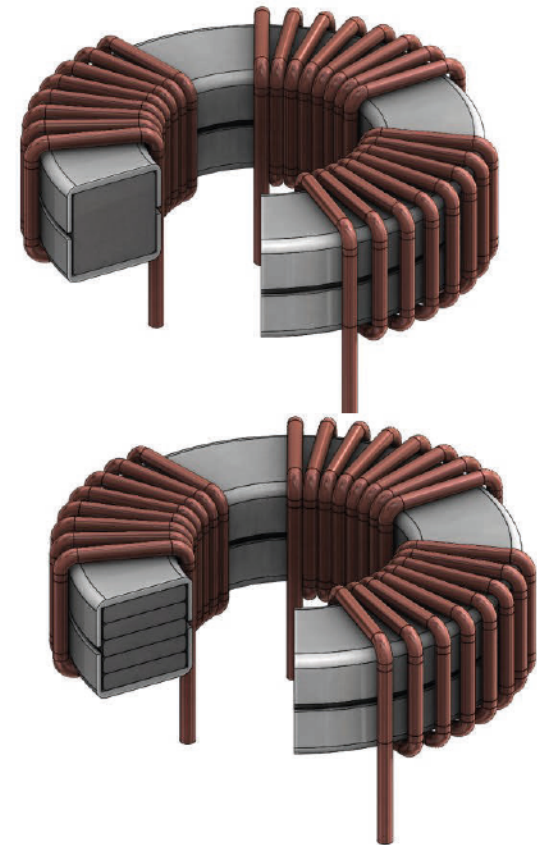
Laminated ferrite ring core



Inductor construction details:

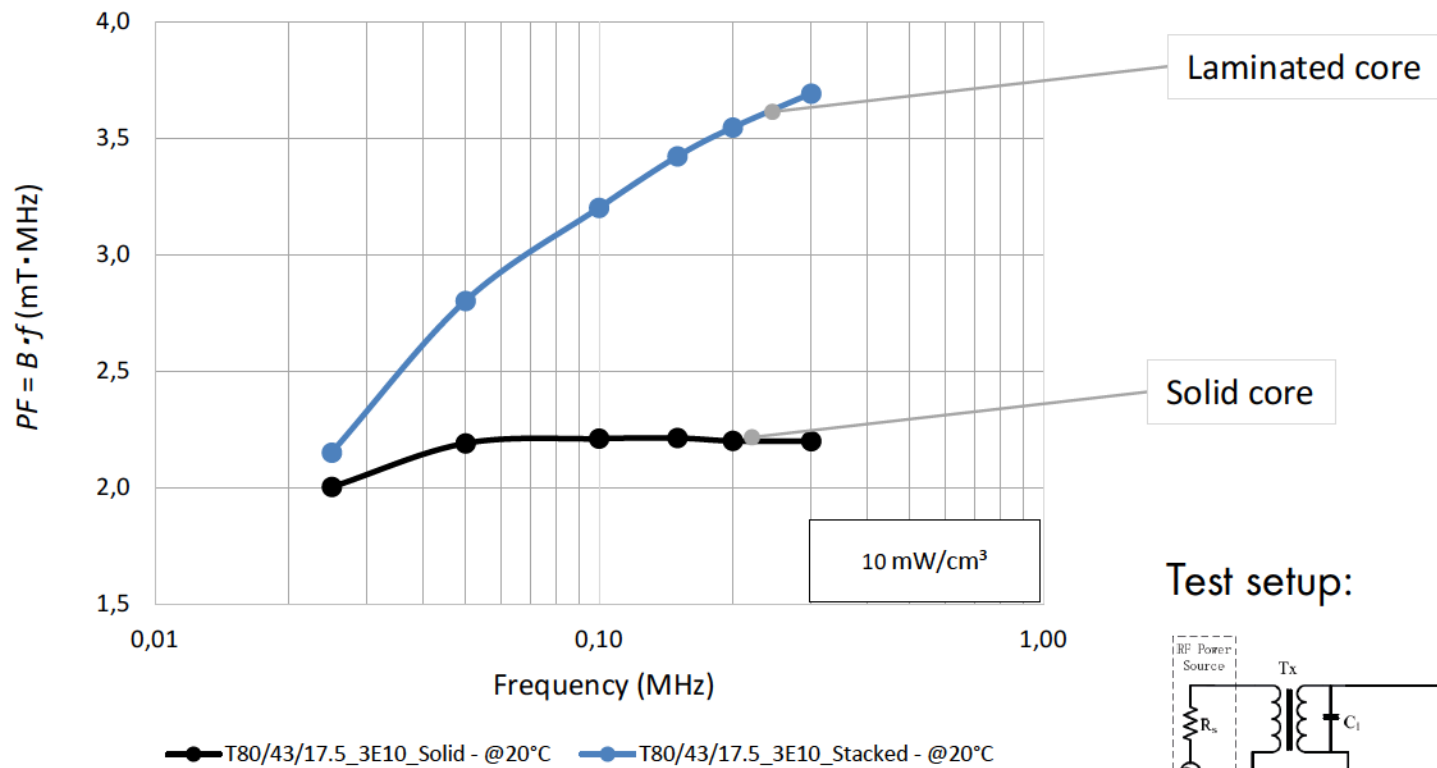
Parameter	Unit	Solid	Laminated
Material name	-	3E10	3E10
Material type		Mn-Zn	Mn-Zn
Dimensions OD x ID x H	mm	80 x 45 x 17.5 solid	80 x 45 x 3.5 5 laminations
Core total cross section	mm ²	324	324
Core volume	cm ³	62.55	62.55
Number of turns		8/phase	8/phase

Designed and built inductors:

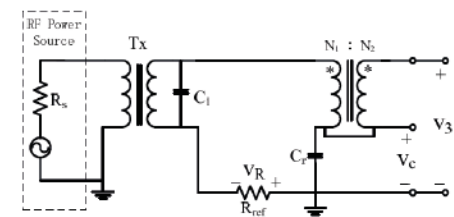


Laminated ferrite ring core

Core performance under sinusoidal excitation:

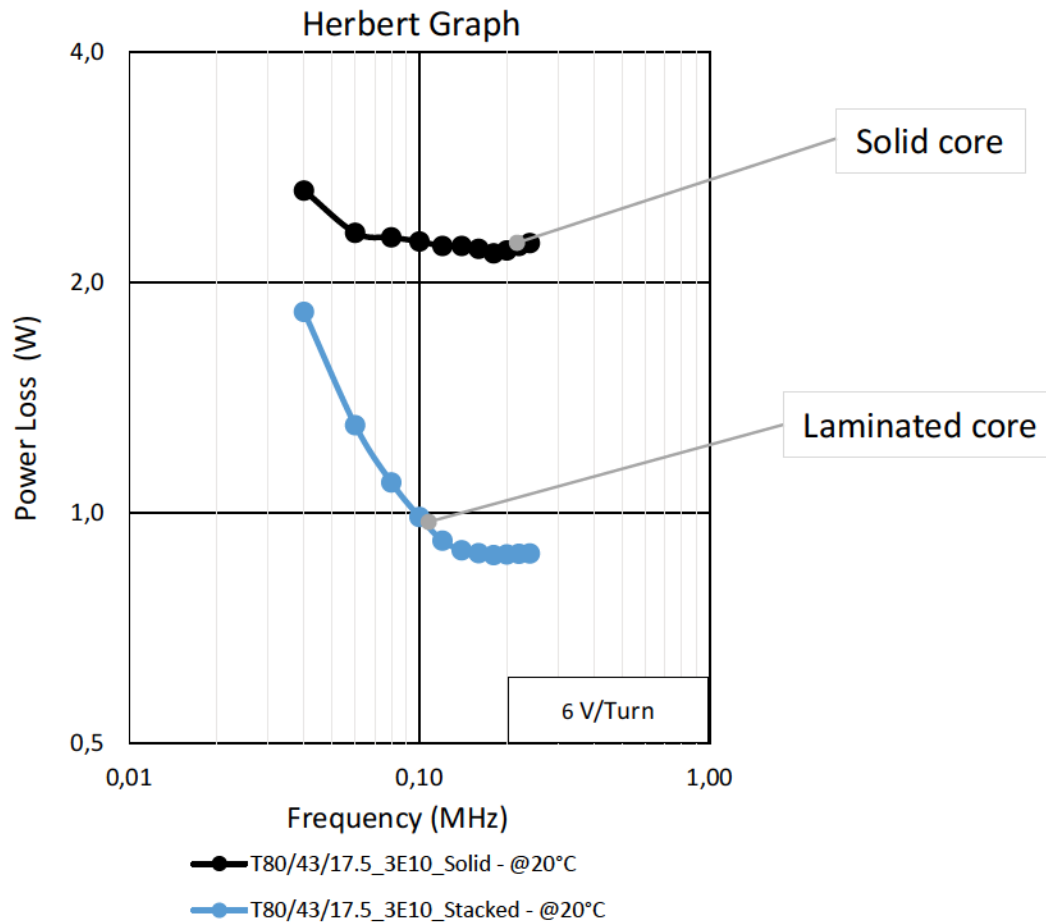


Test setup:

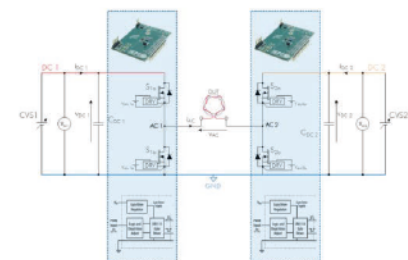


Laminated ferrite ring core

Power losses with rectangular excitation:



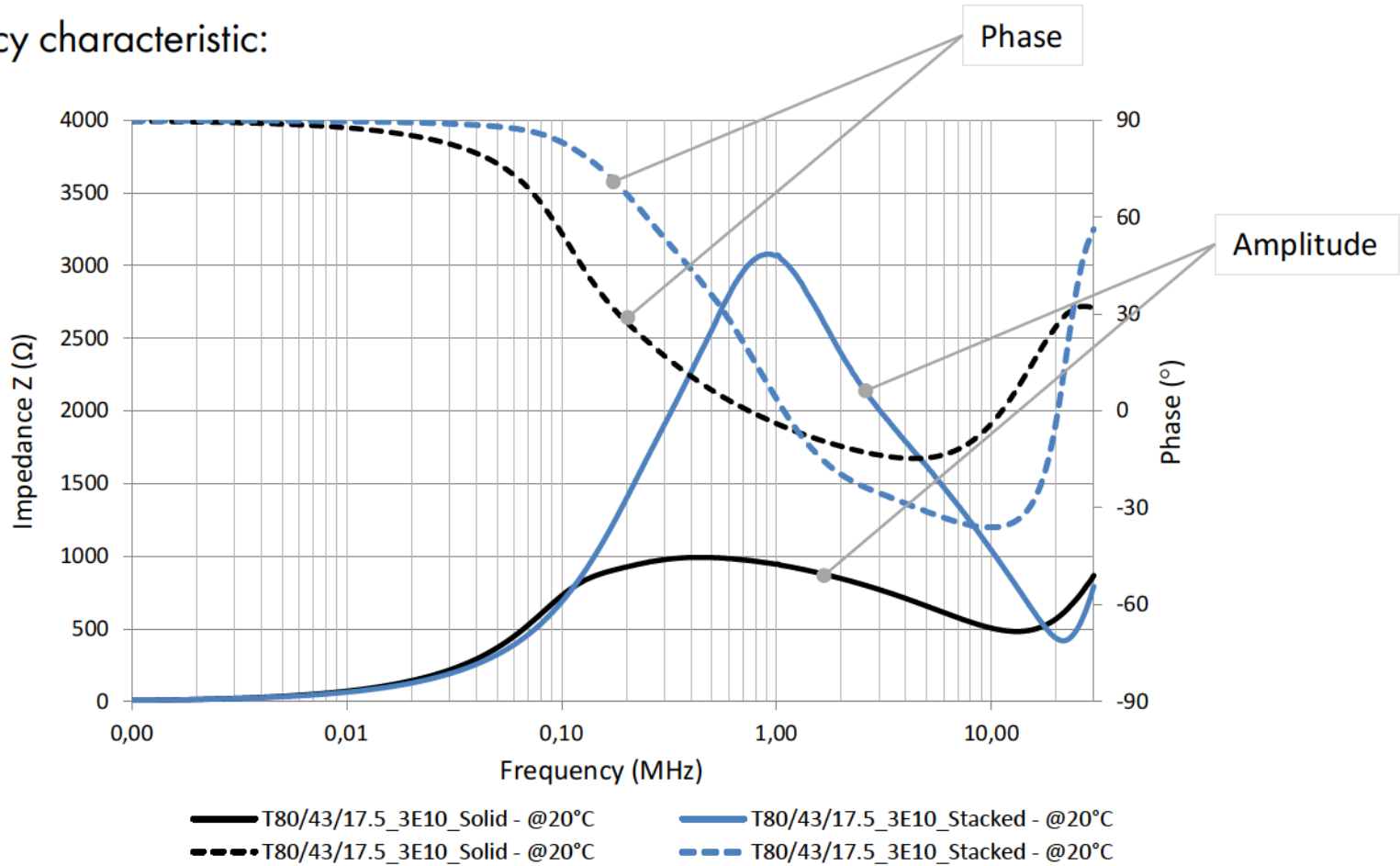
Test setup:



Laminated ferrite ring core



Frequency characteristic:

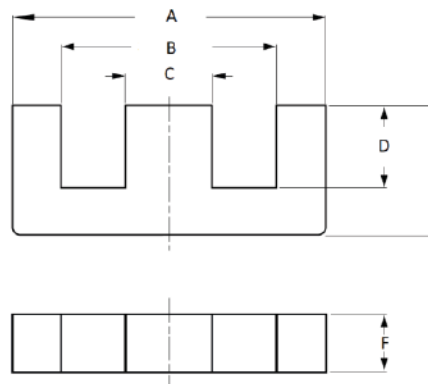


Laminated ferrite E-shape cores

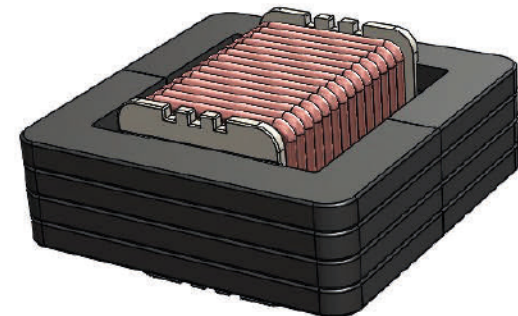
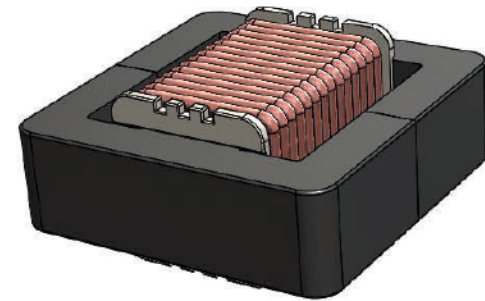


Core construction details:

Parameter	Unit	Solid	Laminated
Material name	-	3C95	3C95
Material type		Mn-Zn	Mn-Zn
Dimensions A	mm	65	65
Dimensions B	mm	45	45
Dimensions C	mm	20	20
Dimensions D	mm	12	12
Dimensions E	mm	22	22
Dimensions F	mm	20	5 4 laminations



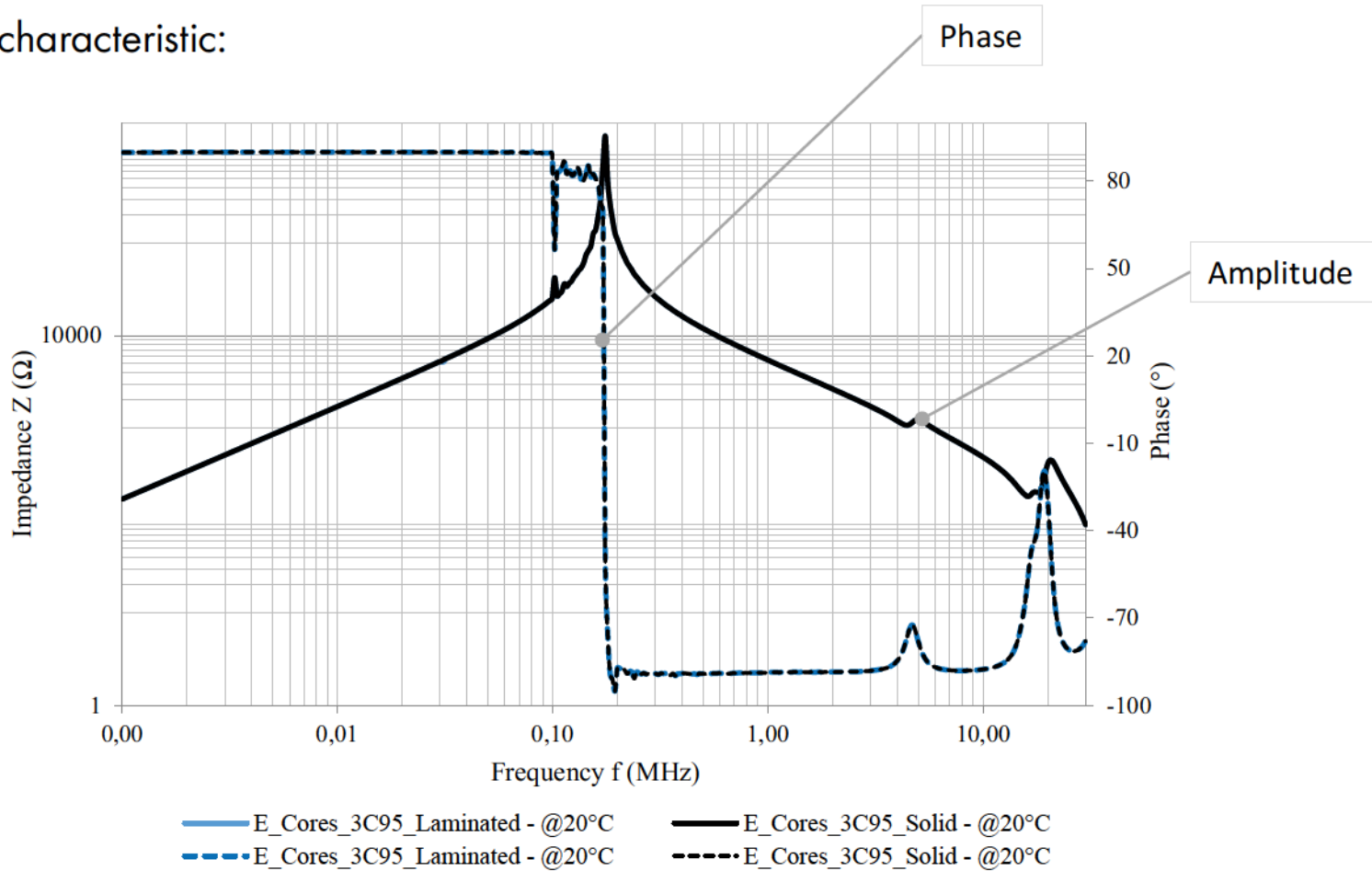
Designed and built inductors:



Laminated ferrite E-shape cores



Frequency characteristic:

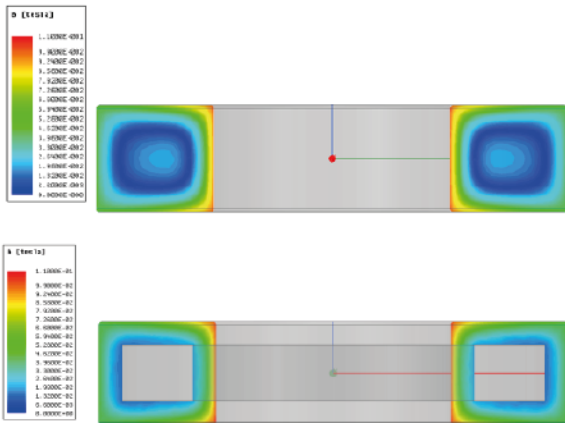
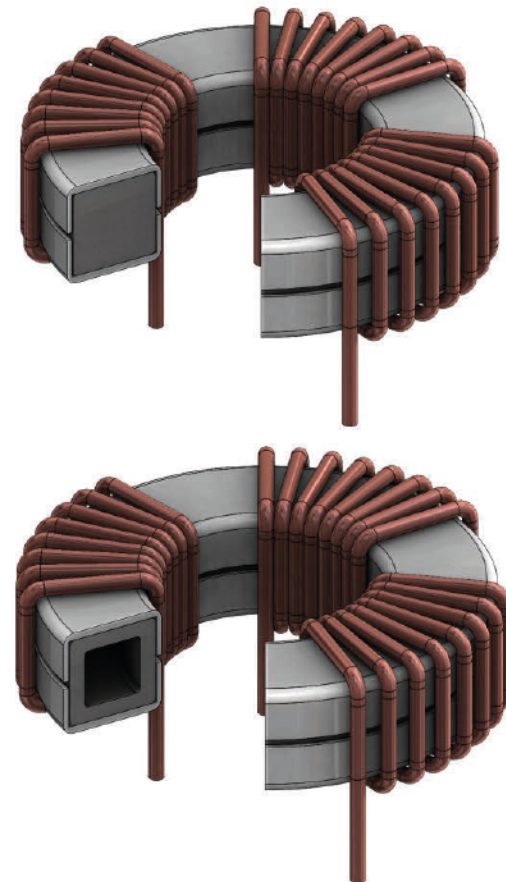


Hollowed ferrite ring core

Inductor construction details:

Parameter	Unit	Solid	Hollowed
Material name	-	3E12	3E12
Material type		Mn-Zn	Mn-Zn
Dimensions OD x ID x H	mm	86 x 60 x 13.5	86 x 60 x 28
Core total cross section	mm ²	177	177
Core volume	cm ³	40.50	40.50

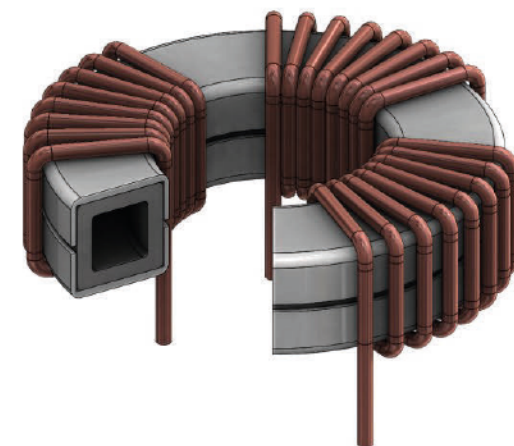
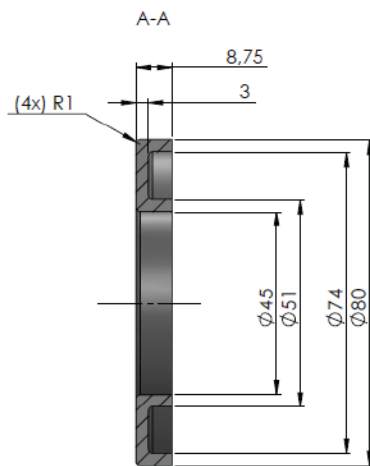
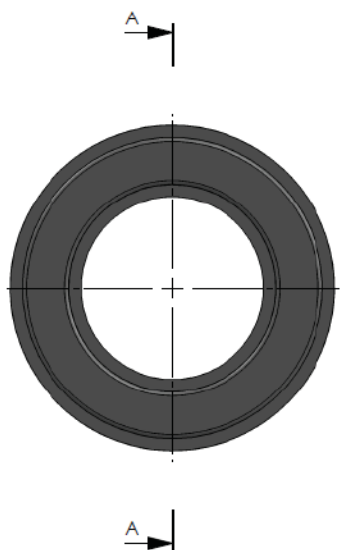
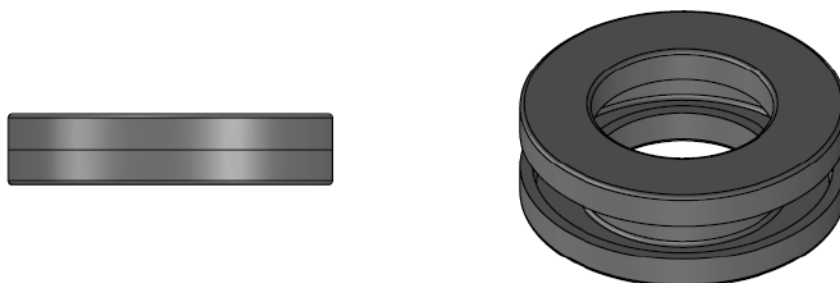
Designed and built inductors:



Hollowed ferrite ring core

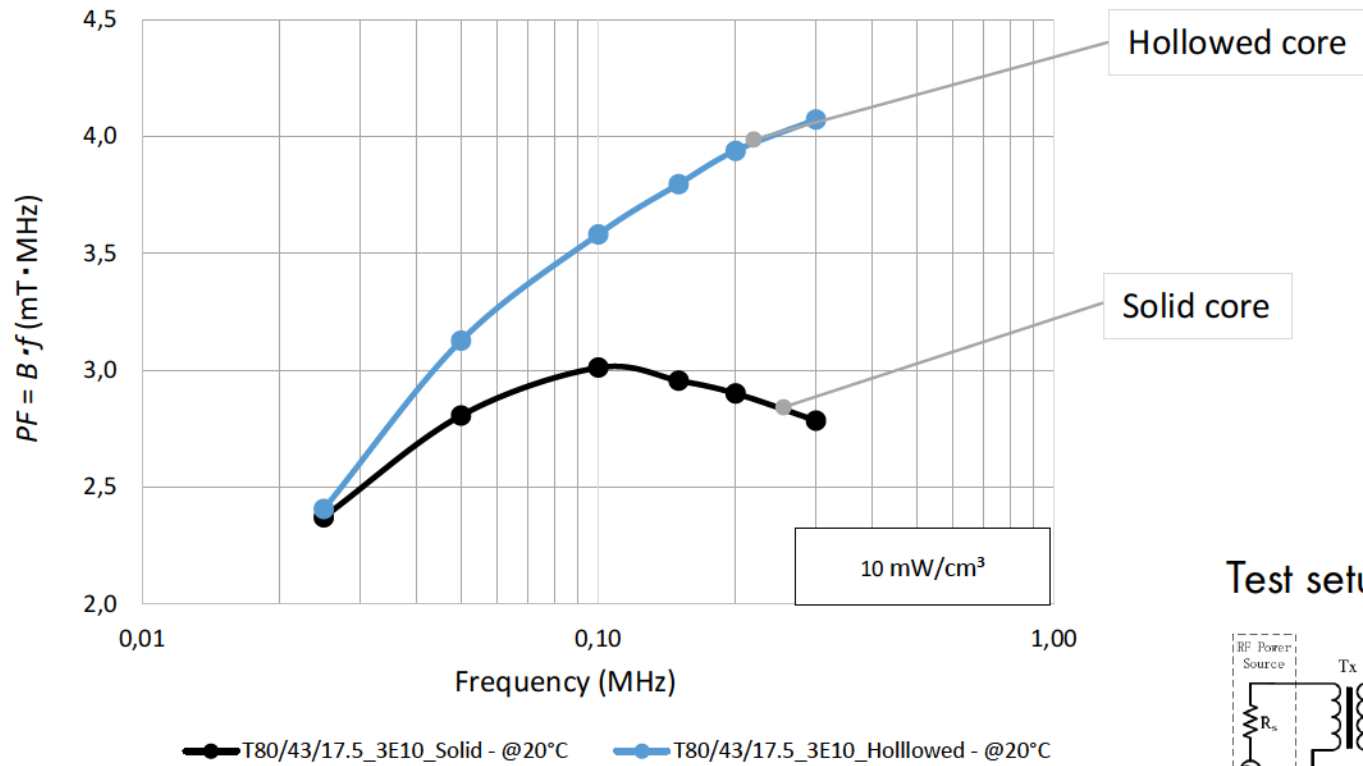


Core construction details:

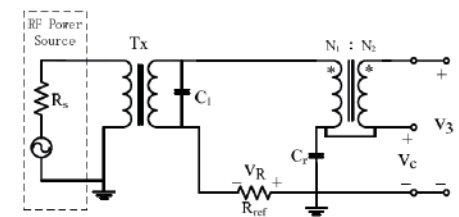


Hollowed ferrite ring core

Core performance under sinusoidal excitation:

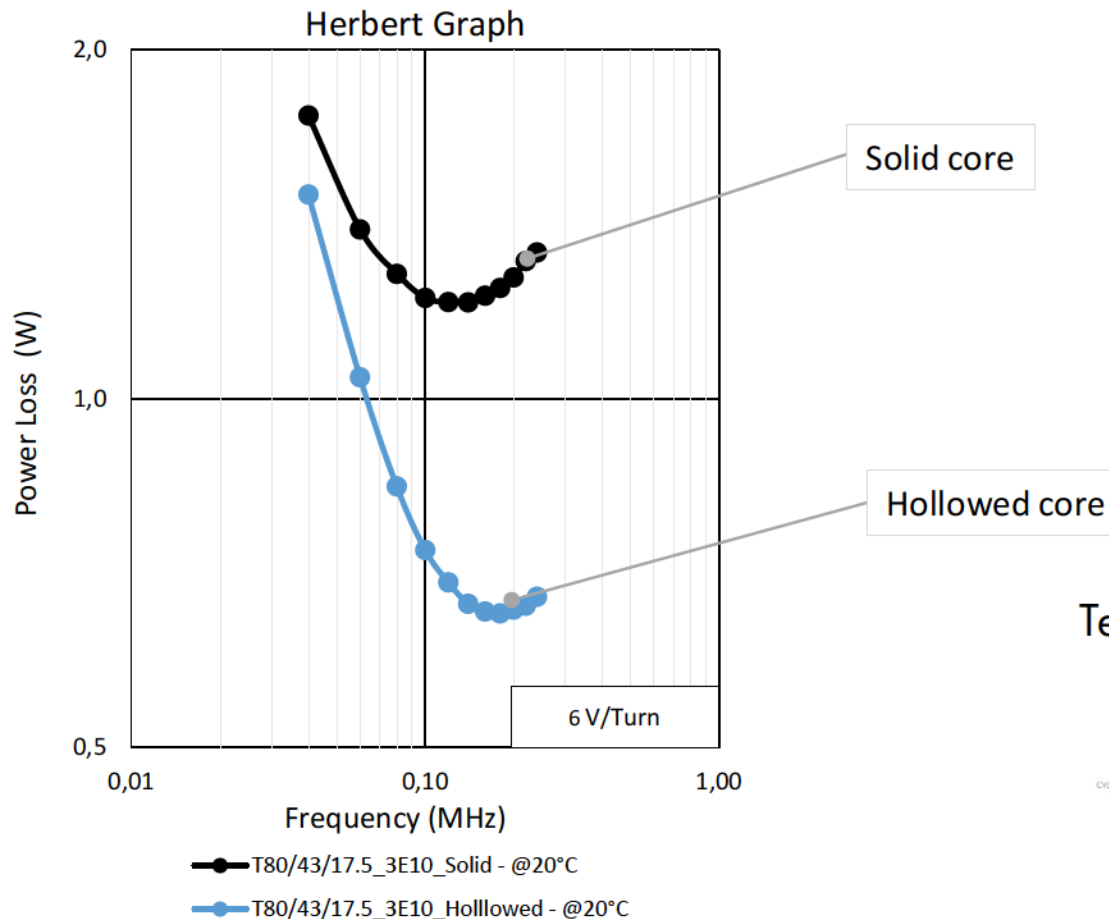


Test setup:

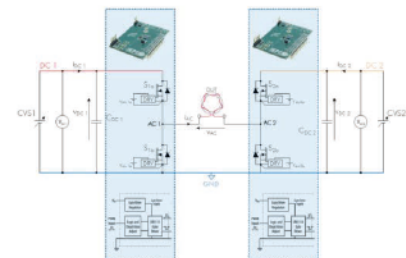


Hollowed ferrite ring core

Power losses with rectangular excitation:



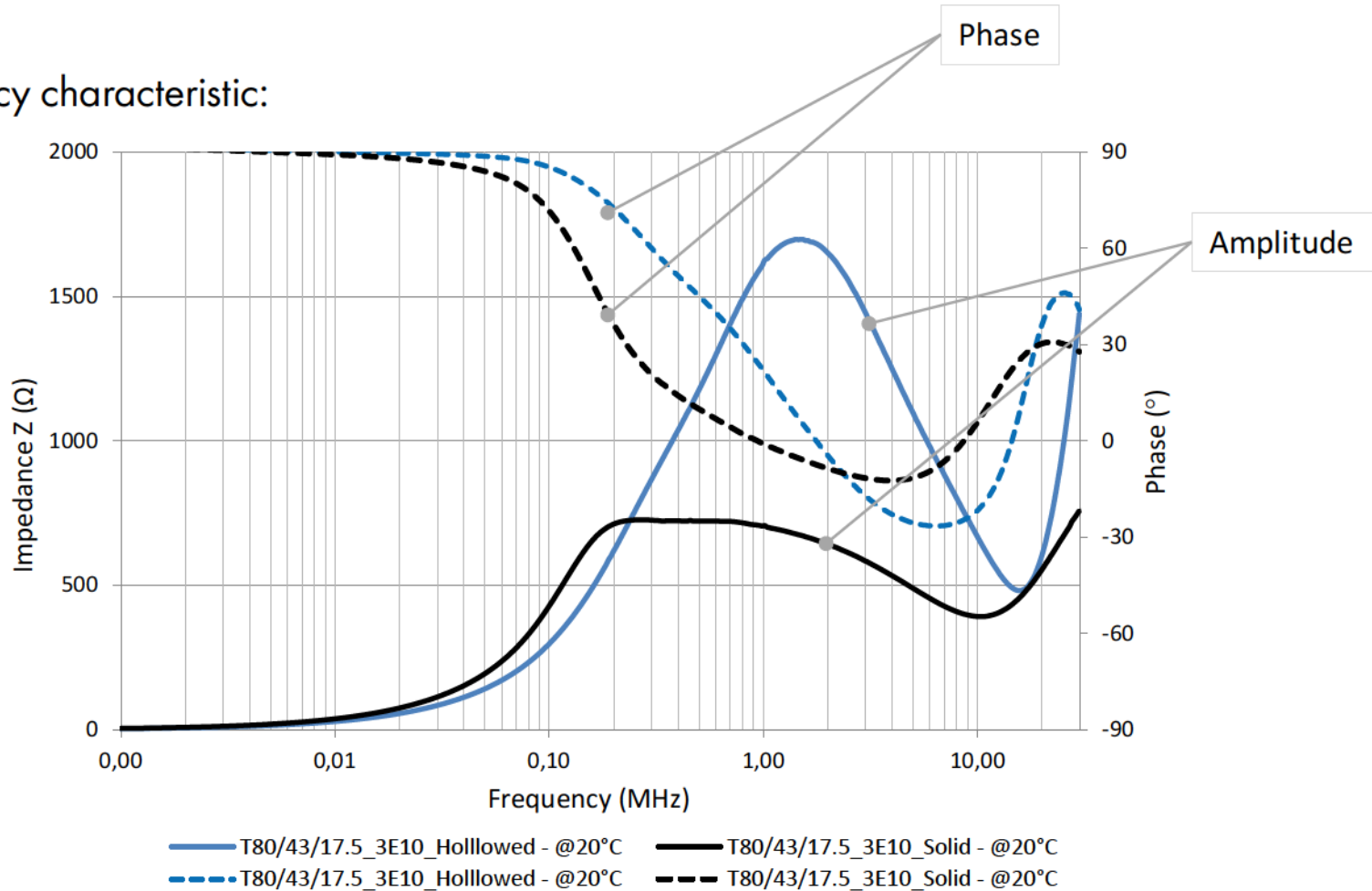
Test setup:



Hollowed ferrite ring core



Frequency characteristic:



String of beads



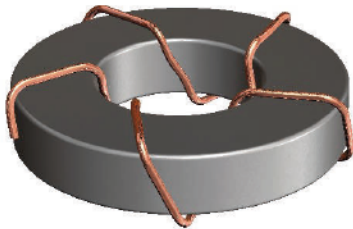
Core construction details:

Parameter	Unit	Core 1	Core 2	Core 3	Core 4
Material name	-	3E10	3E10	3E10	3E10
Material tape		Mn-Zn	Mn-Zn	Mn-Zn	Mn-Zn
Dimensions OD x ID x H	mm	80 x 40 x 15	(60 x 40 x 15) x 2	(50 x 40 x 15) x 4	(14 x 9 x 9) x 64
Core total cross section	mm ²	300	300	300	1472
Core total volume	cm ³	56.55	47.12	42.41	51.58
Turns number	-	5	5	5	1

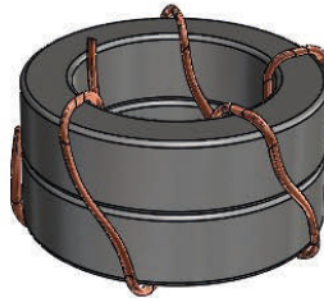
String of beads



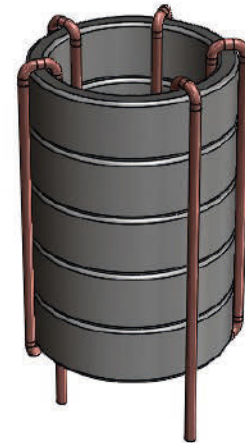
Core setup



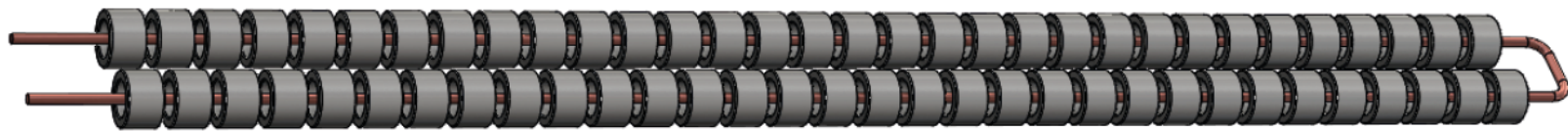
Core 1



Core 2



Core 3

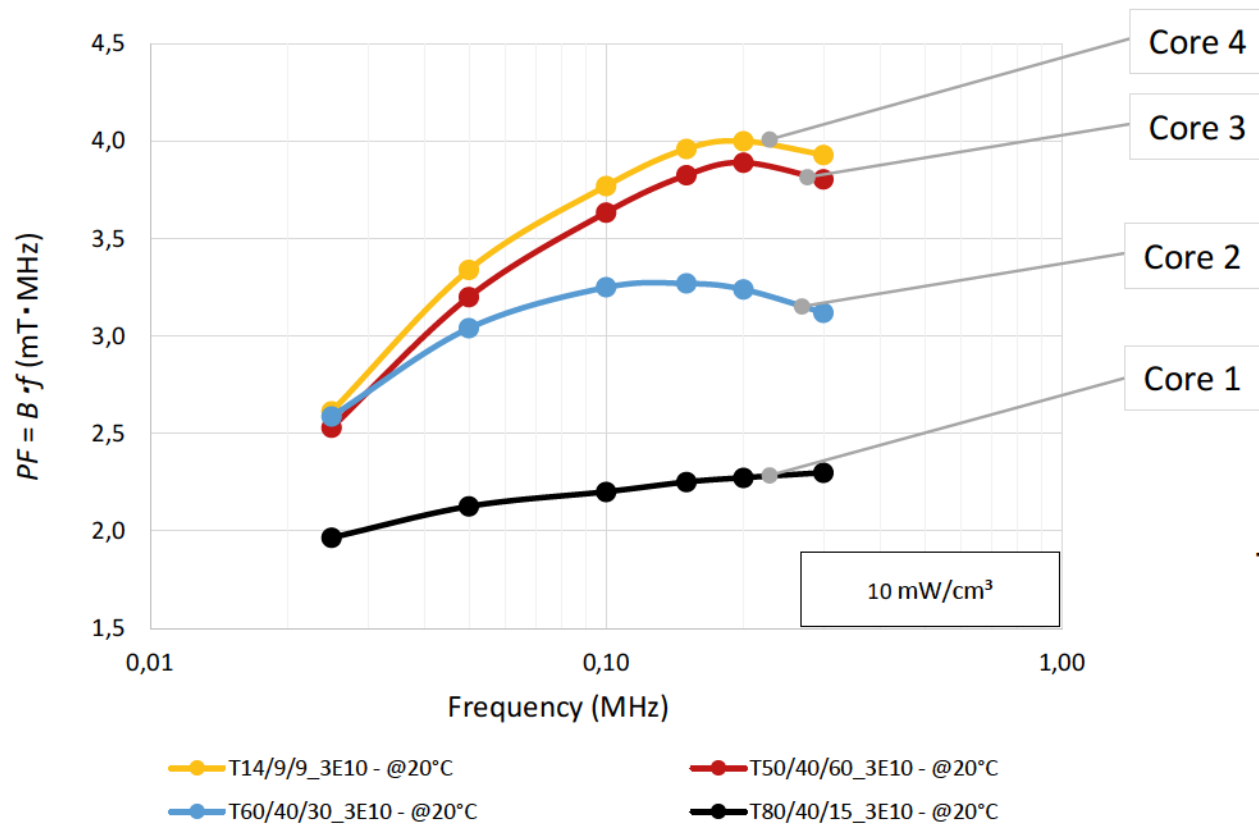


Core 4

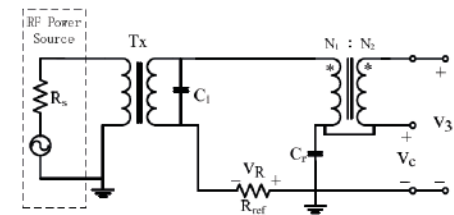
String of beads



Core performance under sinusoidal excitation:

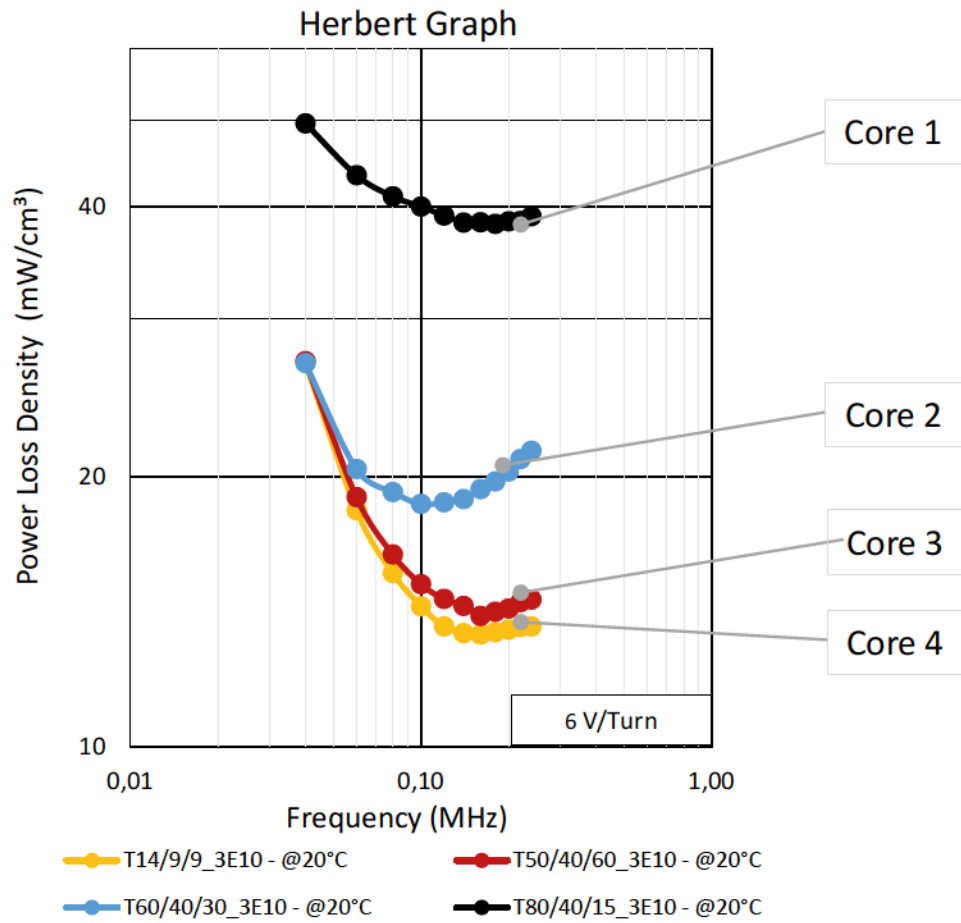


Test setup:

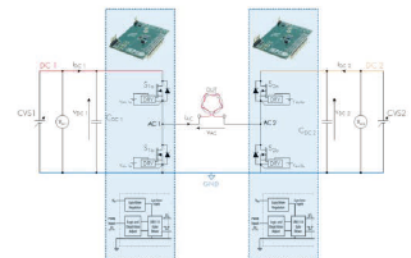


String of beads

Power losses with rectangular excitation:



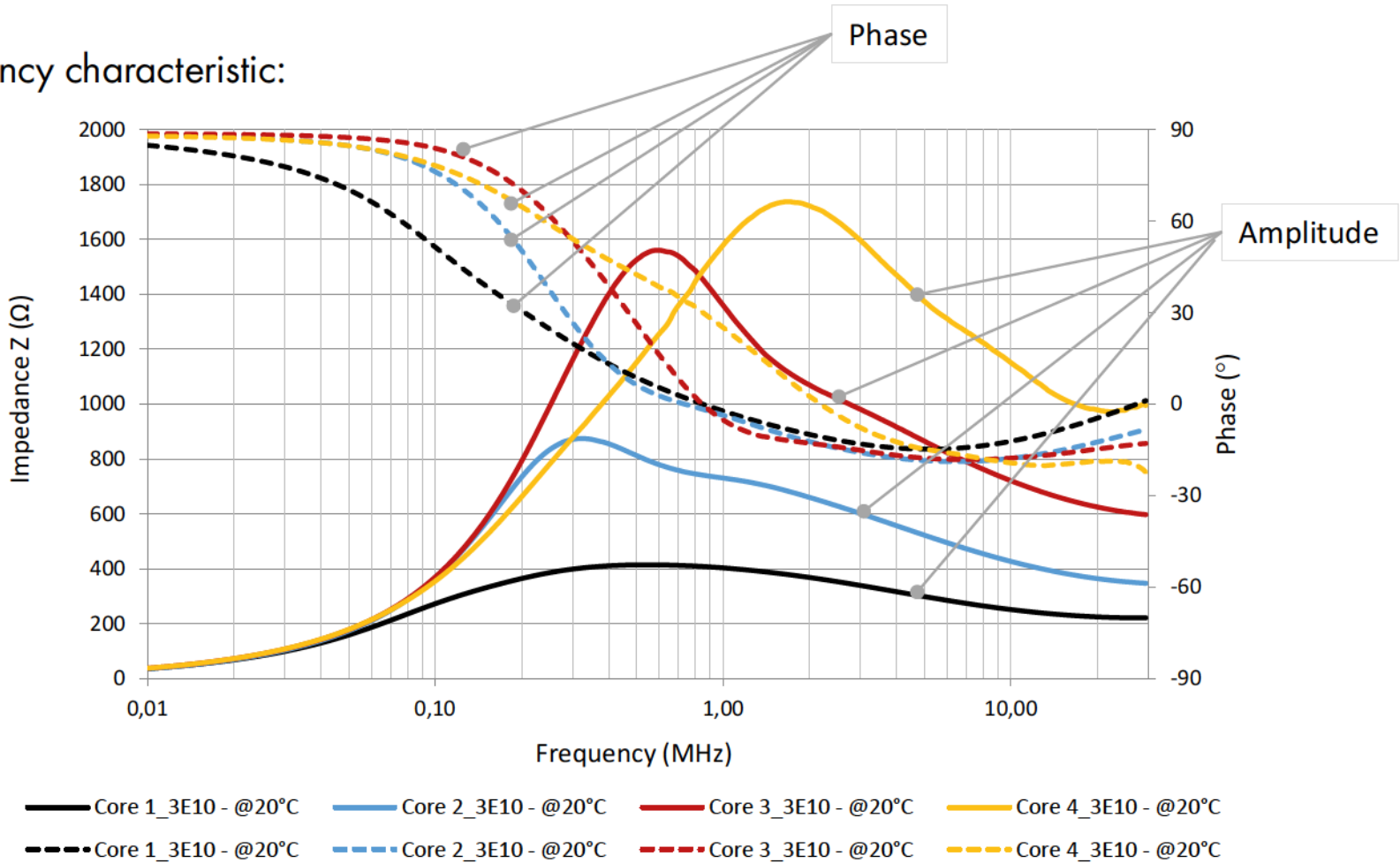
Test setup:



String of beads



Frequency characteristic:



Conclusion and future work



1. Laminar ferrite structure shows significant improvement of the impedance characteristic while maintaining the same core size and mitigate parameters deterioration of the large size bulk cores. The laminar structure reduces high-frequency effects.
2. Hollowed core improve core performance at expense of increased size. The performance is worse than for laminated core.
3. Core shape and size has significant influence on the core parameters. Core overall size optimization is as important as material selection.

ENERGY
THAT
CHANGES



SECTION IV – FERRITES ELECTRICAL PROPERTIES

Marcin Kącki, dr. Marek S. Ryłko, Edward Herbert, Dawid Proszak

Sponsored by

The Power Sources Manufacturers Association

e-mail: power@psma.com, <http://www.psm.com/>

P.O. Box 418, Mendham, NJ 07945-0418

The state-of-the-art magnetic modelling assumes high frequency effects in ferrites as negligible where material parameters as permeability and permittivity are provided as a constant that is valid for the ferrite family range. Market available measurement fixtures to determine ferrite's electrical properties are limited to the ring cores with an external diameter up to 30 mm; and thus, effective up to 1 MHz due to sample size and associated frequency effects. The common sense perception of ferrites performance is insufficient as frequency effects become significant; therefore, the new approach to ferrite electrical properties measurements is required to determine magnetic material performance beyond 1 MHz.

Project development:

1. Custom measurement fixture design and construction
2. Sample size selection
3. Preliminary material test – proof of the operation
4. Data post-processing (ferrite electrical properties calculation)

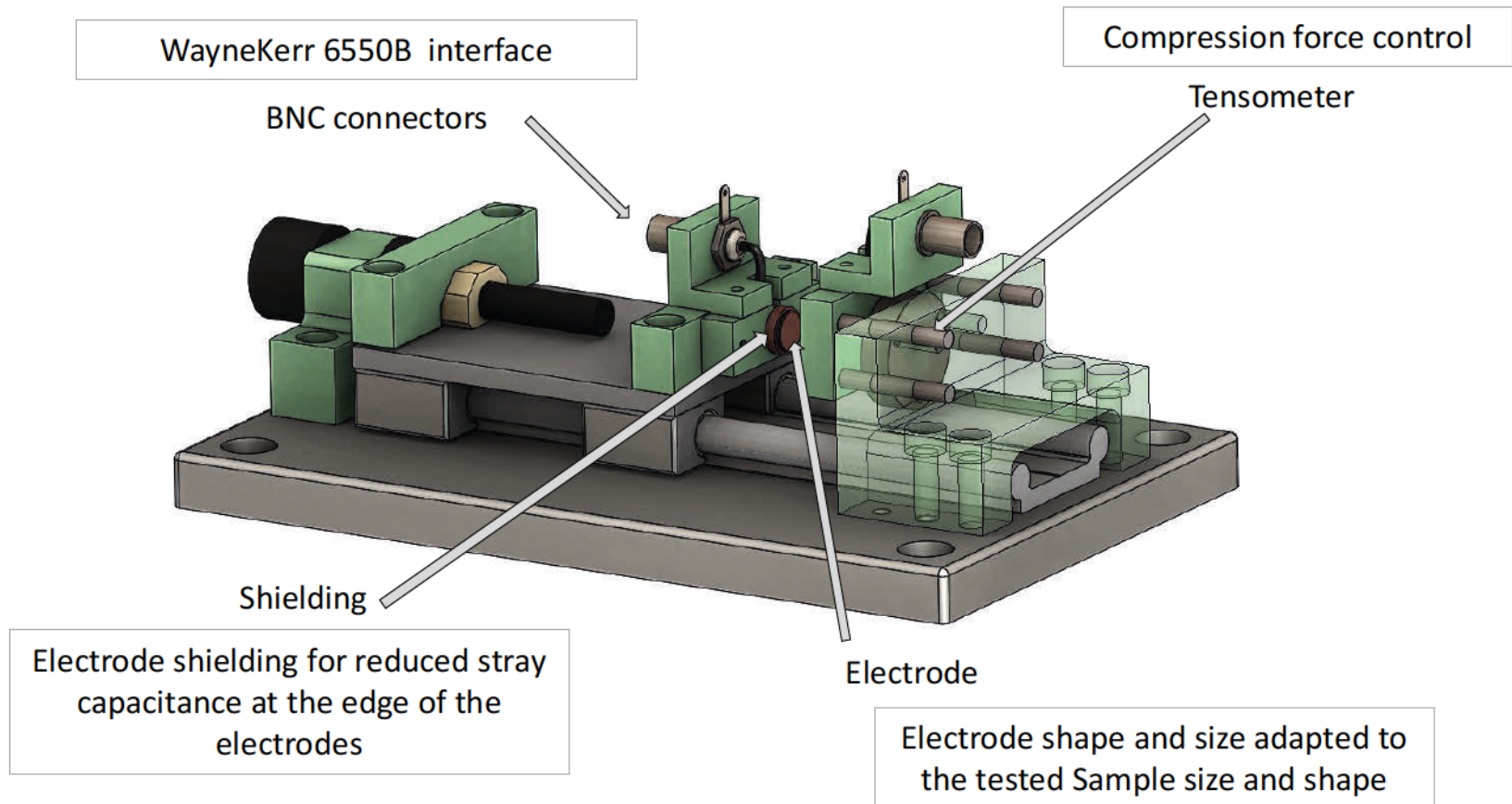
Content



1	Measurements fixture development
2	Sample size selection for material testing
3	Magnetic material electrical properties
4	Conclusion and future work
5	Appendices

Measurements fixture development

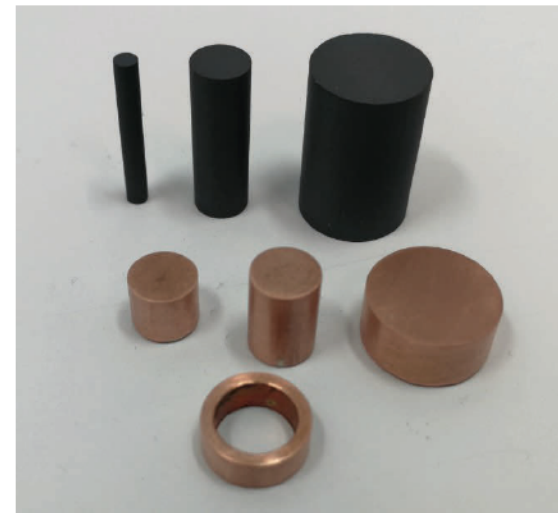
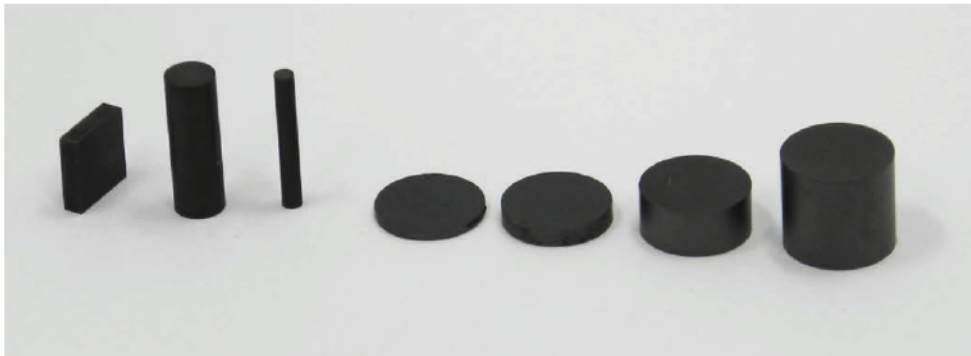
In order to define ferrite electrical characteristics for dielectric constant, ϵ and conductivity, σ dedicated test fixture was developed as below:



Measurements fixture development








The test fixture has three exchangeable sets of electrodes that can be used for measurement of custom shape samples: two electrodes for testing round cross section samples with diameter 10 and 1.8 mm and one electrode for testing rectangular cross section samples with dimensions 2.4 and 10 mm. Each electrode is shielded to minimize fringing fields' effect.



Sample size selection for material testing



The sample size selection plays an important role in magnetic material testing. The dimensions of the tested sample may become within the range of the electromagnetic wave wavelength for the frequencies of interest and developed dimensional resonance can dominate measurement.

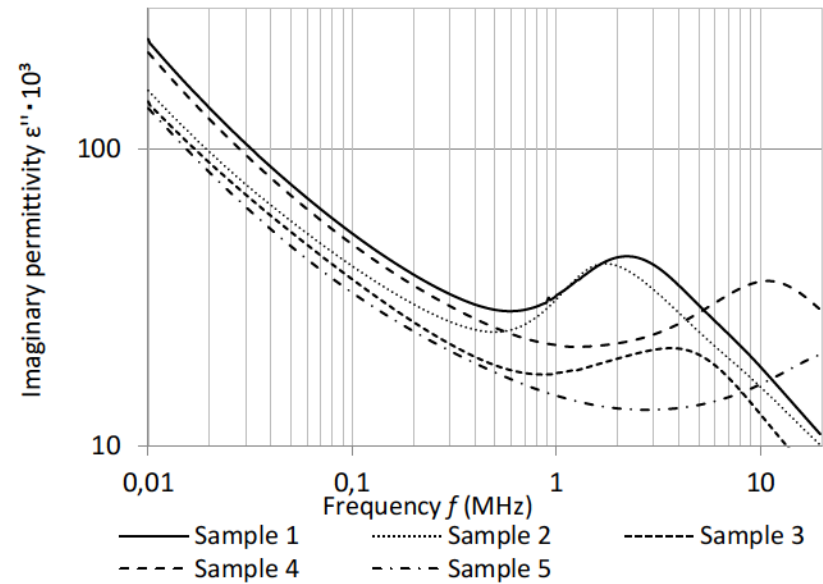
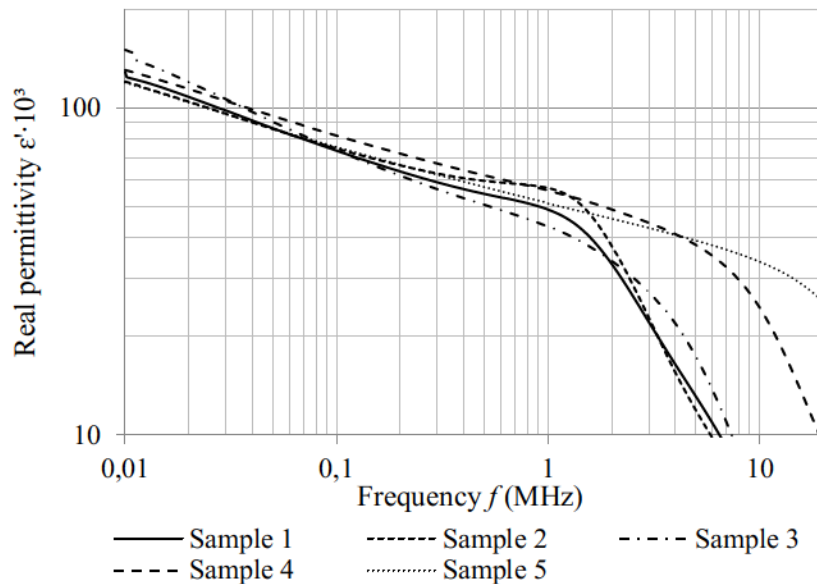
Sample No.	Sample 1	Sample 2	Sample 3	Sample 4	Sample 5
Shape					
Contact surface cross section	78.5 mm ²	78.5 mm ²	78.5 mm ²	1.5x8 mm ²	2.54 mm ²
Thickness/Height	2 mm	5 mm	10 mm	10 mm	18 mm
Material 3C90	✓	✓	✓	✓	✓
Tension	0.5 N/mm ²	0.5 N/mm ²	0.5 N/mm ²	0.5 N/mm ²	0.5 N/mm ²

Sample size selection for material testing



Measured material properties:

Measurement condition:
Tension - 0.5 N/mm²
Temperature - 20 °C






Measurement of the material properties are dominated by the dimensional resonance at certain sample size.

Sample size selection for material testing



The sample length influence on measured magnetic material properties was tested on three samples:

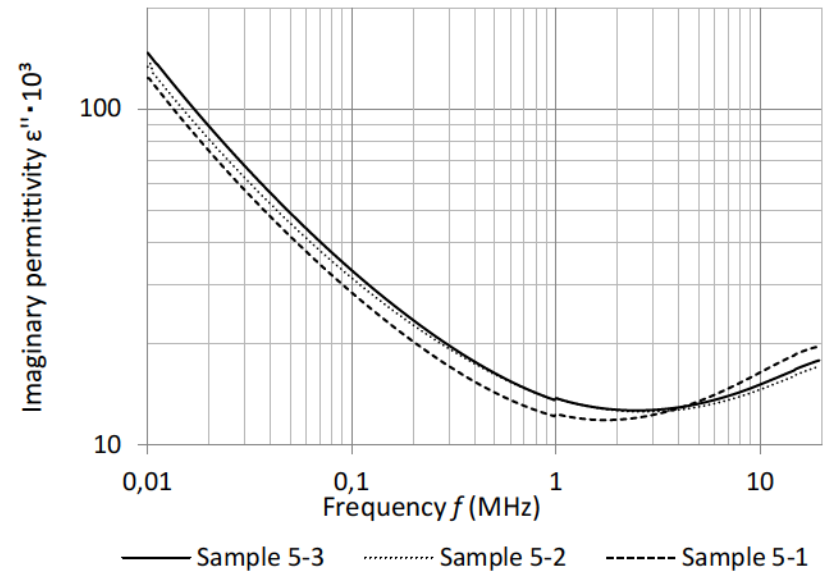
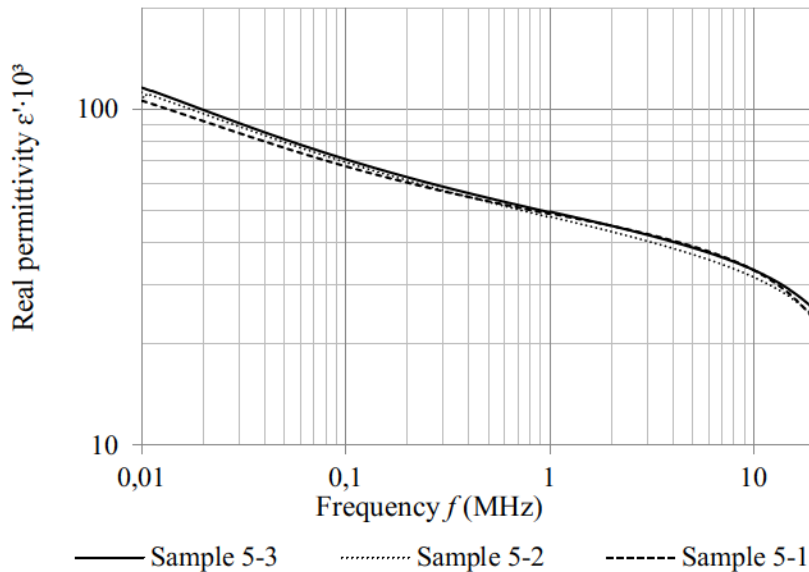
Sample No.	Sample 5-1	Sample 5-2	Sample 5-3
Shape			
Contact surface cross section	2.54 mm ²	2.54 mm ²	2.54 mm ²
Height	18 mm	10 mm	5 mm
Material 3C90	✓	✓	✓
Tension	0.5 N/mm ²	0.5 N/mm ²	0.5 N/mm ²

Sample size selection for material testing



Measured material properties:

Measurement condition:
Tension - 0.5 N/mm²
Temperature - 20 °C








Sample length has no impact on measured parameters.

Sample size selection for material testing



The proposed test fixture is equipped with strain gauges for compression force control. The force applied during measurements allows minimizing the negative impact of sample contact resistance. However, excessive force would cause significant parameter deterioration.

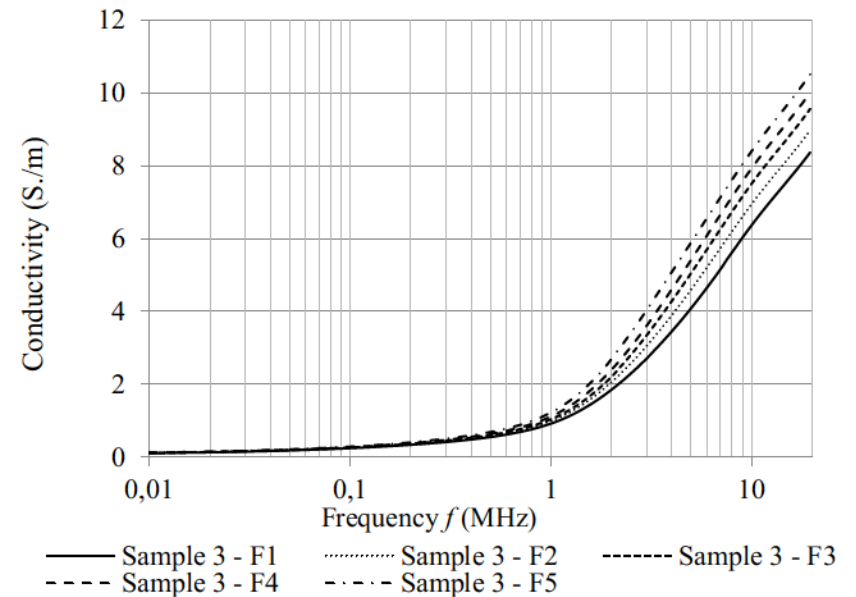
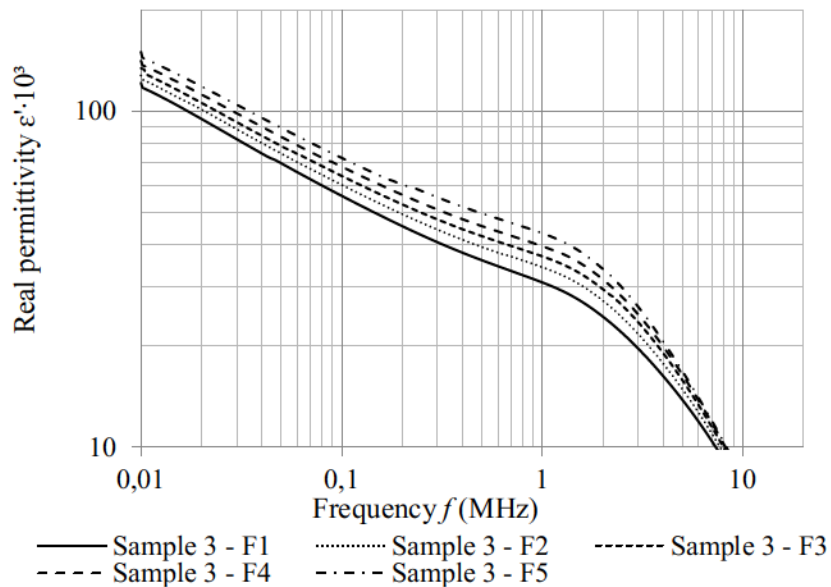
Sample No.	Sample 3 -F ₁	Sample 3 -F ₂	Sample 3 -F ₃	Sample 3 -F ₄	Sample 3 -F ₅
Shape					
Contact surface cross section	78.5 mm ²	78.5 mm ²	78.5 mm ²	78.5 mm ²	78.5 mm ²
Height	10 mm	10 mm	10 mm	10 mm	10 mm
Material 3C90	✓	✓	✓	✓	✓
Force	40 N	80 N	120 N	160 N	200 N
Tension	0.5 N/mm ²	1.0 N/mm ²	1.5 N/mm ²	2.0 N/mm ²	2.5 N/mm ²

Sample size selection for material testing



Measured material properties:






Measurement condition:
Tension - variable
Temperature - 20 °C



Sample size selection for material testing



Ferrite materials show a high temperature dependency. Temperature increase causes an increase in real. Imaginary permeability also increase together with temperature; the biggest parameters variation is observed at low frequencies.

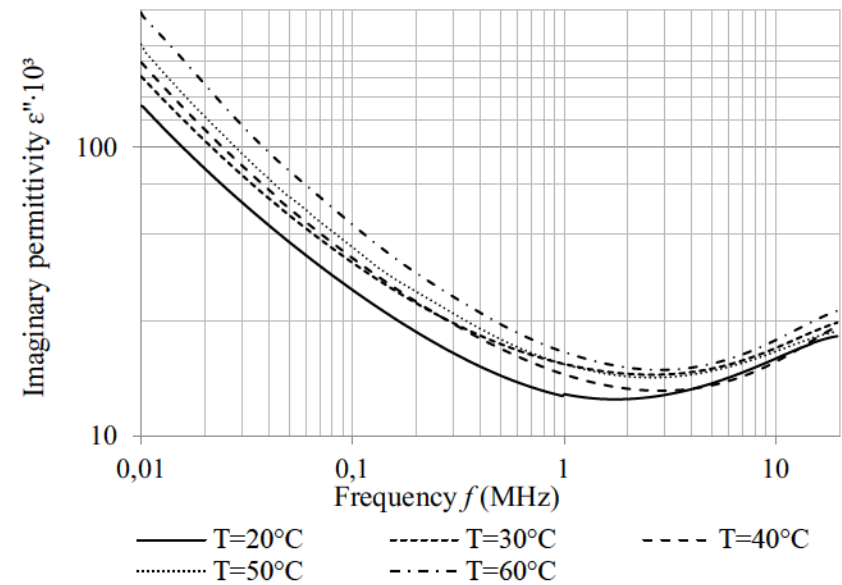
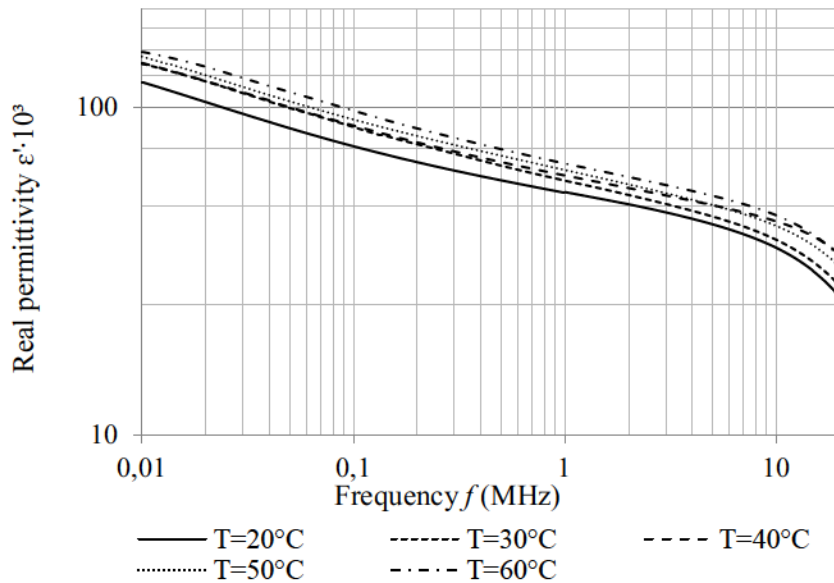
Sample No.	Sample 5 -T ₁	Sample 5-T ₂	Sample 5-T ₃	Sample 5-T ₄	Sample 5-T ₅
Shape					
Contact surface cross section	2.54 mm ²	2.54 mm ²	2.54 mm ²	2.54 mm ²	2.54 mm ²
Height	18 mm	18 mm	18 mm	18 mm	18 mm
Material 3C90	✓	✓	✓	✓	✓
Tension	0.5 N/mm ²	0.5 N/mm ²	0.5 N/mm ²	0.5 N/mm ²	0.5 N/mm ²
Temperature	20 °C	30 °C	40 °C	50 °C	60 °C

Sample size selection for material testing

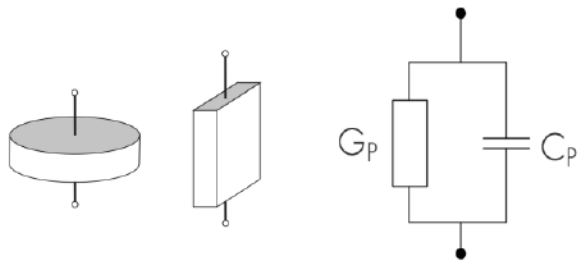


Measured material properties:

Measurement condition:
Tension - 0.5 N/mm²
Temperature - variable



The permittivity and conductivity characteristics are measured using a Wayne Kerr 6550B analyzer up to 20 MHz. The real part of the admittance determines frequency dependent conductance G_p . The imaginary permittivity is calculated based on the conductance characteristic. The imaginary part of the admittance gives the core real permittivity characteristics



Equivalent circuit for parallel representation of complex permittivity

$$Y_p = G_p + j\omega C_p, \epsilon_p = \epsilon'_p + \epsilon''_p$$

$$\epsilon'_p = \frac{C_p h}{\epsilon_0 A_c}$$

$$\epsilon''_p = \frac{G_p h}{\omega \epsilon_0 A_c} = \frac{\sigma}{\omega \epsilon_0}, \sigma = \omega \epsilon_0 \epsilon''_p$$

G_p - measured conductance

C_p - measured capacitance

ϵ_p - parallel relative complex permittivity

ϵ' - real component of the parallel relative complex permittivity

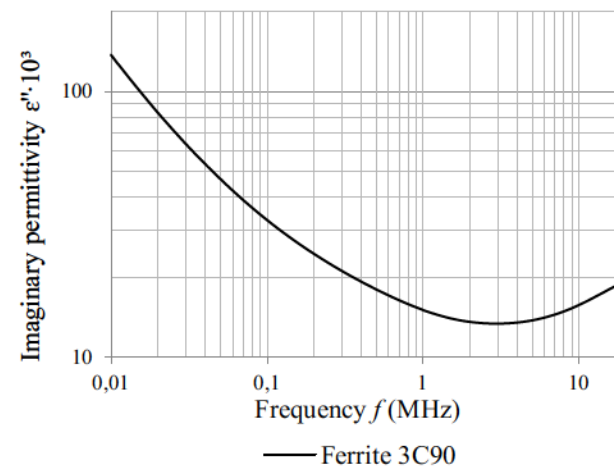
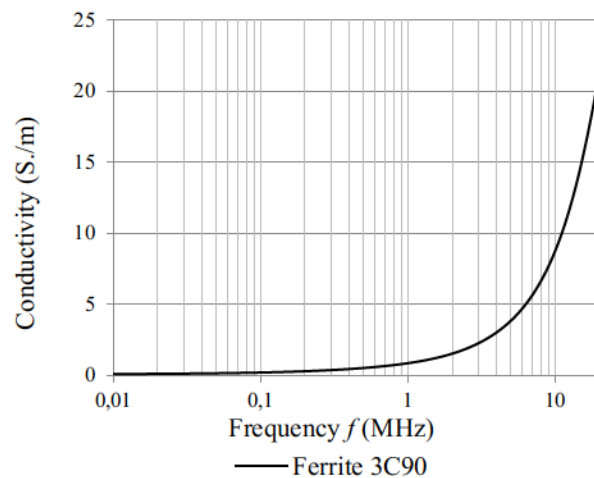
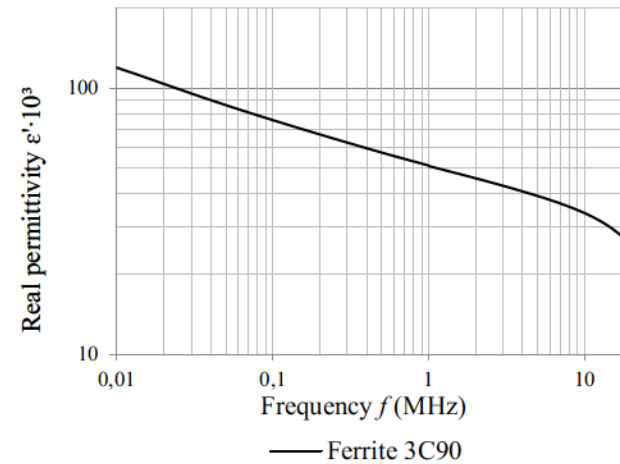
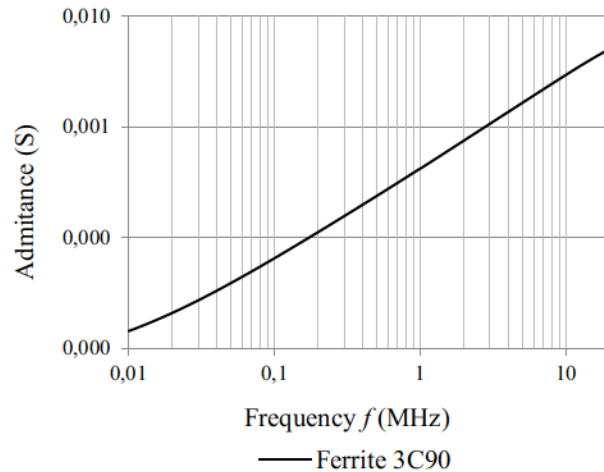
ϵ'' - imaginary component of the parallel relative complex permittivity

ϵ_0 - free space permittivity

h - tested sample height/length

A_c - tested samples cross section

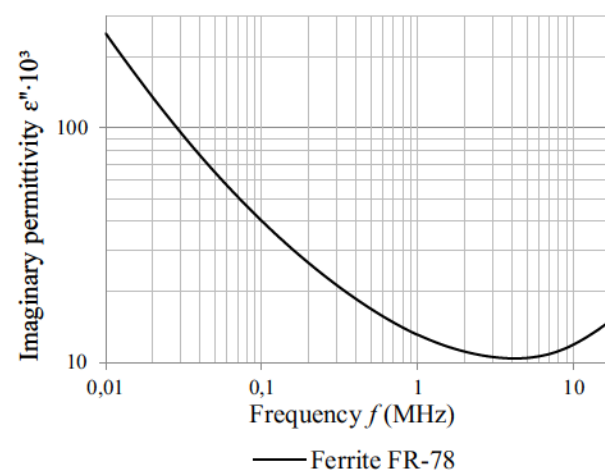
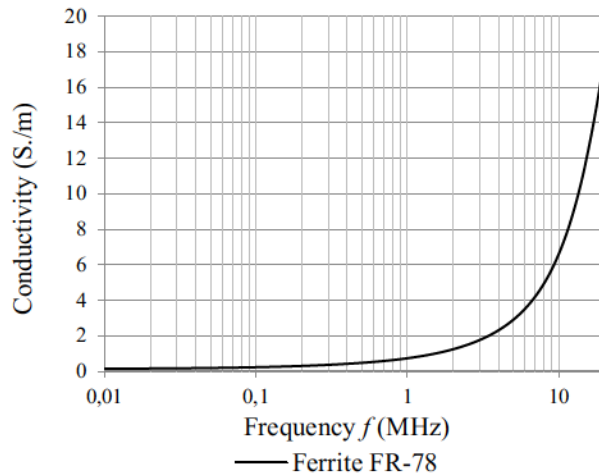
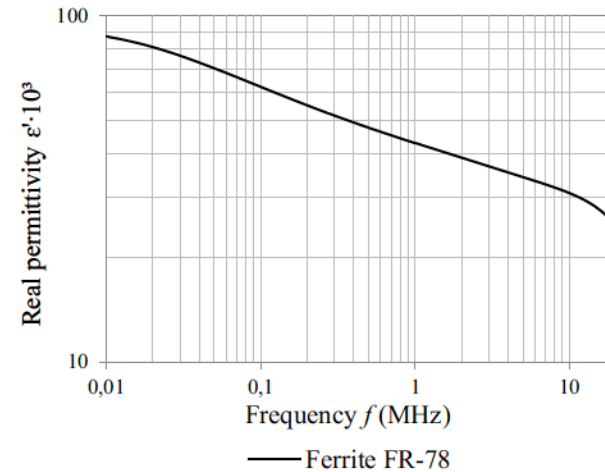
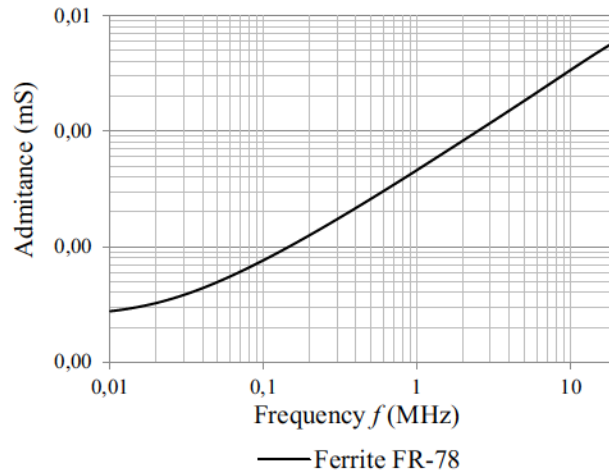
Ferrite 3C90



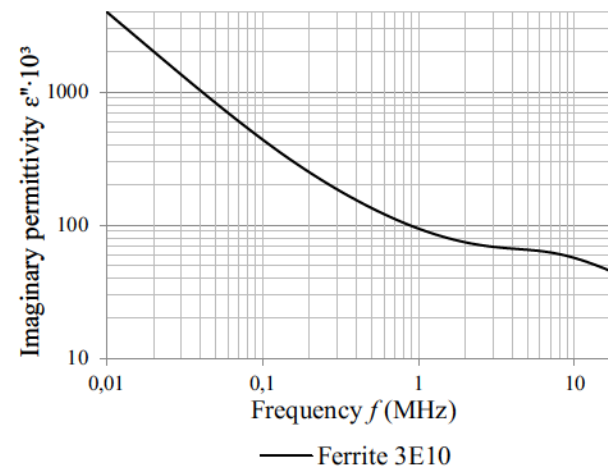
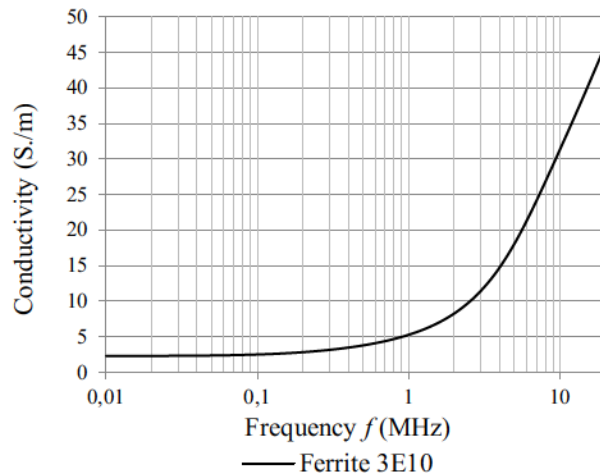
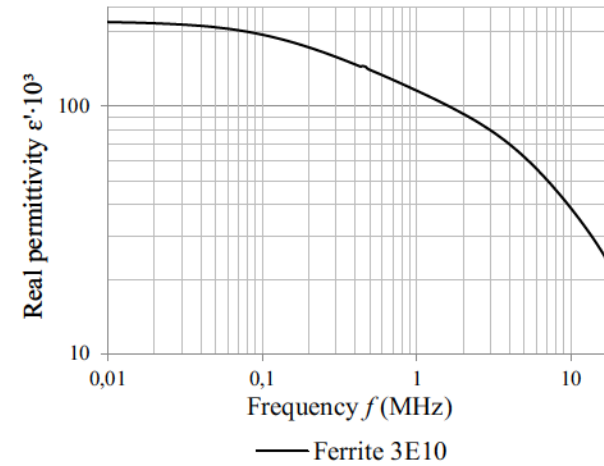
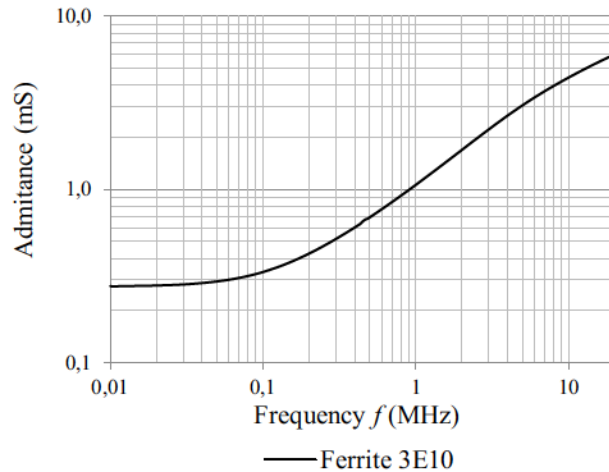
Magnetic material electrical properties



Ferrite FR78



Ferrite 3E10



Conclusion and future work



1. Measurement fixture was designed, built and tested
2. Tests based on five samples of various dimensions made of the same material 3C90 allows for selection of the best sample size to determine ferrite's permittivity and conductivity.
3. Three materials: 3C90, FR-78 and 3E10 are validated up to 5 MHz due to sample's minimum size due to high frequency effect development.
4. Presented methods for core parameters measurement are base for further discussion on the standardized test for magnetic material properties and a generic specification.

Future work

1. Ferrite validation up to 110°C during the tests
2. Ferrite validation under high density magnetic field

Appendices



The Appendices can be found on the PSMA website:

1. Ferrite 3C90 Measurement results.xls
2. Ferrite FR78 Measurement results.xls
3. Ferrtie 3E10 Measurement results.xls

ENERGY
THAT
CHANGES



SECTION V – RECTANGULAR WAVE CORE LOSS TESTER

Marcin Kącki, dr. Marek S. Ryłko, Edward Herbert, dr. Miłosz Szarek

Sponsored by

The Power Sources Manufacturers Association

e-mail: power@psma.com, <http://www.psm.com/>

P.O. Box 418, Mendham, NJ 07945-0418

Accurate core loss calculation is essential part of magnetic component design process in power electronics applications. State of the art methods become insufficient due to the input data which are based on the sinusoidal excitation core loss measurement. Therefore this section of the project deals with core loss tester development for rectangular wave excitation.

Project development:

1. H-bridge design and construction
2. Automated data acquisition to CSV excel file
(interface between power supply, arbitrary waveform generator and oscilloscope)
3. Data post-processing (result compatible with Dartmouth studies)
4. Preliminary material test – proof of the operation

Content



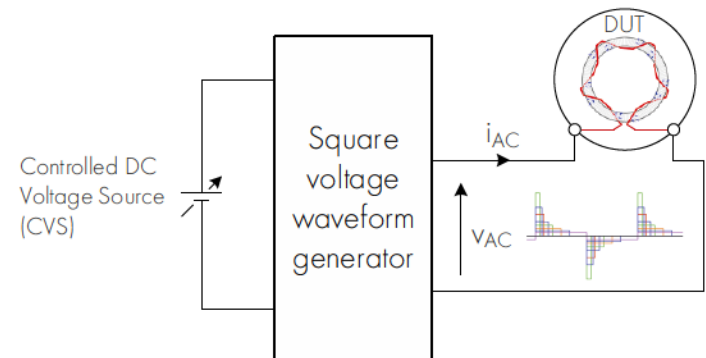
- 1** H-bridge tester development and component selection
- 2** Software development for interfacing measurement setup and data acquisition
- 3** Data post-processing on the example of selected cores
- 4** Conclusion and future work
- 5** Appendices

H-bridge tester development

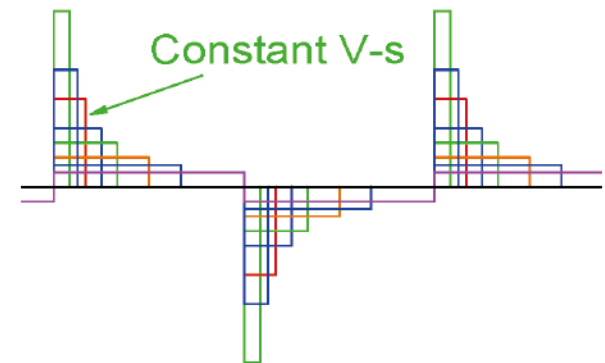


System requirements:

- > Input voltage range ($V_{AC\ peak}$): $\pm 60\text{ V}$
- > Input current range ($I_{AC\ peak}$): $\pm 10\text{ A}$
- > Switching frequency (f_{SW}): 10–500 kHz
- > Rectangular voltage wave generation with variable duty cycle ($D = 0-1$)
- > Asymmetric rectangular voltage wave generation (constant volt-seconds in each half)
- > Minimized transition time: $T_{ON}, T_{OFF} < 5\text{ ns}$
- > Optimized dead-time and on-resistance



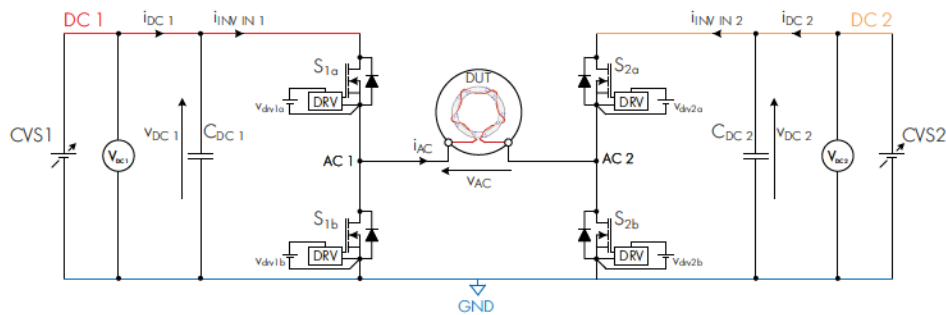
General system schematic



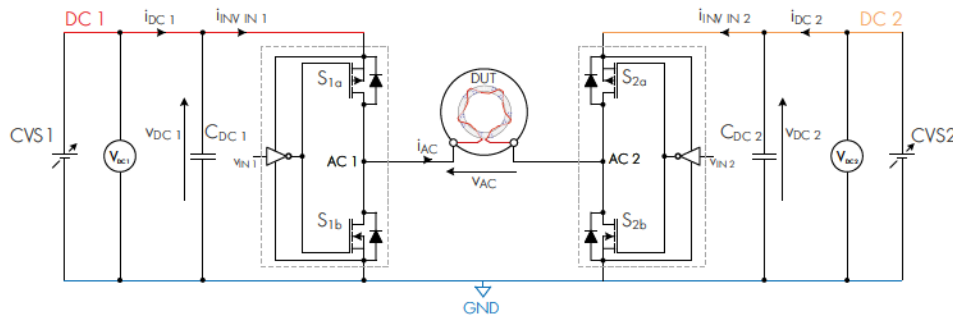
H-bridge tester development

Analyzed topology:

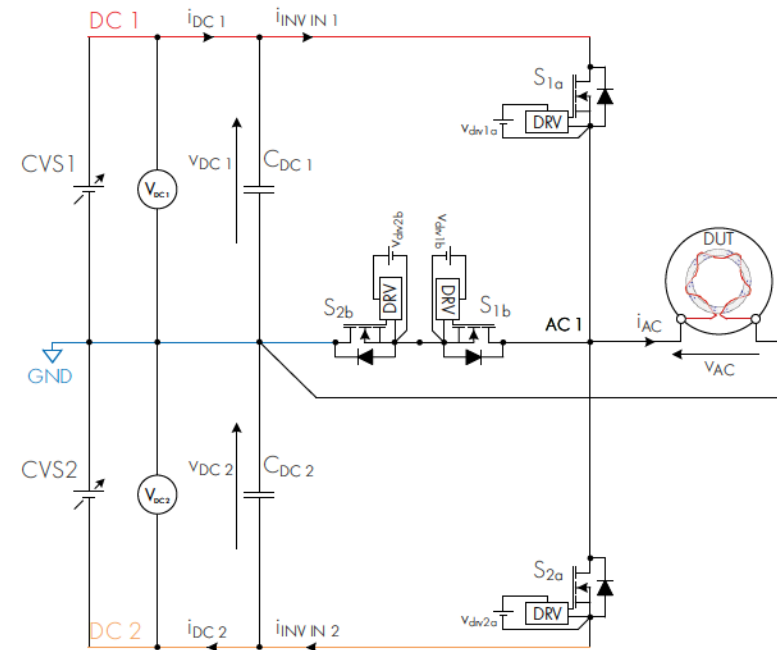
1) Full bridge topology - selected for tester



2) Two half-bridges



3) T-NPC topology



H-bridge tester development



Manufacturer	Code	Type	Structure	V [V]	I [A]	RdsON [mOhm]	Vf [V]	tdON [ns]	tr [ns]	tdOFF [ns]	tf [ns]	Package	Driver
Infineon	BSC0924ND1	N-MOSFET	Half-bridge	30	60	3.8 @ Vgs=10V	0.56 @ If=3A	4.7	3.8	17	3	TISON	Hi/Low side driver required
Texas Instruments	CSD88584Q5DC	N-MOSFET	Half-bridge	40	50	0.7 @ Vgs=10V	0.75 @ If=30A	11	24	53	17	DualCool	Hi/Low side driver required. e.g. DRV832X
ON SEMICONDUCTOR	FDMD240LET40	N-MOSFET	Half-bridge	40	103	2.0 @ Vgs=10V	0.7 @ If=1.6A	12	8	36	9	Dual Power	Hi/Low side driver required
ON SEMICONDUCTOR	FDMD8530	N-MOSFET	Half-bridge	30	201	0.77 @ Vgs=10V	0.7 @ If=2.0A	14	13	71	21	Power-33-8	Hi/Low side driver required

Half bridge Si MOSFET

Half bridge Si MOSFET drivers

Manufacturer	Code	Type	Structure	V [V]	I [A]	RdsON [mOhm]	Vf [V]	tdON [ns]	tr [ns]	tdOFF [ns]	tf [ns]	Package	Driver
Analog Devices	ADuM4120 ADuM4120-1	Isolated, High-Side Precision Gate Drivers	Half-bridge PN-MOSFET	35	2.3, peak	ROH = 800 ROL = 600 @ Vcc = 15V	Not defined	33	14	43	12	SOIC	Not required
Infineon	2EDF7275F	Isolated, High-Side	Half-bridge PN-MOSFET	22	8, peak	ROH = 850 ROL = 350 @ Iout = 50mA	Not defined	37	6.5	35	4.5	SOIC	Not required
IXYS	IXRFD630	Low-Side RF MOSFET Driver	Half-bridge PN-MOSFET	30	30, peak	ROH = 210 ROL = 130 @ Vcc = 30V	Not defined, external Schottky recommended	24	4	22	4	Low inductance RF	Not required
IXYS	IXDN609	Low-Side, Ultrafast MOSFET Drivers	Half-bridge PN-MOSFET	40	9, peak	ROH = 600 ROL = 400 @ Vcc = 18V	Not defined, external Schottky recommended	40	22	42	15	Power SOIC, TO-263	Not required
Vishey / Siliconix	SQJ504EP-T1_GE3	N-Channel, P-Channel MOSFET	2-pack	40-40	30	Rrip = 13 Rripn = 6 @ Vgs=10V	0.8 @ If=8.0A	11/15	4/6	21/45	5/7	PowerPAK-SO-8	Low side only

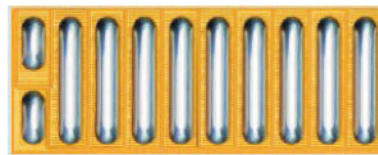
H-bridge tester development



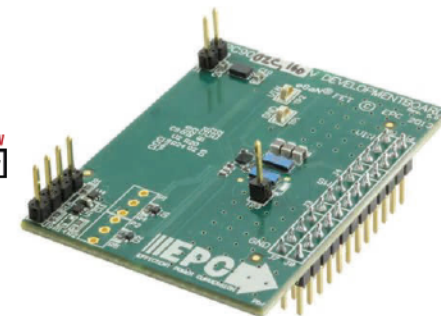
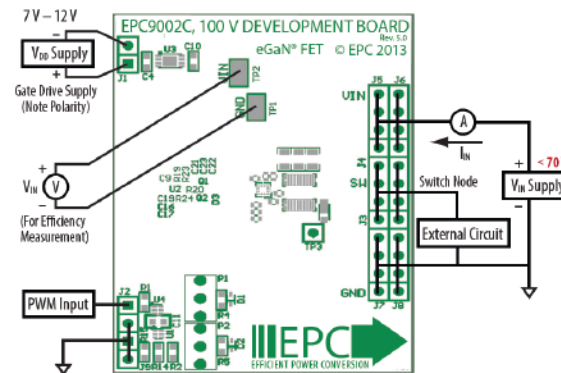
Selected semiconductors for the core loss tester:

Manufacturer	Code	Type	Structure	V	I	RdsON	Q _{G-TOTAL}	Q _{GS}	Q _{GD}	Q _{OSS}
				[V]	[A]	[mOhm]	[nC]	[nC]	[nC]	[nC]
EPC	EPC2001C	GaN FETs	Single	100	36	7 @ V _{gs} =5V	7.5	2.4	1.2	31

Package: LGA 4.1x1.6 mm

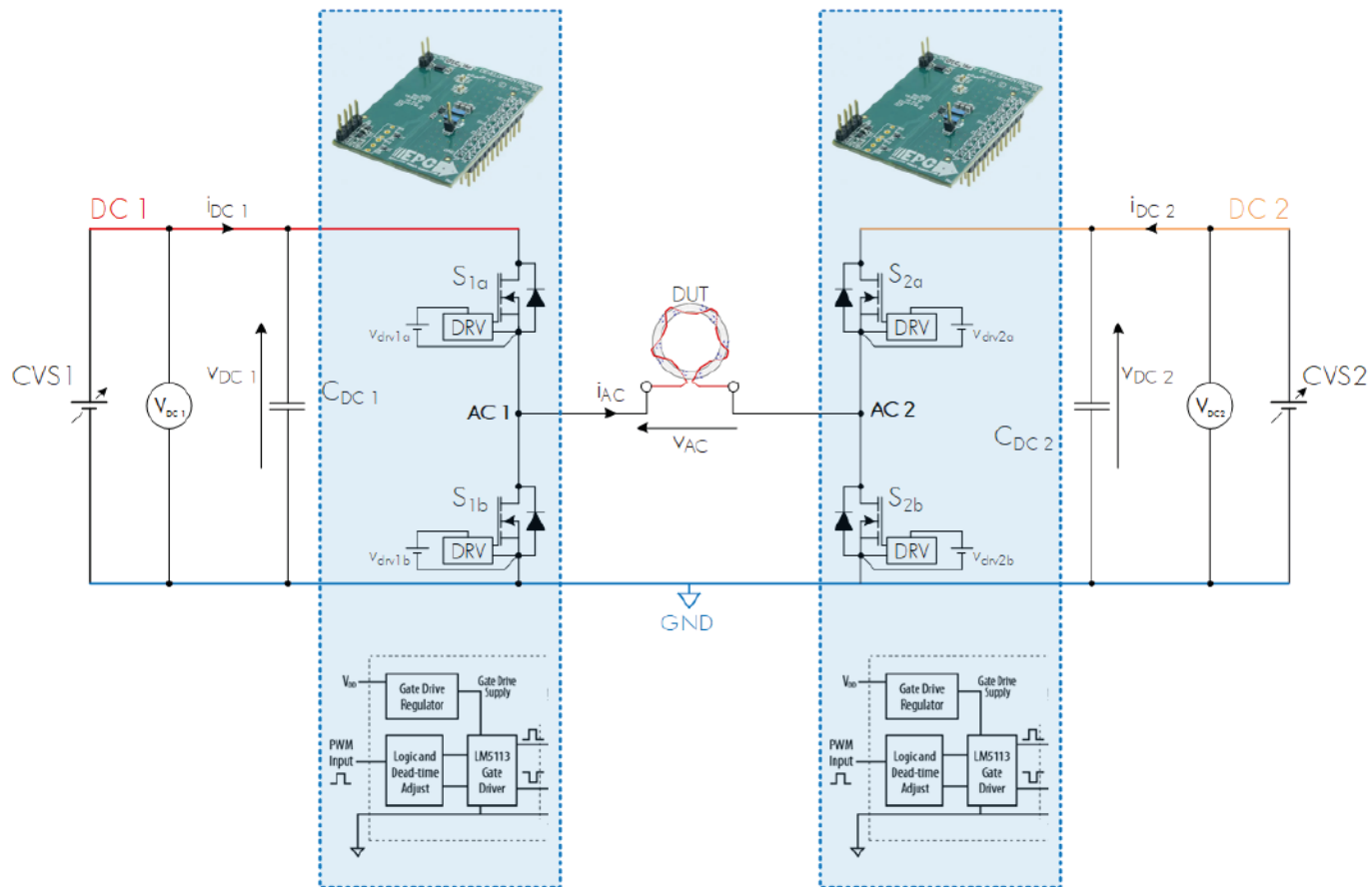


Semiconductors are integrated into the designed system on evaluation boards:

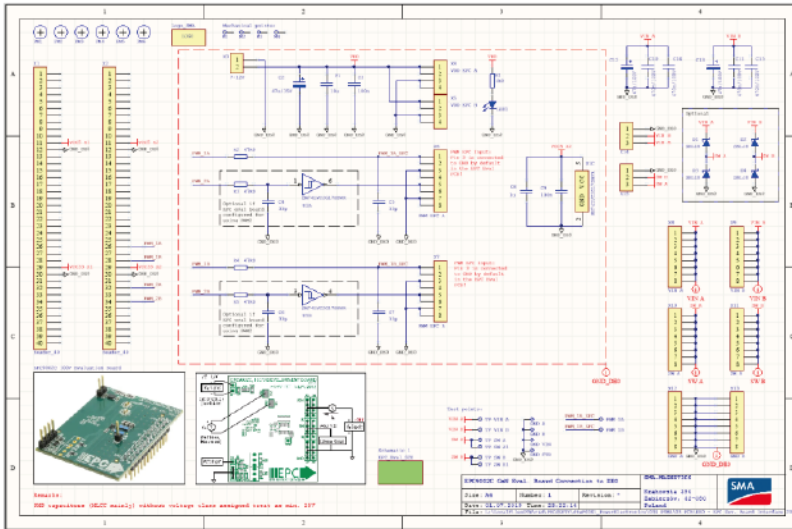


H-bridge tester development

Prototype core loss tester for rectangular wave excitation:

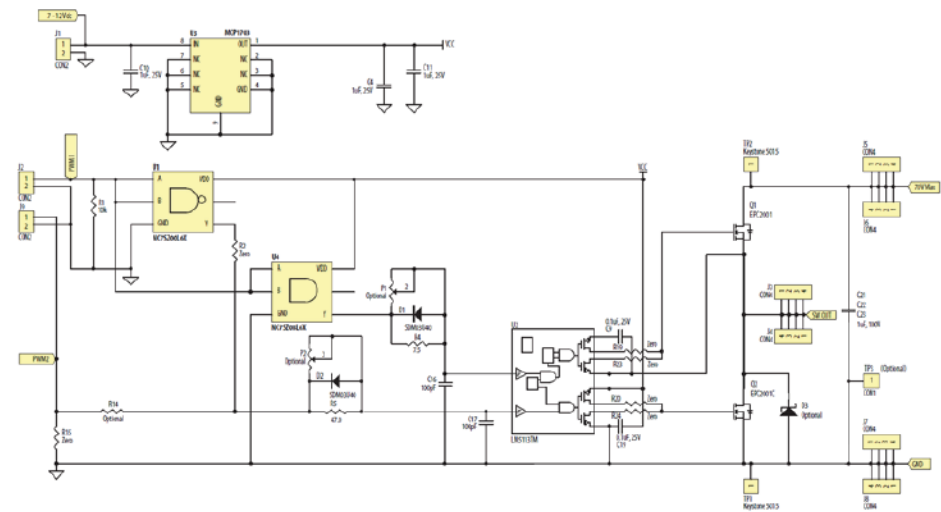


H-bridge tester development



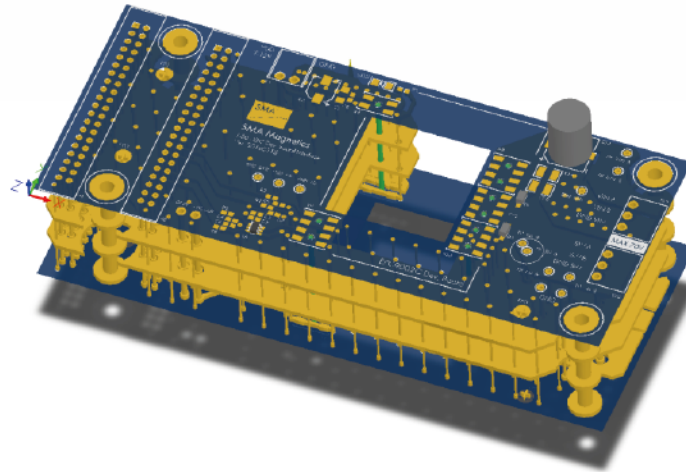
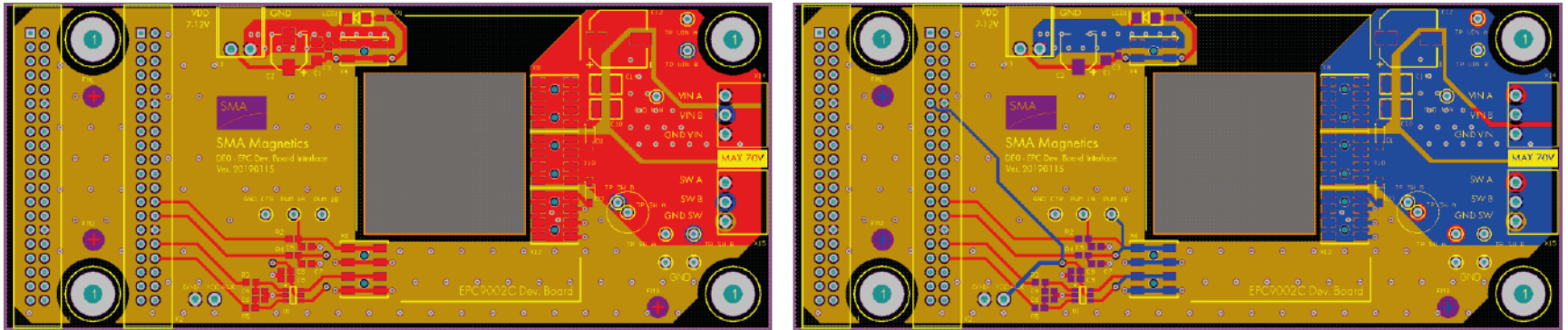
EPC evaluation PCB board

Main PCB board



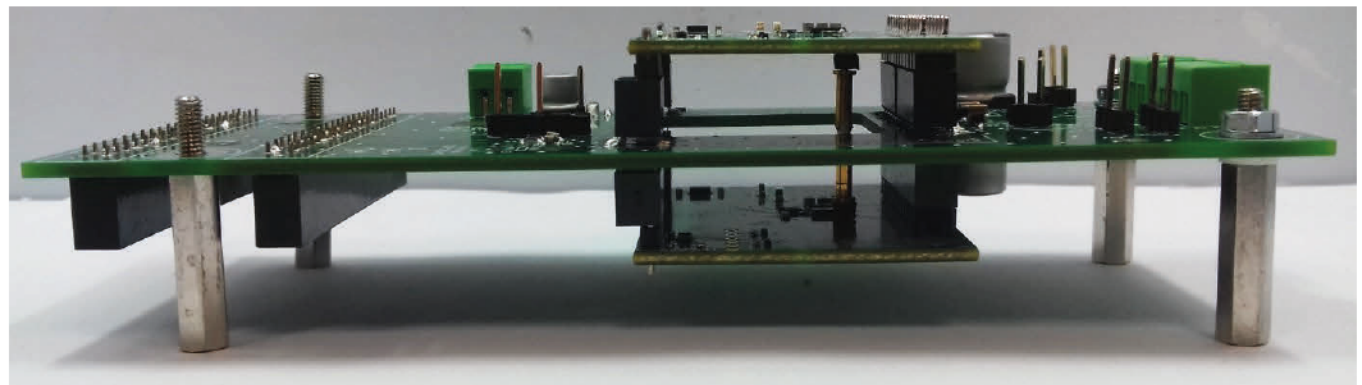
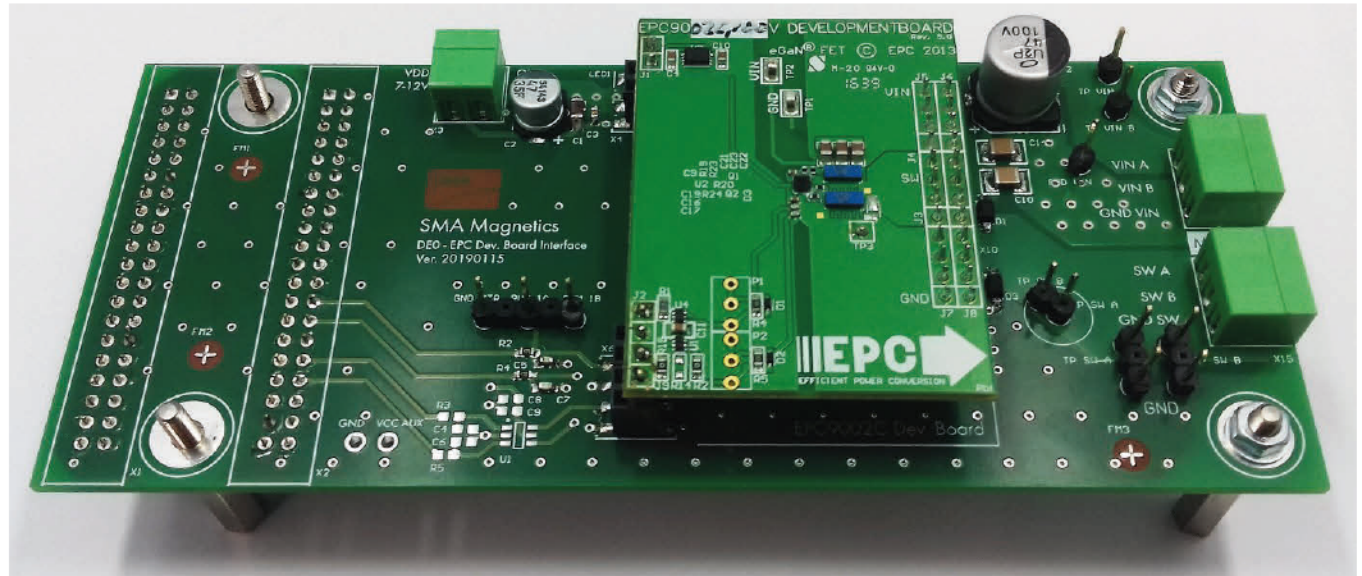
Details provided in the Appendix 1 - Main_PCB.pdf

H-bridge tester development



Details provided in the Appendix 1 - Main_PCB.pdf

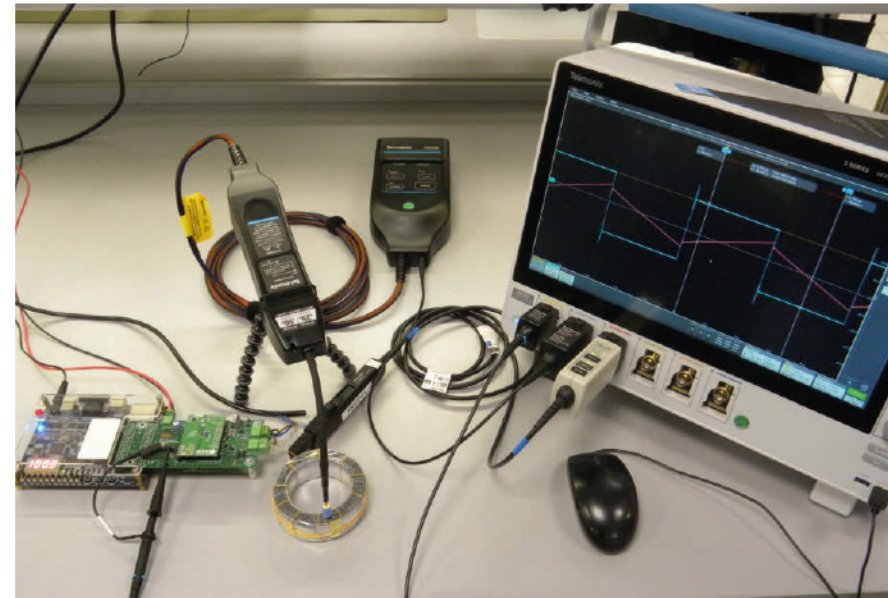
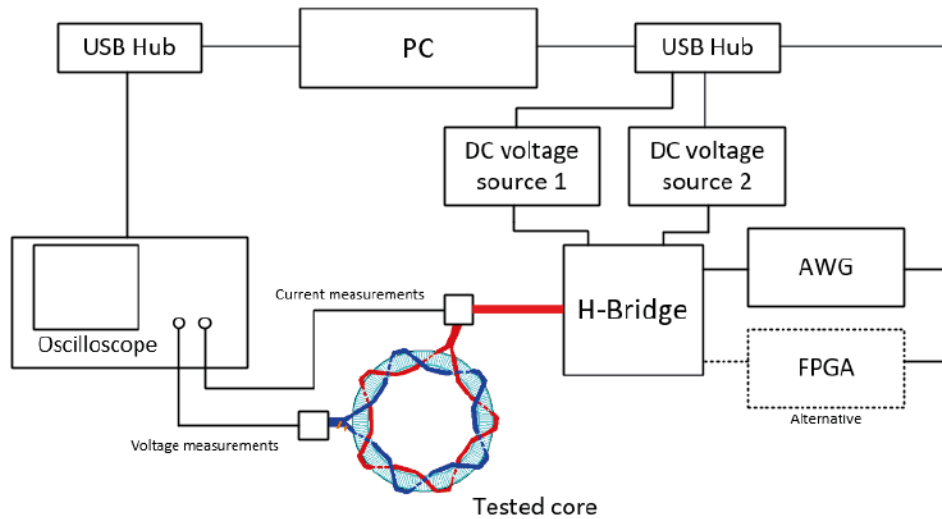
H-bridge tester development



Software development for interfacing measurement setup and data acquisition



Measurement system:

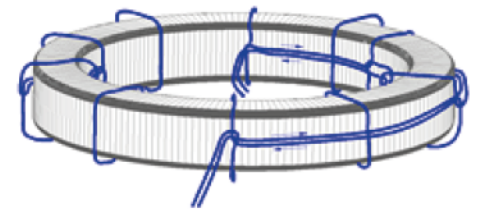
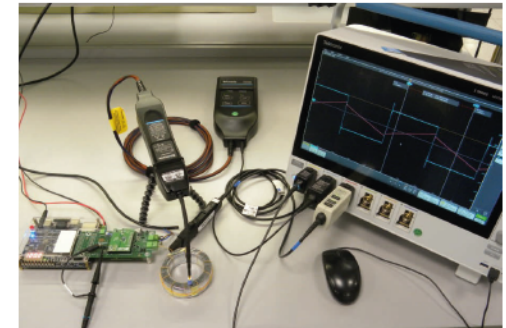


Software development for interfacing measurement setup and data acquisition



Measurement system elements:

- > Oscilloscope - Tektronix MSO56
- > Arbitrary waveform generator - Tektronix AFG31000
- > DC power source 1&2 - Keithley 2230G-60-3
- > Voltage probe - Tektronix TIVH08
- > Current probe - Tektronix TCP0030A
- > FPGA control board - Altera DE0
- > Core under test - magnetic core with two: excitation and sensing winding (Both winding made to have an H-filed which is aligned with the circumference of the core to compensate any circumferential H-field as well as reducing stray inductance)

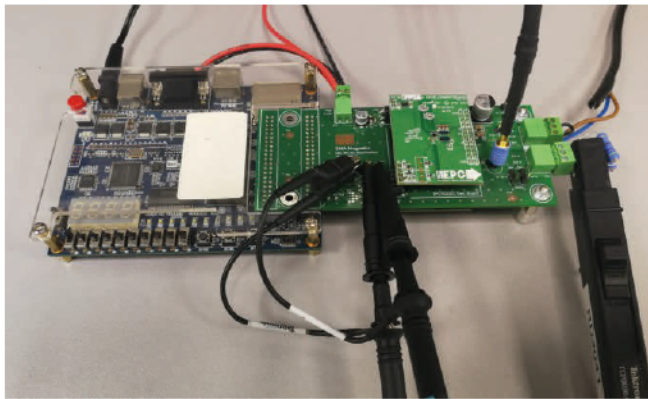


Software development for interfacing measurement setup and data acquisition

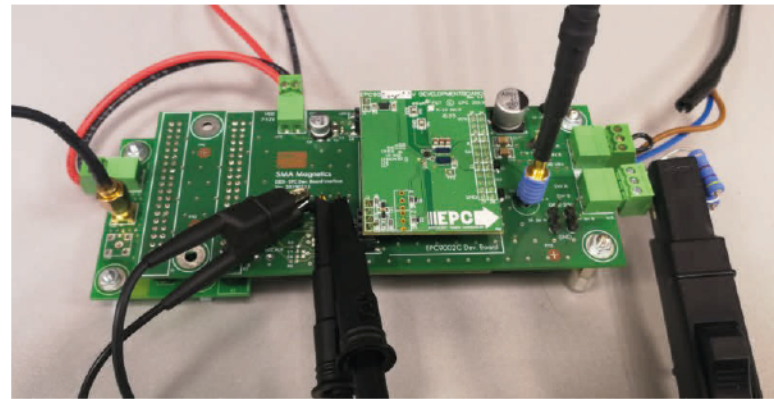


Designed system allows to generate pulses by:

1. FPGA algorithm
(frequencies and voltages are defined in the control algorithm. All parameters can be adjusted by user via controller's buttons)
2. Arbitrary waveform generator
(frequencies and voltages are defined in the excel file, parameter could be easily adjusted during the test)



H-bridge controlled by FPGA

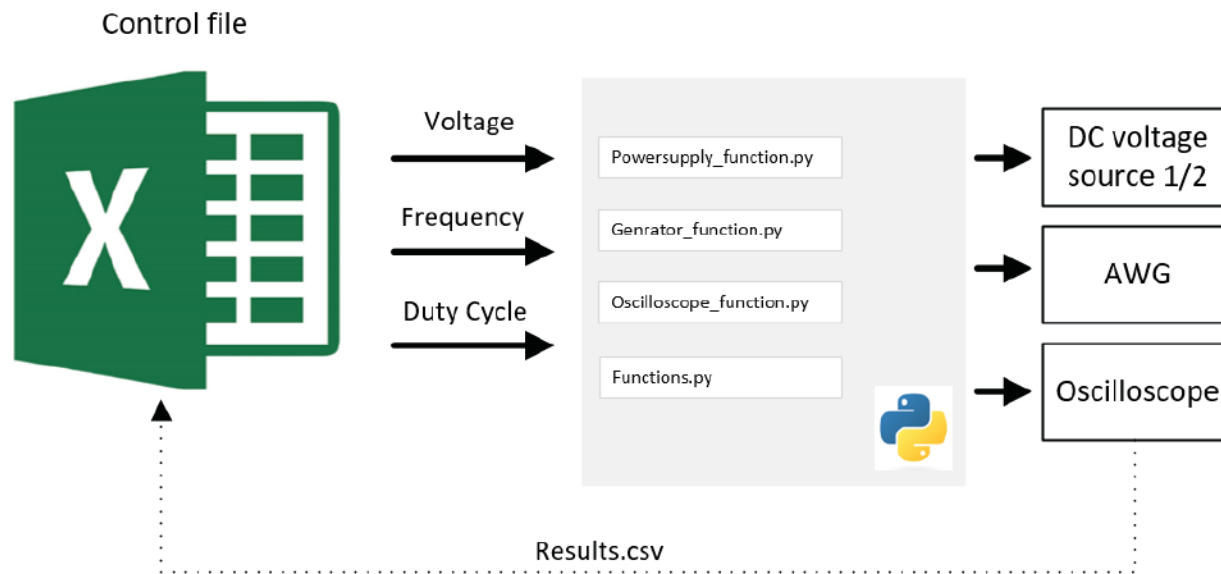


H-bridge controlled by AWG

Software development for interfacing measurement setup and data acquisition



Excel file control all connected devices: oscilloscope, power supply, pulse generator and also provides data acquisition and data postprocessing. Communication is done using Python.

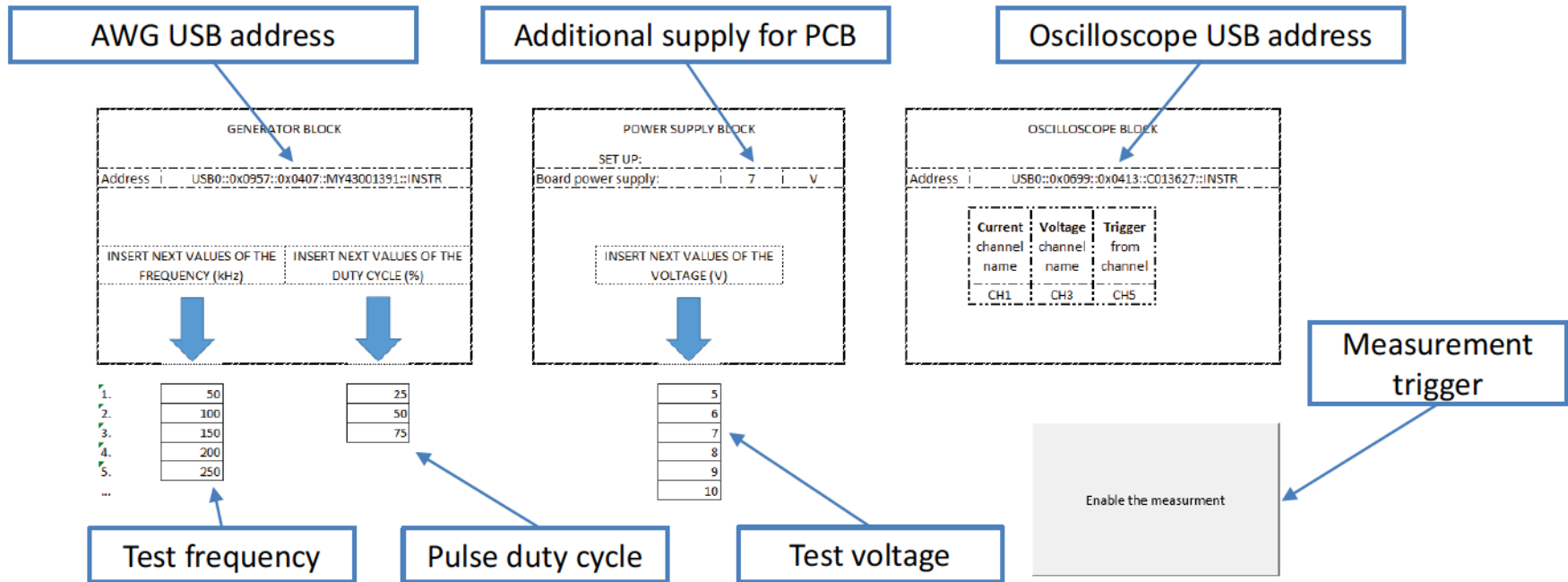


All control scripts are presented in Appendices 3 – 6.

Software development for interfacing measurement setup and data acquisition



Control file description:



Presented file will test core with every combination of listed parameters: frequency, duty cycle, voltage

The excel file is presented in Appendix 7 - Main_control_file

Software development for interfacing measurement setup and data acquisition



Measurements data are collected in one folder as presented below:

- 5.0V_25_50.0kHz_ALL.csv
- 5.0V_25_75.0kHz_ALL.csv
- 5.0V_25_100.0kHz_ALL.csv
- 5.0V_25_125.0kHz_ALL.csv
- 5.0V_25_150.0kHz_ALL.csv
- 5.0V_50_50.0kHz_ALL.csv
- 5.0V_50_75.0kHz_ALL.csv
- 5.0V_50_100.0kHz_ALL.csv
- 5.0V_50_125.0kHz_ALL.csv
- 5.0V_50_150.0kHz_ALL.csv

Test frequency

Pulse duty cycle

Test voltage



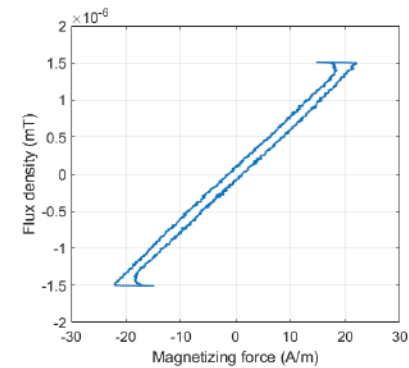
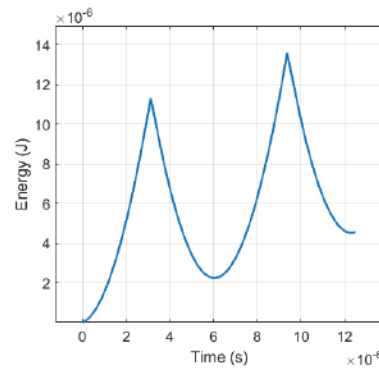
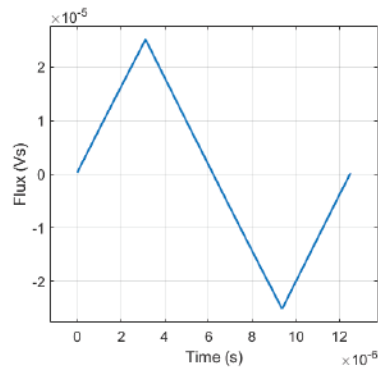
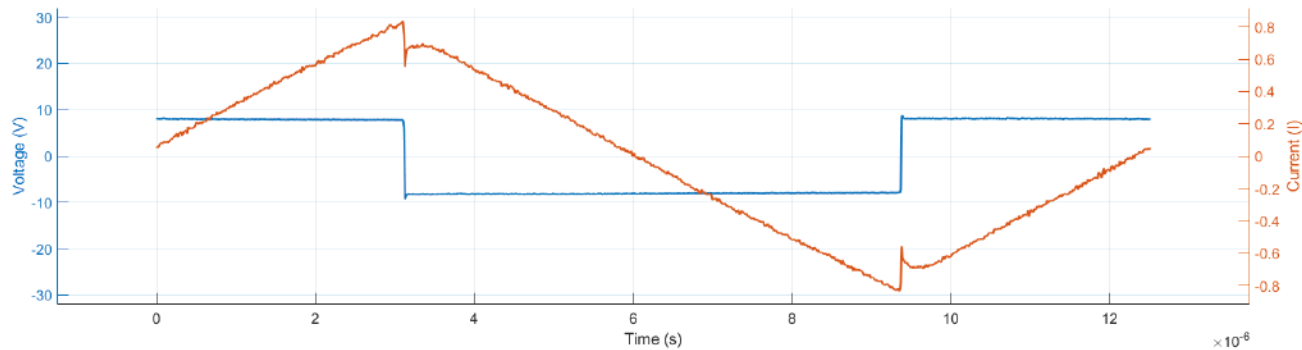
	A	B	C	D	E
1	50 kHz				
2	Time (s)	Voltage (V)	Current (A)		
3	-2.001300E-05	4.424600E+00	5.181500E-02		
4	-1.997300E-05	3.858000E+00	5.121200E-02		
5	-1.993300E-05	4.354100E+00	5.004600E-02		
6	-1.989300E-05	4.486900E+00	5.022000E-02		
7	-1.985300E-05	4.458300E+00	5.100600E-02		
8	-1.981300E-05	4.460700E+00	5.053100E-02		
9	-1.977300E-05	4.478400E+00	5.084800E-02		
10	-1.973300E-05	4.476000E+00	5.103300E-02		
11	-1.969300E-05	4.469300E+00	5.040900E-02		
12	-1.965200E-05	4.503300E+00	5.024100E-02		
13	-1.961200E-05	4.483900E+00	5.015300E-02		
14	-1.957200E-05	4.452000E+00	4.954300E-02		
15	-1.953200E-05	4.454300E+00	5.008500E-02		
16	-1.949200E-05	4.442900E+00	4.943200E-02		
17	-1.945200E-05	4.401300E+00	4.948600E-02		
18	-1.941200E-05	4.459800E+00	4.916000E-02		
19	-1.937200E-05	4.481400E+00	4.882300E-02		
20	-1.933200E-05	4.415400E+00	4.875100E-02		
21	-1.929200E-05	4.453000E+00	4.845600E-02		
22	-1.925200E-05	4.485500E+00	4.843900E-02		
23	-1.921200E-05	4.469400E+00	4.812200E-02		
24	-1.917200E-05	4.484700E+00	4.802900E-02		
25	-1.913200E-05	4.482100E+00	4.737800E-02		
26	-1.909200E-05	4.422400E+00	4.734300E-02		
27	-1.905200E-05	4.461000E+00	4.727200E-02		
28	-1.901200E-05	4.432200E+00	4.742100E-02		
29	-1.897100E-05	4.437000E+00	4.675000E-02		
30	-1.893100E-05	4.442700E+00	4.674700E-02		
31	-1.889100E-05	4.424000E+00	4.638100E-02		
32	-1.885100E-05	4.438100E+00	4.634800E-02		
33	-1.881100E-05	4.451700E+00	4.584500E-02		
34	-1.877100E-05	4.430200E+00	4.583400E-02		
35	-1.873100E-05	4.363200E+00	4.551100E-02		

Results are compatible with scripts developed during previous studies.

Data post-processing



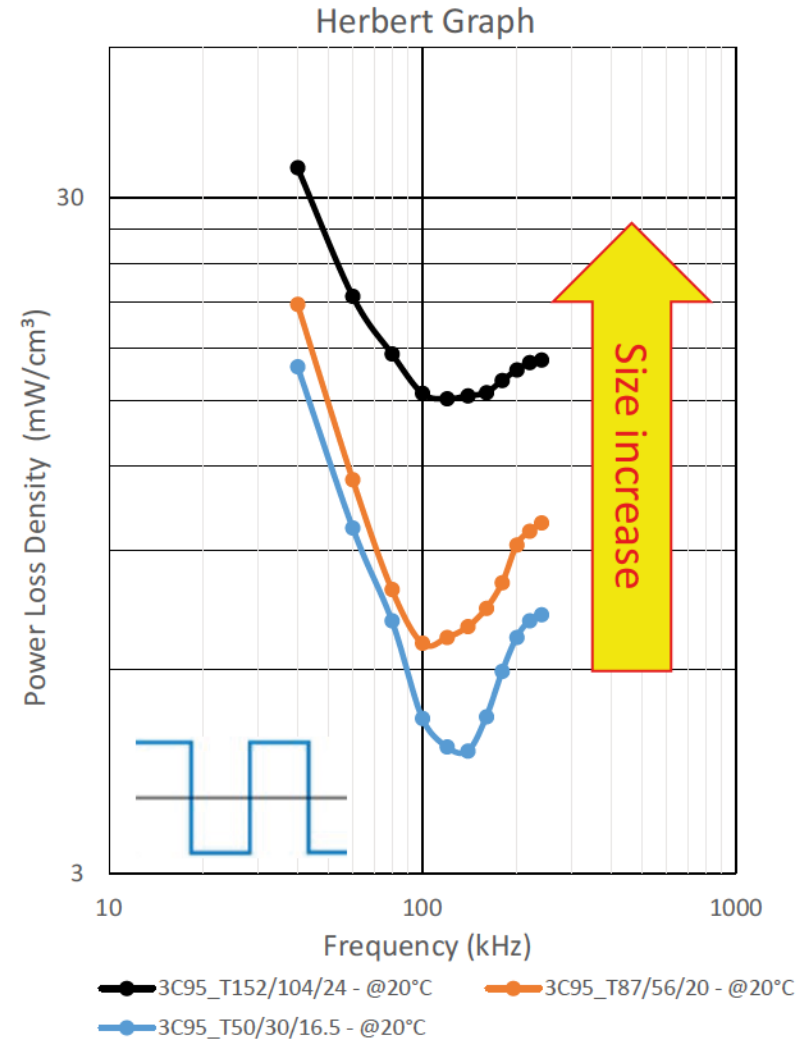
Matlab script is employed for detailed analysis (e.g. power loss calculation).
Calculation example for toroidal core T50/30/16.5mm, 4V/turn, 80 kHz :



Data post-processing on the example of selected cores

Power loss measured for three toroidal cores made of the same material 3C95 in three sizes:

Tested samples			
Material	3C95	3C95	3C95
Dimensions OD x ID x H	152x104x24 mm	87x56x20 mm	50x30x16.5 mm
Core total cross section	558 mm ²	310 mm ²	164 mm ²
Core volume	224 cm ³	69.6 cm ³	20.47 cm ³



Data post-processing on the example of selected cores

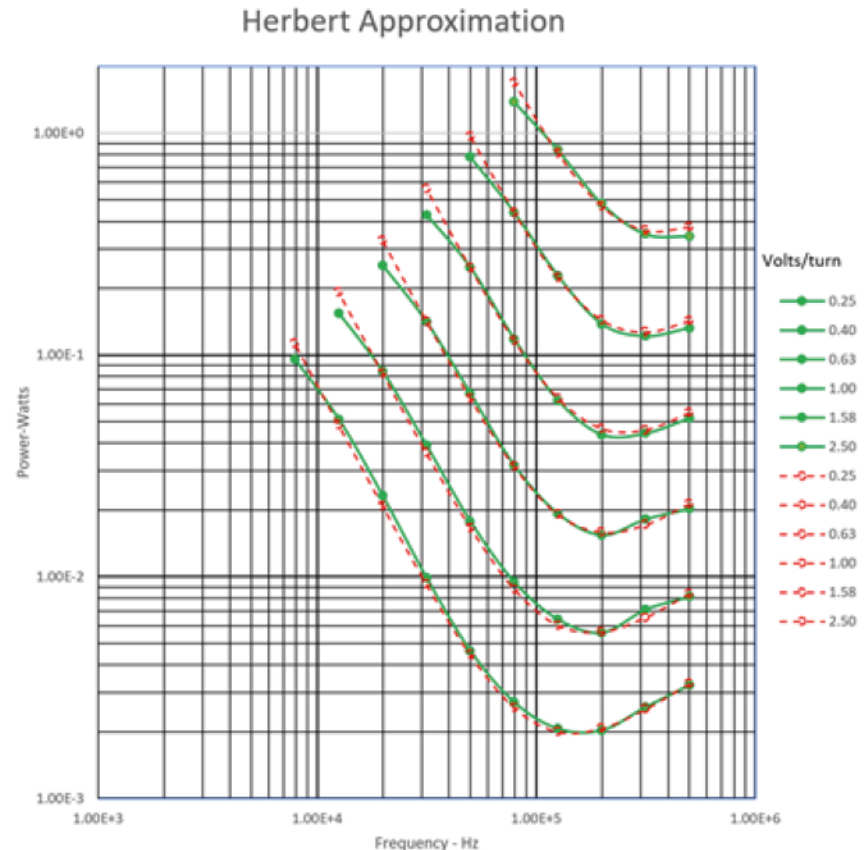


Measured data are presented on the Herbert graph.

Optimum operating point for a core is directly identified as well as core losses at the other operating points.

Curve fitting formula

$$P_c = k * f^\delta * \left(1 + \left(\frac{v}{V_b} \right)^\alpha * \left(\frac{f_b}{f} \right)^\beta \right) * v^2$$



Conclusion and future work



1. H-bridge was designed, built and tested
2. Automated data acquisition excel file was developed
3. Measured data are compatible with previous studies
4. Preliminary tests based on the three toroidal cores made of the same material 3C95 in three sizes were performed
5. Presented methods for core parameters measurement are base for further discussion on the standardized test for magnetic material properties and a generic specification

Future work

1. Study on flux propagation under rectangular waveform
2. Characterization of power losses under various rectangular flux pattern conditions in range of ambient temperature

Appendices



The Appendices can be found on the PSMA website:

1. Main_PCB.pdf
2. AWG_PCB.pdf
3. Python - Powersupply_function.py
4. Python - Generator_function.py
5. Python - Oscilloscope_function.py
6. Python - Functions_function.py
7. Excel - Main_control_file.xlsm

ENERGY
THAT
CHANGES



SOCIAL MEDIA
www.SMA.de/Newsroom

